DESIGNING AND BUILDING A NEUTRON INSTRUMENT

XIV School of Neutron Scattering Francesco Paolo Ricci (SoNS)

Erice, 1-9 April 2016

Scattering Techniques: DIFFRACTION

Thomas Hansen

Institut Laue-Langevin

Diffraction

- ***Diffraction*** vs. ***interference***
  - *__Diffraction__ is the __interference__ of waves from __many__ sources, usually __scattering__ objects*
  - Focus on ***Bragg*** diffraction (diffraction on periodic 3D lattices)
- Neutron ***diffraction*** ≈ ***elastic*** neutron ***scattering***
  - Introduction to neutron scattering (again ...?)
    - ***Nuclear*** scattering
    - (***Magnetic*** scattering)
  - Single crystal Neutron Diffraction
    - Structure determination left out
  - Neutron Powder Diffraction
    - Rietveld method
    - Peak shape and microstructure

Neutron Scattering

- Interactions of slow (thermal) neutrons with condensed matter
  - Nuclear scattering
  - Magnetic scattering
  - Nuclear absorption
- Energy and momentum conservation
- Diffraction ≈ elastic scattering
- Inelastic scattering
- Features of the neutron scattering technique
- The Master formula

Nuclear scattering

- Simple scattering experiment
  - Neutrons beam : incident wave vector $\mathbf{k}_0$ falls on sample
  - Interaction probability rather small: most neutrons transmitted
  - Few scattered neutrons measured with detector in direction $\mathbf{k}_1$
  - incident beam
    - uniform flux Φ (neutrons crossing unit area per unit time)
  - sample
  - *N* identical atoms in the beam
  - detector
    - solid angle $\Delta\Omega$ and efficiency η

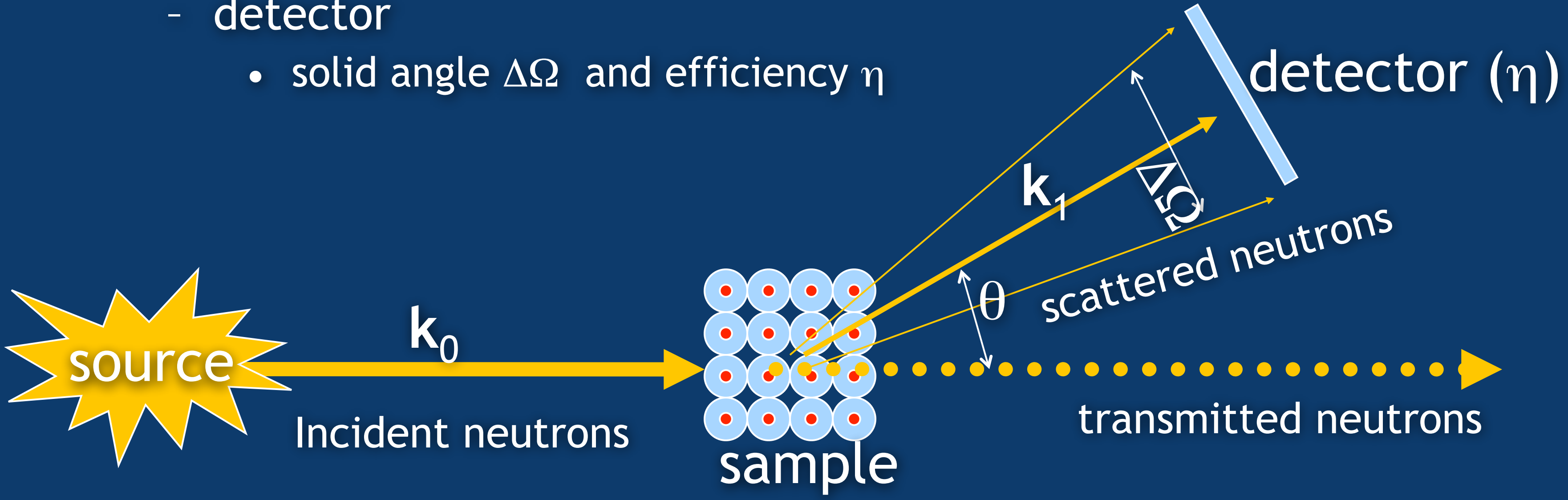

Scattering: differential cross section

- count rate *C* in the detector
  - proportional to all quantities
  - constant of proportionality: *differential cross section*
- $d\sigma/d\Omega = C/(\Phi N(\Delta\Omega)\eta)$.
- differential cross section
  - function of magnitude and directions of $\mathbf{k}_0$ and $\mathbf{k}_1$
  - property of sample ...
    - ... and (sometimes) neutron spin state
- types of interaction in condensed matter studies
  - nuclear interaction and ...
  - ... magnetic dipole interaction
  - neglect weaker interactions [C.G. Shull]

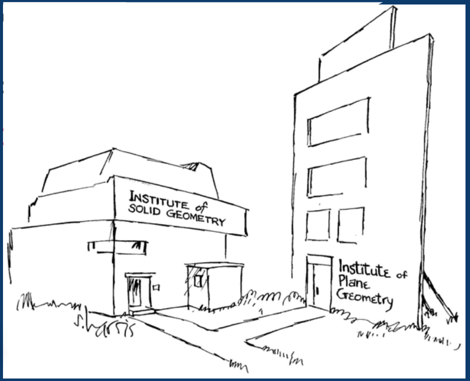

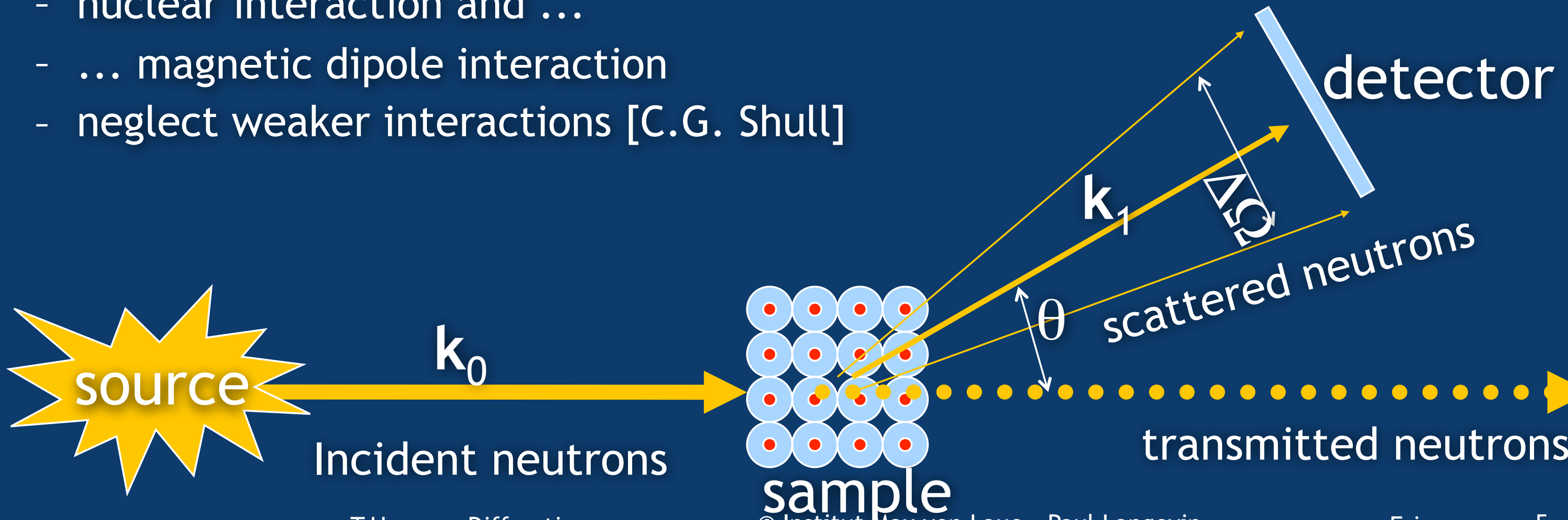

detector

$\mathbf{k}_1$

$\Delta\Omega$

θ

scattered neutrons

source

$\mathbf{k}_0$

Incident neutrons

transmitted neutrons

sample

Nuclear scattering: scattering length

- Interaction between slow neutrons and atoms through nuclear force
  - wavelength >> range of nuclear force
  - atoms in the sample are both non-interacting and identical
- Differential cross section constant:
  - $d\sigma/d\Omega \propto b^2$.
- *Scattering length b*
  - property of nucleus of scattering atom
    - atomic number *Z* and atomic weight *A*
    - spin state relative to that of the neutron

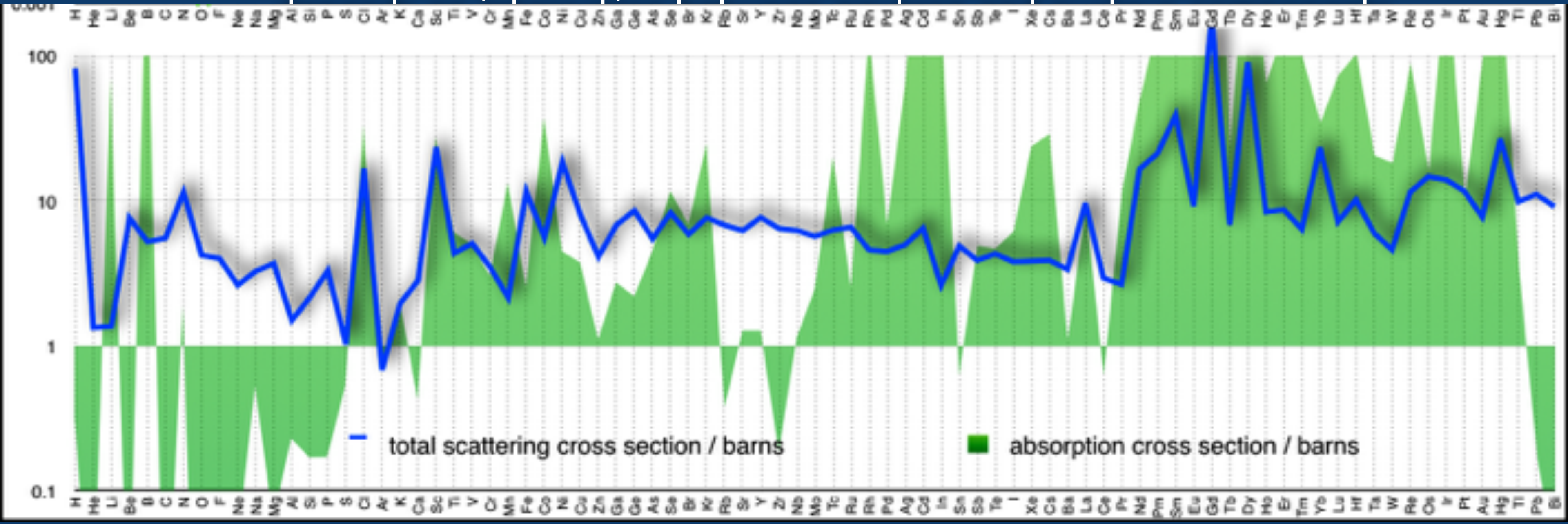

Nuclear Scattering: scattering length (cont'd)

- Two spin states, (*I* ± 1/2) of neutron-nucleus system
  - Quite different scattering lengths possible
    - Incoherent scattering *(I'll be back …)*
    - In case of polarized nuclei
      - measure the configuration of the nuclear spins
      - nuclear magnetism is a much weaker phenomenon than electronic magnetism
- Low-lying resonance of neutron-nucleus system
  - scattering and absorption cross sections depending on wavelength
  - scattering length becomes complex.
- Scattering length in laboratory system smaller by a factor (*A*/*A*+1)
  - Only, if the nucleus is free to recoil.
  - Neutron scattering on condensed-matter:
    - Fixed atom more appropriate limiting case
    - "bound-atom" values quoted for scattering lengths and cross sections
      - http://www.ncnr.nist.gov/resources/n-lengths/
    - (A/A+1) to be considered for scattering experiments on gases

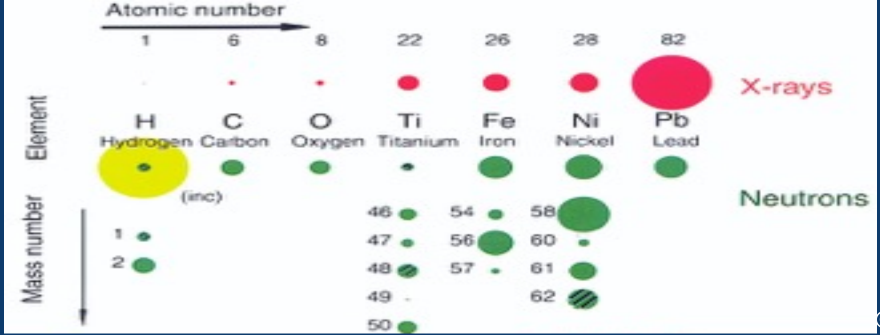

© Institut Max von Laue - Paul Langevin

Magnetic scattering

- Neutron’s magnetic moment interacts with unpaired electrons
- Paramagnet with electrons localized in specific ions
  - Random spin orientations and no external magnetic field
- Differential cross section $d\sigma/d\Omega = (\gamma\, r_0)^2\, [\, f\, (\mathbf{k}_1-\mathbf{k}_0)\,]^2\, S(S+1)$
    - $\gamma\, r_0 = 0.54 \cdot 10^{-12}$ cm
    - Spin quantum number for the ions: S
- Magnetic form factor $f(\mathbf{Q}) = f\,(\mathbf{k}_1-\mathbf{k}_0)$
    - Fourier transform of the density distribution of the unpaired electrons
    - normalized to $f(\mathbf{0}) = 1$
  - Nuclear scattering length constant, considering the nucleus as a point
    - Good intensities for higher scattering angles, larger wave vectors Q
  - Magnetic neutron scattering like X-ray and electron scattering:
    - Form factor decreases with scattering angle, less information for higher Q.
- Orbital contribution to the magnetic interaction
  - Additional scattering from current associated with a moving electron

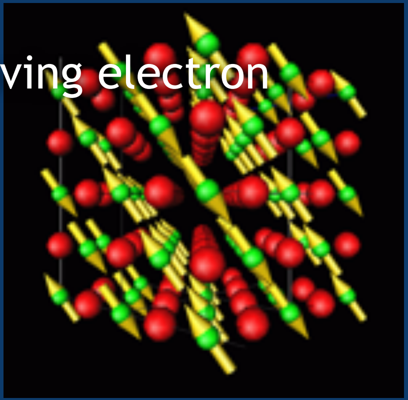

Ferromagnetic and antiferromagnetic oxides

Nuclear absorption

  - Incident neutron on sample: beside transmission and scattering,
- Absorption as a third possible outcome
  - Treated as simple attenuation of incident and scattered beams
    - Numerical factor in general expression for differential cross section
  - Other things leading to attenuation
    - Beam removal from multiple scattering involving the same neutron
  - Strong absorption due to resonance capture
    - Wavelength-dependent complex scattering length.

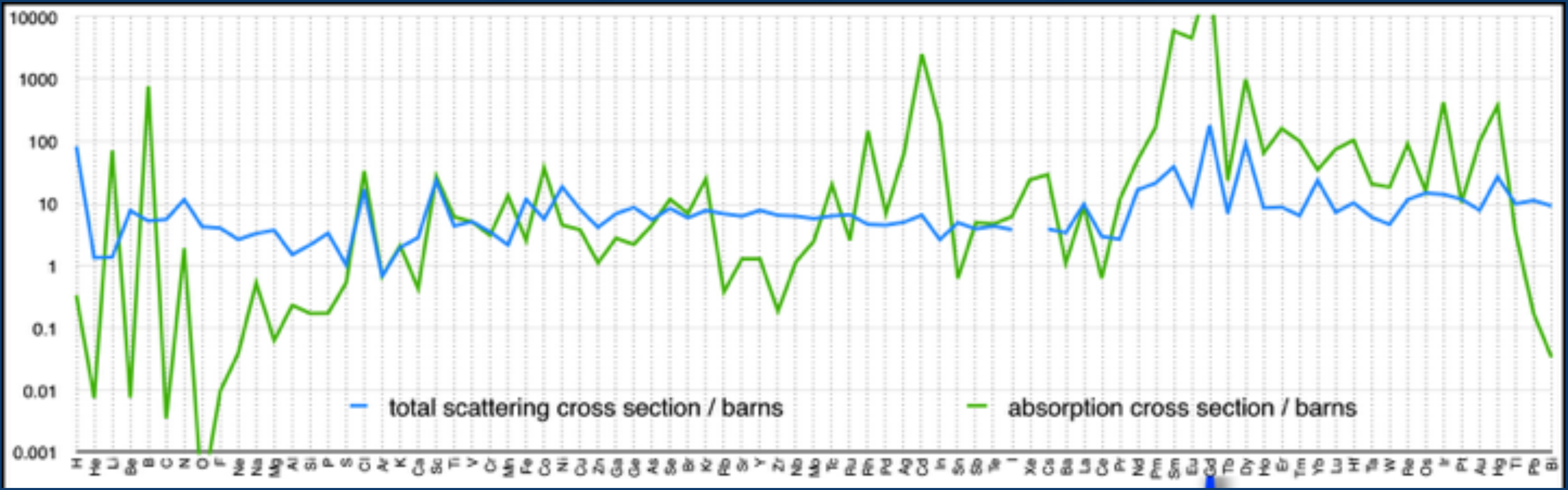

Energy & momentum conservation

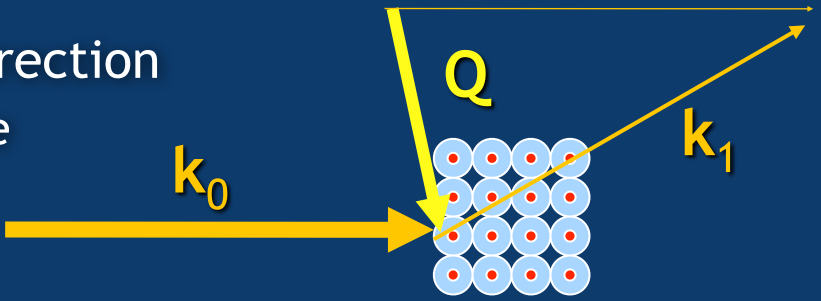

- Wave vector **k** suffers change in direction
  - momentum exchanged with sample
  - corresponding wave vector **Q**
  - law of momentum conservation as
    - $\mathbf{k}_0 - \mathbf{k}_1 = \mathbf{Q}$.
- Momentum $h/2\pi\cdot\mathbf{Q}$ taken up by the scattering atom
    - Subsequently shared with the rest,
    - or, single crystals, the sample as a whole recoils
- Magnitude of **k** can change as well
  - neutron exchanges energy
  - law of energy conservation,
  - $(h/2\pi)^2 k_0^2/2m - (h/2\pi)^2 k_1^2/2m = E$,
  - E is the energy transferred to the sample
    - two terms on the left-hand side: incident and scattered neutron energies

© Institut Max von Laue - Paul Langevin

Energy & momentum conservation …

- Process, in which a neutron is scattered from $\mathbf{k}_0$ to $\mathbf{k}_1$
  - associated with a set of values of **Q** and *E*
- Intensity of scattering: function of the variables (**Q**, *E*)
  - Property of the particular sample and its environment
    - Temperature, pressure, magnetic field, etc.
  - Neutron experiments try to measure this function
    - description of its form
      - for different materials
      - in different environments

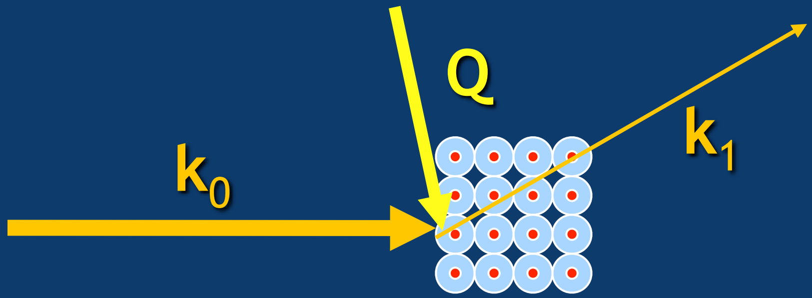

Diffraction

- Sample of individual, non-interacting scattering units of mass M
  - Relation between E and $\mathbf{Q}$ takes the simple form $E = (h/2\pi)^2 Q^2/2m$.
  - Two-body collision problem, with $E = 2E_0\, m/M\, (1 - \cos\theta) + O\,(m/M)^2$
    - θ : scattering angle between $\mathbf{k}_0$ and $\mathbf{k}_1$
    - $E_{0:}$ incident neutron energy
    - m: **neutron** mass, M: **sample** mass
- Energy transfer tends to zero as mass M of scattering unit increases
  - Solid sample: significant amount of scattering is “elastic”, i.e., $E = 0$
    - Sample recoils as rigid unit, scattering unit = whole sample
    - $|\mathbf{k}_1| = |\mathbf{k}_0|$
  - $2k_0 \sin(\theta/2) = Q$.
- Crystalline materials:
  - Strong elastic scattering when **Q** equal to a reciprocal lattice vector
- $\mathbf{Q} = 2\pi\,(h/a,\ k/b,\ l/c)$ or $Q = 2\pi/d$.
  - d : spacing of the (h, k, l) set of crystal planes (I’ll be back on this …)
    - With $k_0 = 2\pi/\lambda_0$, we derive the common Bragg condition for diffraction:

$$\lambda_0 = 2d\,\sin(\theta/2)$$

Diffraction: Bragg’s law

- $\lambda_0 = 2d \sin(\theta/2)$
    - Waves scattered from successive lattice planes interfere constructively
    - Giving an intensity maximum in the diffraction pattern
    - Single-crystal sample
        - crystal orientation : **Q** parallel to reciprocal lattice vector
- 2 scanning methods through different lattice plane spacings
    - varying θ at constant λ_0
    - varying λ_0 at constant θ
- Involving either definition or measurement of λ_0: 2 ways
    - Using mosaic single-crystal monochromators/analysers (Bragg condition)
    - Velocity, determining/measuring travel time for a known distance

Diffraction: Elastic scattering

- Truly *elastic scattering*,
  - Determine the wavelength of both incident and scattered beams
  - Ensure that $|\mathbf{k}_1| = |\mathbf{k}_0|$
  - Structural measurements in crystalline materials
    - Elastic scattering is dominant contribution
  - *Total scattering* corresponding to certain λ_0 and θ measured
      - regardless of energy transfer.
    - Inelastic ($E \neq 0$) contribution either neglected of removed by data analysis
  - Non-crystalline samples (glasses or liquids)
    - Total scattering usually quantity of interest
    - Corrections have to be made for inelastic scattering
- Count rate *C* in a typical neutron diffraction experiment
- $C \approx \Phi(\lambda_0)\ (\Delta\lambda_0)\ N\ b^2\ (\Delta\Omega)\ \eta \approx 10^{-22}N$
    - 1% resolution
    - $\Phi(\lambda_0)\lambda_0 \approx 10^9 \mathrm{n/cm^2s}$, $\Delta\lambda_0/\lambda_0 \approx 10^{-2}$, $b^2 \approx 2\cdot10^{-25}\mathrm{cm}^2$, $\Delta\Omega \approx 10^{-4}$, $\eta \approx 0.5$
  - 1 count/s: 10^{22} atoms, 1 g sample

Bragg Diffraction for crystal structure

- Crystalline matter:
  - Each single atom scatters an incoming wave serving as a secondary isotropic point source
  - Constructive interference in certain directions
  - Atoms arranged on many infinite sets of equidistant parallel lattice planes

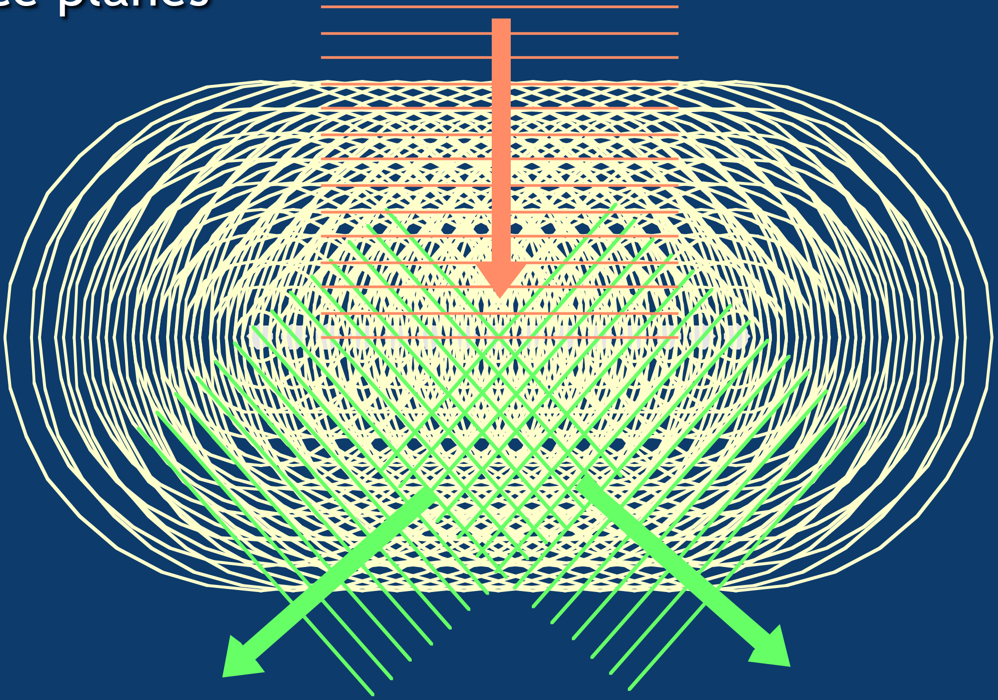

Bragg’s law: interference

- Lattice planes regarded as semi-transparent mirrors
  - Constructive interference if reflected beams in phase:
- **$2d \sin\theta = n\lambda$**
  - Total cancellation if not, due to infinite number of planes

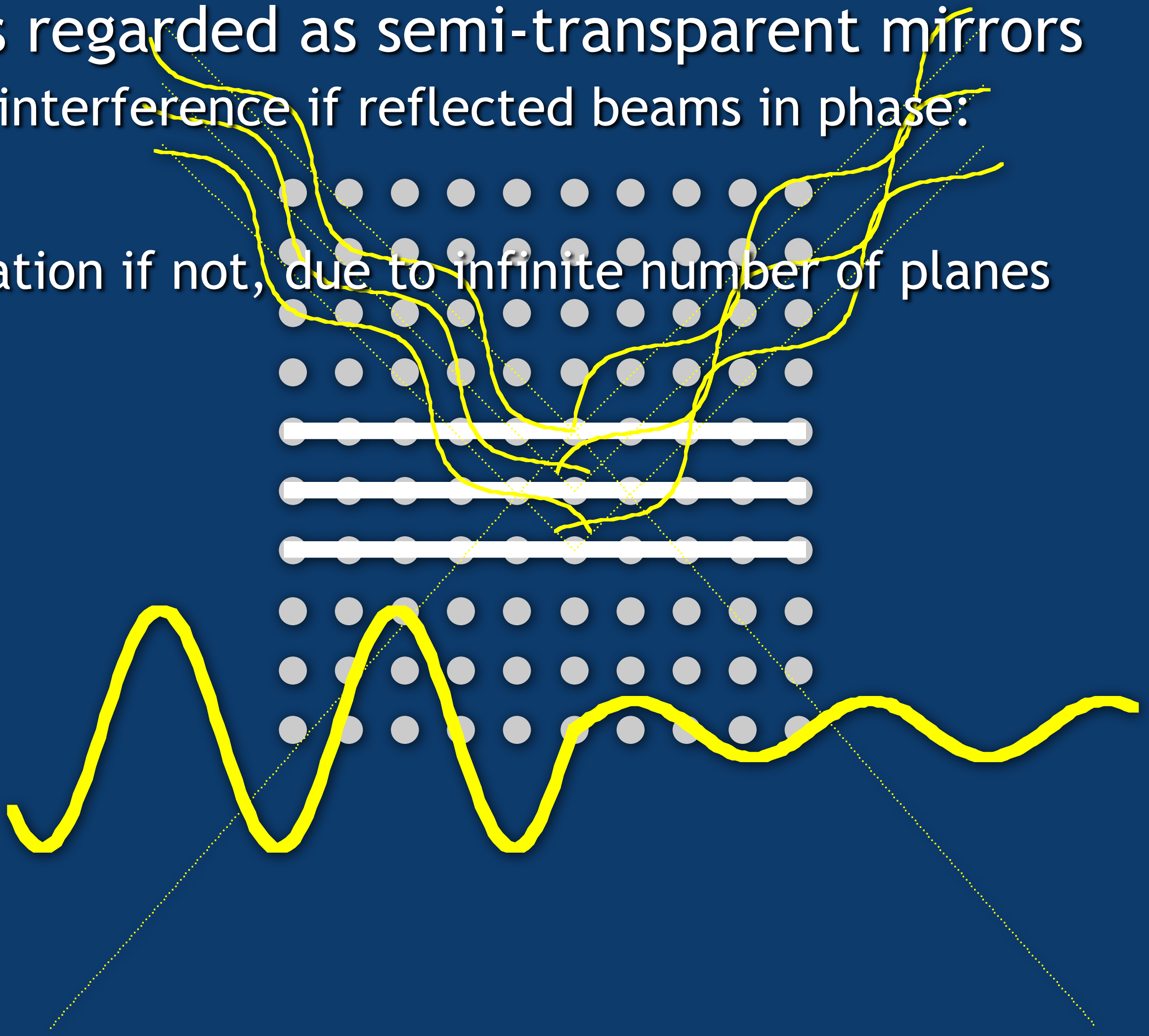

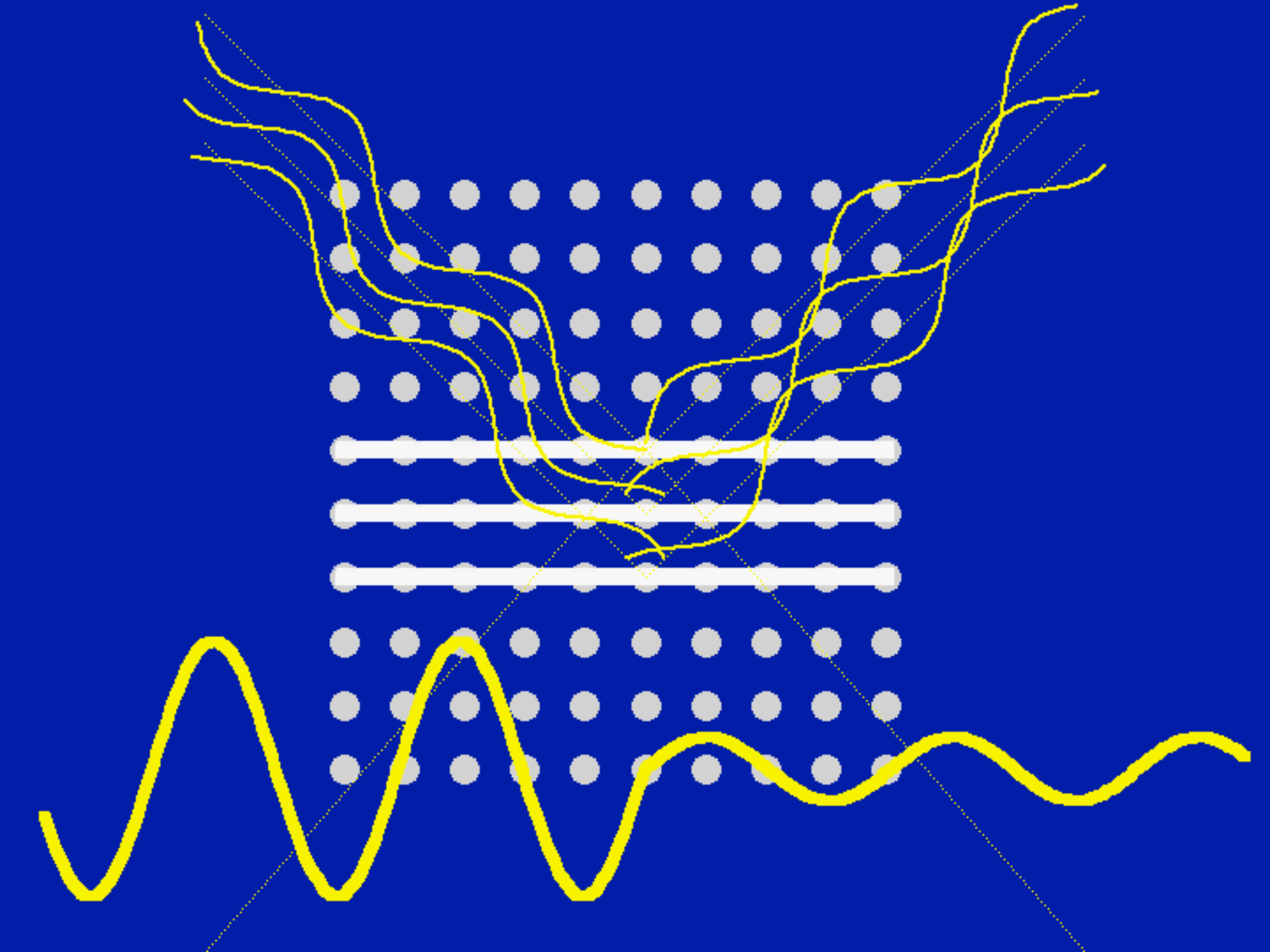

Bragg diffraction as specular reflection on semi-transparent mirrors of lattice planes

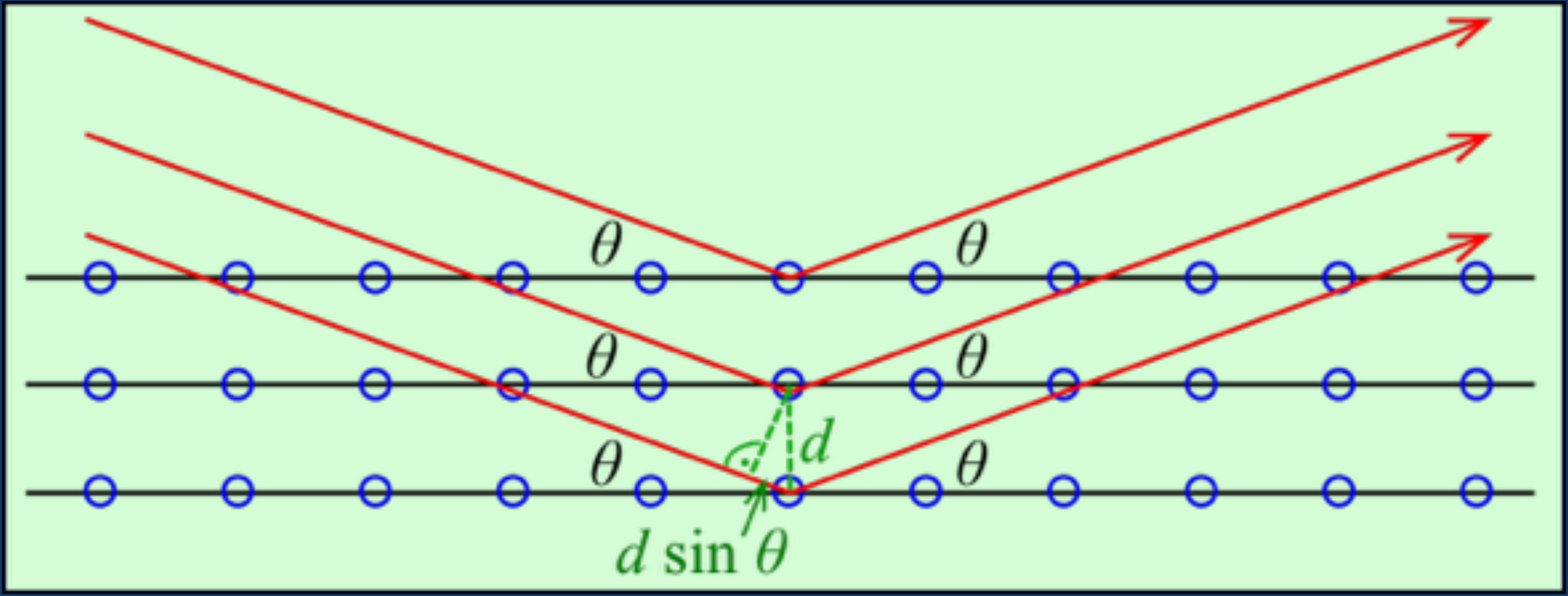

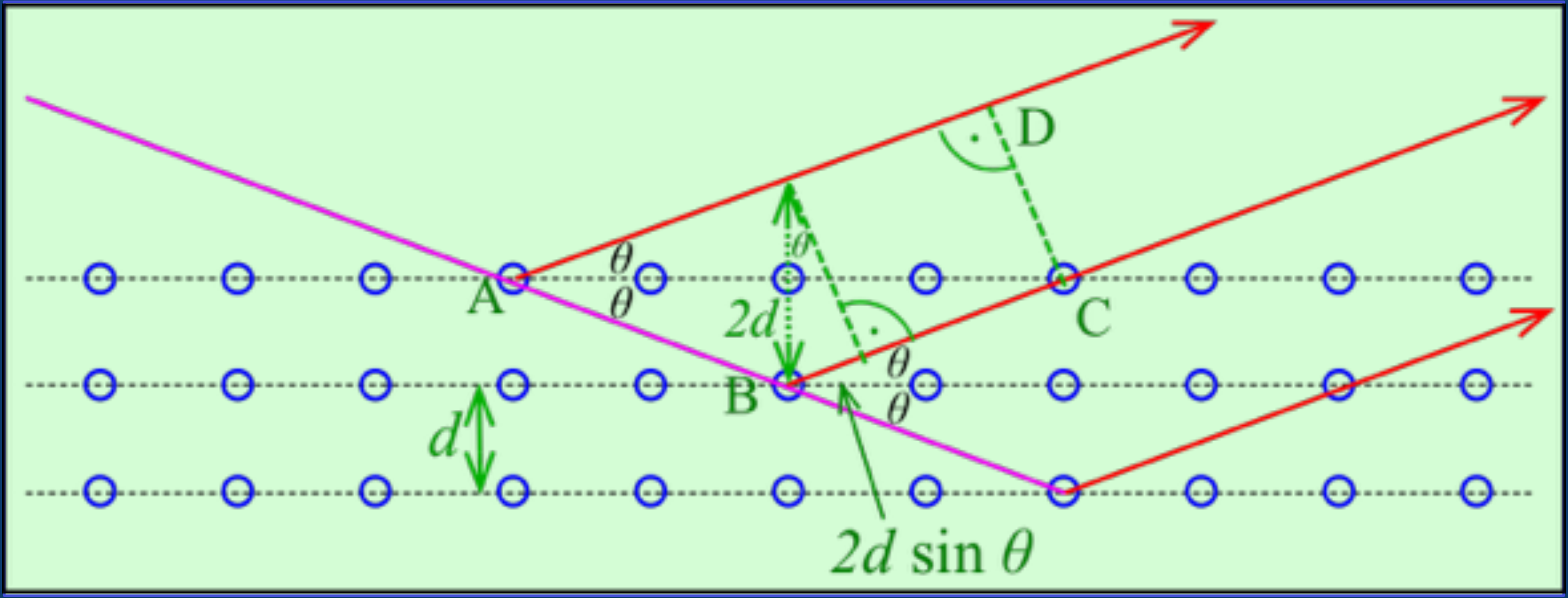

The Master Formula

- Possible changes in scattering experiments:
  - Sample state $\lambda_0 \to \lambda_1$, neutron spin $\sigma_0 \to \sigma_1$
- Differential cross section
  - W: number of transitions per second

$$\left(\frac{d\sigma}{d\Omega}\right)_{\mathbf{k}_0\sigma_0\lambda_0\to\mathbf{k}_1\sigma_1\lambda_1} = \frac{1}{N\Phi\Delta\Omega} W_{\mathbf{k}_0\sigma_0\lambda_0\to\mathbf{k}_1\sigma_1\lambda_1}$$

  - Fermi's Golden Rule
    - First order perturbation theory

$$W_{\mathbf{k}_0\sigma_0\lambda_0\to\mathbf{k}_1\sigma_1\lambda_1} = \frac{1}{h}\left|\langle\mathbf{k}_1\sigma_1\lambda_1|V|\mathbf{k}_0\sigma_0\lambda_0\rangle\right|^2 \rho_{\mathbf{k}_1\sigma_1}(E_1)$$

      - Valid for nuclear scattering: nuclear potential short-ranged
  - *V*: interaction potential, ρ: density of states
  - Wave function $V_0^{-1/2}e^{\mathbf{kr}}|\sigma>$ for sample volume V_0
    - Energy interval $dE_1 = (h/2\pi)^2 k_1 dk_1/m$

$$\rho_{\mathbf{k}_1\sigma_1}(E_1)\,dE_1 = \frac{V_0}{8\pi^3}d\mathbf{k}_1 = \frac{V_0}{8\pi^3}k_1^2\,dk_1\Delta\Omega$$

$$\rho_{\mathbf{k}_1\sigma_1}(E_1) = \frac{V_0}{2\pi}\frac{mk_1}{h^2}\Delta\Omega$$

  - Incident flux

$$\Phi = \frac{1}{V_0}v = \frac{hk_0}{2\pi V_0 m}$$

$$\left(\frac{d\sigma}{d\Omega}\right)_{\mathbf{k}_0\sigma_0\lambda_0\to\mathbf{k}_1\sigma_1\lambda_1} = \left(\frac{1}{N}\right)\frac{k_1}{k_0}\left(\frac{2\pi V_0 m}{h^2}\right)^2\left|\langle\mathbf{k}_1\sigma_1\lambda_1|V|\mathbf{k}_0\sigma_0\lambda_0\rangle\right|^2$$

The Master Formula (cont'd)

- Energy conservation condition as a δ function

$$\left(\frac{d\sigma}{d\Omega}\right)_{\mathbf{k}_0\sigma_0\lambda_0\to\mathbf{k}_1\sigma_1\lambda_1} = \left(\frac{1}{N}\right)\frac{k_1}{k_0}\left(\frac{2\pi V_0 m}{h^2}\right)^2 \left|\left\langle \mathbf{k}_1\sigma_1\lambda_1\right|V\left|\mathbf{k}_0\sigma_0\lambda_0\right\rangle\right|^2 \times \delta(E + E_{\lambda_0} + E_{\lambda_1})$$

- sum over all final states,
- average over initial states, occurring with probability *p*

$$\left(\frac{d^2\sigma}{d\Omega dE}\right)_{\mathbf{k}_0\to\mathbf{k}_1} = \left(\frac{1}{N}\right)\frac{k_1}{k_0}\left(\frac{2\pi V_0 m}{h^2}\right)\sum_{\lambda_0\sigma_0} p_{\lambda_0}p_{\sigma_0} \times \sum_{\lambda_1\sigma_1}\left|\left\langle \mathbf{k}_1\sigma_1\lambda_1\right|V\left|\mathbf{k}_0\sigma_0\lambda_0\right\rangle\right|^2 \delta(E + E_{\lambda_0} + E_{\lambda_1})$$

- "master-formula"
  - basis for the interpretation of all neutron scattering experiments

Nuclear scattering

$$\left(\frac{d^2\sigma}{d\Omega\, dE}\right)_{\mathbf{k}_0\to\mathbf{k}_1} = \left(\frac{1}{N}\right)\frac{k_1}{k_0}\left(\frac{2\pi V_0 m}{h^2}\right)\sum_{\lambda_0\sigma_0} p_{\lambda_0}p_{\sigma_0}\times\sum_{\lambda_1\sigma_1}\left|\langle \mathbf{k}_1\sigma_1\lambda_1|V|\mathbf{k}_0\sigma_0\lambda_0\rangle\right|^2\delta(E+E_{\lambda_0}+E_{\lambda_1})$$

- Nuclear potential range 3 orders of magnitude < wavelength
  - δ function: Fermi pseudo-potential: $$V = \frac{h^2}{2\pi m} b_{\sigma\lambda}\delta(\mathbf{r}-\mathbf{R})$$
  - *b* scattering length, **r** and **R** neutron and nucleus positions
- Interaction potential neutron-sample: sum over atoms in samples
- Average over neutron wave function: $$V(\mathbf{r}) = \frac{h^2}{2\pi m}\sum_i b_i\delta(\mathbf{r}-\mathbf{R}_i)$$
- Master formula ⇒

$$\langle \mathbf{k}_1|V|\mathbf{k}_0\rangle = \frac{h^2}{2\pi m}\sum_i b_i\int d\mathbf{r}\, e^{-i\mathbf{k}_1\cdot\mathbf{r}}\delta(\mathbf{r}-\mathbf{R}_i)e^{i\mathbf{k}_0\cdot\mathbf{r}} = \frac{h^2}{2\pi m}\sum_i b_i e^{i\mathbf{Q}\cdot\mathbf{R}_i}$$

- Unpolarised neutrons : $$\frac{d^2\sigma}{d\Omega\, dE} = \frac{1}{N}\frac{k_1}{k_0}\sum_{\lambda_0\sigma_0} p_{\lambda_0}p_{\sigma_0}\left|\sum_{\lambda_0\sigma_0}\sum_i b_i\langle\sigma_1\lambda_1|e^{i\mathbf{Q}\cdot\mathbf{R}_i}|\sigma_0\lambda_0\rangle\right|^2\delta(E+E_{\lambda_0}+E_{\lambda_1})$$

$$\frac{d^2\sigma}{d\Omega\, dE} = \frac{1}{N}\frac{k_1}{k_0}\sum_{\lambda_0} p_{\lambda_0}\left|\sum_{\lambda_0}\sum_i b_i\langle\lambda_1|e^{i\mathbf{Q}\cdot\mathbf{R}_i}|\lambda_0\rangle\right|^2\delta(E+E_{\lambda_0}+E_{\lambda_1})$$

Real time presentation

$$\frac{d^2\sigma}{d\Omega dE} = \frac{1}{N}\frac{k_1}{k_0}\sum_{\lambda_0} p_{\lambda_0}\left|\sum_{\lambda_0}\sum_{i} b_i \left\langle \lambda_1 \middle| e^{i\mathbf{Q}\cdot\mathbf{R}_i} \middle| \lambda_0 \right\rangle\right|^2 \delta(E + E_{\lambda_0} + E_{\lambda_1})$$

$$\delta\left(E + E_{\lambda_0} - E_{\lambda_1}\right) = \frac{1}{2\pi h}\int_{-\infty}^{\infty} \exp\left[-2\pi i\left(E + E_{\lambda_0} - E_{\lambda_1}\right)t/h\right]dt$$

$$\frac{d^2\sigma}{d\Omega dE} = \frac{1}{N}\frac{k_1}{k_0}\frac{1}{h}\sum_{\lambda_0} p_{\lambda_0}\sum_{\lambda_0}\sum_{ii'} b_i^* b_{i'}\int_{-\infty}^{\infty}\left\langle \lambda_0 \middle| e^{i\mathbf{Q}\cdot\mathbf{R}_i} \middle| \lambda_1 \right\rangle\left\langle \lambda_1 \middle| e^{2\pi iHt/h} e^{i\mathbf{Q}\cdot\mathbf{R}_{i'}} e^{-2\pi iHt/h} \middle| \lambda_0 \right\rangle e^{-2\pi iEt/h} dt \quad \text{with} \quad e^{2\pi iHt/h}\left|\lambda_{0,1}\right\rangle = e^{2\pi iE_{0,1}t/h}\left|\lambda_{0,1}\right\rangle$$

$$\frac{d^2\sigma}{d\Omega dE} = \frac{1}{N}\frac{k_1}{k_0}\frac{1}{h}\int_{-\infty}^{\infty}\sum_{ii'}\left\langle b_i^* b_{i'} e^{-i\mathbf{Q}\cdot\mathbf{R}_i} e^{2\pi iHt/h} e^{i\mathbf{Q}\cdot\mathbf{R}_{i'}} e^{-2\pi iHt/h}\right\rangle e^{-2\pi iEt/h} dt$$

Angular brackets: thermal average of expectation values of operator
Heisenberg time-dependent representation of the operators:

$$\frac{d^2\sigma}{d\Omega dE} = \frac{1}{N}\frac{k_1}{k_0}\frac{1}{h}\int_{-\infty}^{\infty}\sum_{ii'}\left\langle b_i^* b_{i'} e^{-i\mathbf{Q}\cdot\mathbf{R}_i(0)} e^{i\mathbf{Q}\cdot\mathbf{R}_{i'}(t)}\right\rangle e^{-2\pi iEt/h} dt$$

Decoupled nuclear parameters

$$\frac{d^2\sigma}{d\Omega dE}=\frac{1}{N}\frac{k_1}{k_0}\frac{1}{h}\int_{-\infty}^{\infty}\sum_{ii'}\left\langle b_i^* b_{i'} e^{-i\mathbf{Q}\cdot\mathbf{R}_i(0)} e^{i\mathbf{Q}\cdot\mathbf{R}_{i'}(t)}\right\rangle e^{-2\pi iEt/h}dt$$

Nuclear spins and isotopes ($\Delta A/A$) randomly distributed,
Scattering without nuclear states, only in terms of atomic coordinates

$$\frac{d^2\sigma}{d\Omega dE}=\frac{1}{N}\frac{k_1}{k_0}\frac{1}{h}\int_{-\infty}^{\infty}\sum_{dd'}\sum_{i\in d,i'\in d'}\overline{b_i^* b_{i'}}\left\langle e^{-i\mathbf{Q}\cdot\mathbf{R}_i(0)} e^{i\mathbf{Q}\cdot\mathbf{R}_{i'}(t)}\right\rangle e^{-2\pi iEt/h}dt$$

Coherent and incoherent scattering

$$\frac{d^2\sigma}{d\Omega dE} = \frac{1}{N}\frac{k_1}{k_0}\frac{1}{h}\int_{-\infty}^{\infty}\sum_{dd'}\sum_{i\in d, i'\in d'}\overline{b_i^* b_{i'}}\left\langle e^{-i\mathbf{Q}\cdot\mathbf{R}_i(0)} e^{i\mathbf{Q}\cdot\mathbf{R}_{i'}(t)}\right\rangle e^{-2\pi i E t/h}dt$$

$$S_{ii'}\left(\mathbf{Q},E\right) = \frac{1}{h}\int_{-\infty}^{\infty}\left\langle e^{-i\mathbf{Q}\cdot\mathbf{R}_i(0)} e^{i\mathbf{Q}\cdot\mathbf{R}_{i'}(t)}\right\rangle e^{-2\pi i E t/h}dt$$

Scattering function

$$\frac{d^2\sigma}{d\Omega dE} = \frac{1}{N}\frac{k_1}{k_0}\sum_{dd'}\sum_{i\in d, i'\in d'}\overline{b_i^* b_{i'}} S_{ii'}$$

$$\overline{b_i^* b_{i'}} = \begin{cases} \overline{b_d^*}\,\overline{b_{d'}} & : i \neq i' \\ \left|\overline{b_d^2}\right| & : i = i' \end{cases} = \overline{b_d^*}\,\overline{b_{d'}} + \left(\left|\overline{b_d^2}\right| - \left|\overline{b_d}\right|^2\right)\delta_{ii'}\delta_{dd'}$$

(Uncorrelated spins and isotopes)

$$\frac{d^2\sigma}{d\Omega dE} = \frac{1}{N}\frac{k_1}{k_0}\sum_{dd'}\sum_{i\in d, i'\in d'}\left[\overline{b_d^*}\,\overline{b_d} + \left(\left|\overline{b_d^2}\right| - \left|\overline{b_d}\right|^2\right)\delta_{ii'}\delta_{dd'}\right]S_{ii'} = \frac{1}{N}\frac{k_1}{k_0}\sum_{dd'}\overline{b_d^*}\,\overline{b_{d'}}\sum_{i\in d, i'\in d'}S_{ii'} + \frac{1}{N}\frac{k_1}{k_0}\sum_{d}\left(\left|\overline{b_d^2}\right| - \left|\overline{b_d}\right|^2\right)\sum_{i\in d}S_{ii}$$

Coherent Incoherent
scattering cross section

$$\sigma_{coh}^d \equiv 4\pi\left|\overline{b_d}\right|^2$$

$$\sigma_{inc}^d \equiv 4\pi\left[\left|\overline{b_d^2}\right| - \left|\overline{b_d}\right|^2\right]$$

$$\sigma_s^d \equiv 4\pi\left|\overline{b_d^2}\right|$$

$$\frac{d^2\sigma}{d\Omega dE} = \frac{1}{N}\frac{k_1}{k_0}\sum_{dd'}\overline{b_d^*}\,\overline{b_{d'}}\sum_{i\in d, i'\in d'}S_{ii'} + \frac{1}{N}\frac{k_1}{k_0}\sum_{d}\frac{\sigma_{inc}^d}{4\pi}\sum_{i\in d}S_{ii}$$

Single element

$$\sigma_{coh}^d = 4\pi\left\{\sum_a \frac{c_a}{2I_a+1}\left[\left(I_a+1\right)b_a^+ + I_a b_a^-\right]\right\}^2$$

$$\sigma_s^d = 4\pi\sum_a \frac{c_a}{2I_a+1}\left[\left(I_a+1\right)\left(b_a^+\right)^2 + I_a\left(b_a^-\right)^2\right]$$

$$\sigma_{inc}^d = \sigma_s^d - \sigma_{coh}^d$$

isotopes *a* with abundance c_a and nuclear spin I_a

Coherent & incoherent scattering functions

Scattering function $S_{ii'}\left(\mathbf{Q},E\right)=\frac{1}{h}\int_{-\infty}^{\infty}\left\langle e^{-i\mathbf{Q}\cdot\mathbf{R}_{i}(0)}e^{i\mathbf{Q}\cdot\mathbf{R}_{i'}(t)}\right\rangle e^{-2\pi iEt/h}dt$

$$S_{coh}^{dd'}\left(\mathbf{Q},E\right)\equiv\frac{1}{\sqrt{N_dN_{d'}}}\sum_{i\in d,i'\in d'}S_{ii'}=\frac{1}{\sqrt{N_dN_{d'}}}\frac{1}{h}\sum_{i\in d,i'\in d'}\int_{-\infty}^{\infty}\left\langle e^{-i\mathbf{Q}\cdot\mathbf{R}_{i}(0)}e^{i\mathbf{Q}\cdot\mathbf{R}_{i'}(t)}\right\rangle e^{-2\pi iEt/h}dt$$

$$S_{inc}^{dd'}\left(\mathbf{Q},E\right)\equiv\frac{1}{N_d}\sum_{i\in d}S_{ii}=\frac{1}{N_d}\frac{1}{h}\sum_{i\in d}\int_{-\infty}^{\infty}\left\langle e^{-i\mathbf{Q}\cdot\mathbf{R}_{i}(0)}e^{i\mathbf{Q}\cdot\mathbf{R}_{i}(t)}\right\rangle e^{-2\pi iEt/h}dt$$

$$\frac{d^2\sigma}{d\Omega dE}=\frac{k_1}{k_0}\sum_{dd'}c_d^{\frac{1}{2}}c_{d'}^{\frac{1}{2}}\overline{b_d^*}\,\overline{b_{d'}}S_{coh}^{dd'}\left(\mathbf{Q},E\right)+\frac{k_1}{k_0}\sum_{d}c_d\frac{\sigma_{inc}^{d}}{4\pi}S_{inc}^{dd'}\left(\mathbf{Q},E\right)$$

Total intermediate and self intermediate scattering functions

$$I_{tot}^{dd'}\left(\mathbf{Q},E\right)\equiv\frac{1}{\sqrt{N_dN_{d'}}}\sum_{i\in d,i'\in d'}\left\langle e^{-i\mathbf{Q}\cdot\mathbf{R}_{i}(0)}e^{i\mathbf{Q}\cdot\mathbf{R}_{i'}(t)}\right\rangle$$

$$I_{inc}^{dd'}\left(\mathbf{Q},E\right)\equiv\frac{1}{N_d}\sum_{i\in d}\left\langle e^{-i\mathbf{Q}\cdot\mathbf{R}_{i}(0)}e^{i\mathbf{Q}\cdot\mathbf{R}_{i}(t)}\right\rangle$$

Normal modes

Scattering function

$$S_{ii'}\left(\mathbf{Q},E\right)=\frac{1}{h}\int_{-\infty}^{\infty}\left\langle e^{-i\mathbf{Q}\cdot\mathbf{R}_i(0)}e^{i\mathbf{Q}\cdot\mathbf{R}_{i'}(t)}\right\rangle e^{-2\pi iEt/h}dt$$

Solid: Each atom well defined, fixed equilibrium position

$$S_{coh}^{dd'}\left(\mathbf{Q},E\right)=\frac{1}{N}\frac{1}{h}\sum_{i,i'}\int_{-\infty}^{\infty}\left\langle e^{-i\mathbf{Q}\cdot\mathbf{u}_i(0)}e^{i\mathbf{Q}\cdot\mathbf{u}_{i'}(t)}\right\rangle e^{i\mathbf{Q}\cdot(\mathbf{i}'-\mathbf{i})}e^{-2\pi iEt/h}dt$$

Instantaneous displacement from equilibrium site

$$S_{inc}^{dd'}\left(\mathbf{Q},E\right)=\frac{1}{N}\frac{1}{h}\sum_{i}\int_{-\infty}^{\infty}\left\langle e^{-i\mathbf{Q}\cdot\mathbf{u}_i(0)}e^{i\mathbf{Q}\cdot\mathbf{u}_i(t)}\right\rangle e^{-2\pi iEt/h}dt$$

$$\mathbf{u}_i(t)=\sum_j\left(\frac{h}{4\pi M_i\omega_j}\right)^{\frac{1}{2}}\left[\mathbf{e}_i^j e^{-i\omega_j t}a_j+\mathbf{e}_i^{j*}e^{-i\omega_j t}a_j^+\right]$$

Harmonic forces:

linear function of displacement,

3*N* normal modes

quantum mechanical operators *a*:

annihilation and creation of energy quantum

mode frequency ω, polarisation vector **e**

$$\mathbf{D}_{ii'}=\frac{1}{\left(M_iM_{i'}\right)^{\frac{1}{2}}}\Phi_{ii'}$$

mode frequency ω, polarisation vector **e**:

Eigenvalues/-vectors of dynamical matrix **D**

Force constants Φ

$$U-U_0=\frac{1}{2}\mathbf{u}_i\Phi_{ii'}\mathbf{u}_{i'}$$

Evaluation of scattering functions

$$S_{coh}^{dd'}\left(\mathbf{Q},E\right)=\frac{1}{N}\frac{1}{h}\sum_{i,i'}\int_{-\infty}^{\infty}\left\langle e^{-i\mathbf{Q}\cdot\mathbf{u}_i(0)}e^{i\mathbf{Q}\cdot\mathbf{u}_{i'}(t)}\right\rangle e^{i\mathbf{Q}\cdot(\mathbf{i}'-\mathbf{i})}e^{-2\pi iEt/h}dt$$

$$S_{inc}^{dd'}\left(\mathbf{Q},E\right)=\frac{1}{N}\frac{1}{h}\sum_{i}\int_{-\infty}^{\infty}\left\langle e^{-i\mathbf{Q}\cdot\mathbf{u}_i(0)}e^{i\mathbf{Q}\cdot\mathbf{u}_{i}(t)}\right\rangle e^{-2\pi iEt/h}dt$$

$$\left\langle e^{-i\mathbf{Q}\cdot\mathbf{u}_i(0)}e^{i\mathbf{Q}\cdot\mathbf{u}_{i'}(t)}\right\rangle = e^{-\left[W_i\left(\mathbf{Q}\right)+W_{i'}\left(\mathbf{Q}\right)\right]}e^{\left\langle \mathbf{Q}\cdot\mathbf{u}_i(0)\mathbf{Q}\cdot\mathbf{u}_{i'}(t)\right\rangle}$$

harmonic oscillator

$$e^{-W_i\left(\mathbf{Q}\right)} = e^{-\frac{1}{2}\left\langle\left[\mathbf{Q}\cdot\mathbf{u}_i(0)\right]^2\right\rangle}$$

Debye-Waller factor

$$T_j = \exp(-B_j\frac{\sin^2\theta}{\lambda^2})$$

$$W_i(Q)=\frac{h}{6\pi M_i}\sum_j\frac{\left|Qe_i^j\right|^2}{\omega_j}\left\langle 2n_j+1\right\rangle$$

$$\left\langle n_j\right\rangle=\frac{1}{e^{\frac{h\omega_j}{2\pi k_B T}}-1}$$

population factor

Elastic scattering

$$S_{coh}^{dd'}(\mathbf{Q},E)=\frac{1}{N}\frac{1}{h}\sum_{i,i'}\int_{-\infty}^{\infty}\left\langle e^{-i\mathbf{Q}\cdot\mathbf{u}_i(0)}e^{i\mathbf{Q}\cdot\mathbf{u}_{i'}(t)}\right\rangle e^{i\mathbf{Q}\cdot(\mathbf{i}'-\mathbf{i})}e^{-2\pi iEt/}dt$$

$$S_{inc}^{dd'}(\mathbf{Q},E)=\frac{1}{N}\frac{1}{h}\sum_{i}\int_{-\infty}^{\infty}\left\langle e^{-i\mathbf{Q}\cdot\mathbf{u}_i(0)}e^{i\mathbf{Q}\cdot\mathbf{u}_i(t)}\right\rangle e^{-2\pi iEt/h}dt$$

$$S_{c\,el}(\mathbf{Q},E)=\frac{1}{N}\frac{1}{h}\sum_{i,i'}\int_{-\infty}^{\infty}e^{-[\mathrm{W}_i(\mathbf{Q})+\mathrm{W}_{i'}(\mathbf{Q})]}e^{i\mathbf{Q}\cdot(\mathbf{i}'-\mathbf{i})}e^{-2\pi iEt/h}dt=\frac{1}{N}\sum_{i,i'}e^{-[\mathrm{W}_i(\mathbf{Q})+\mathrm{W}_{i'}(\mathbf{Q})]}e^{i\mathbf{Q}\cdot(\mathbf{i}'-\mathbf{i})}\delta(E)$$

$$S_{el}(\mathbf{Q})=\frac{1}{N}\sum_{i,i'}e^{-[\mathrm{W}_i(\mathbf{Q})+\mathrm{W}_{i'}(\mathbf{Q})]}e^{i\mathbf{Q}\cdot(\mathbf{i}'-\mathbf{i})}$$

elastic structure factor

$$S_{i,el}(\mathbf{Q},E)=\frac{1}{N}\sum_{i}e^{-2\mathrm{W}_i(\mathbf{Q})}\delta(E) \qquad \int S_{i,el}(\mathbf{Q},E)\,dE=\frac{1}{N}\sum_{i}e^{-2\mathrm{W}_i(\mathbf{Q})}$$

average Debye-Waller

$$S_{el}^{dd'}(\mathbf{Q})=\frac{(2\pi)^3}{v_0}e^{-[\mathrm{W}_d(\mathbf{Q})+\mathrm{W}_{d'}(\mathbf{Q})]}e^{i\mathbf{Q}\cdot(\mathbf{d}'-\mathbf{d})}\sum_{\boldsymbol{\tau}}\delta(\mathbf{Q}-\boldsymbol{\tau})$$

long-range order **i=l+d**
crystal lattice made up by **l**
reciprocal lattice vectors τ
Bragg peaks if **Q**=τ

$$\boxed{\left(\frac{d\sigma}{d\Omega}\right)_{c,el}=\frac{2\pi}{v_0}\sum_{\boldsymbol{\tau}}\left|F(\boldsymbol{\tau})\right|^2\delta(\mathbf{Q}-\boldsymbol{\tau})}$$

elastic coherent scattering cross section
unit-cell *structure factor* F(τ)

$$\boxed{F(\boldsymbol{\tau})=\sum_{d}\overline{b_d}e^{-W_d(\boldsymbol{\tau})}e^{i\boldsymbol{\tau}\cdot\mathbf{d}}}$$

$$\left(\frac{d\sigma}{d\Omega}\right)_{i,el}=\sum_{d}c_d\sigma_i^d e^{-2W_d(\mathbf{Q})}$$

Neutron diffraction from crystals

- *In which direction does scattering occur?*
  - Interference and Ewald sphere
    - Reciprocal lattice
- *How strong is the scattering in a given direction?*
  - Structure factor
    - Phase problem
    - Debye-Waller factor
    - coherent scattering length
- *How realistic are perfectly imperfect crystals?*
  - Kinematical and dynamical diffraction theory
  - *How can we get the intensities right?*
    - Corrections to be made: Extinction
- How to properly measure intensities
  - Experimental aspects of single crystal diffraction

Crystal lattice

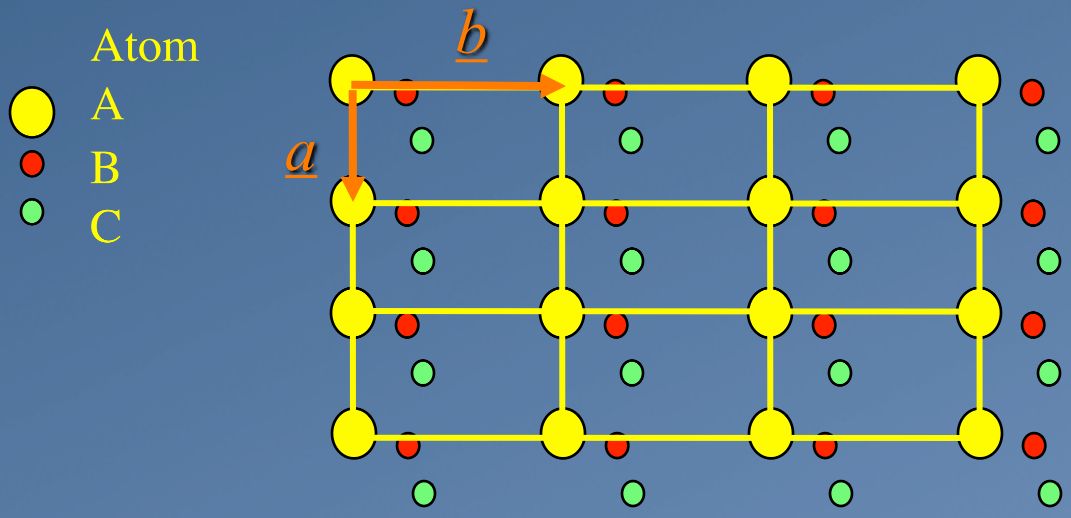

Structure

=

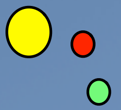

Base

+

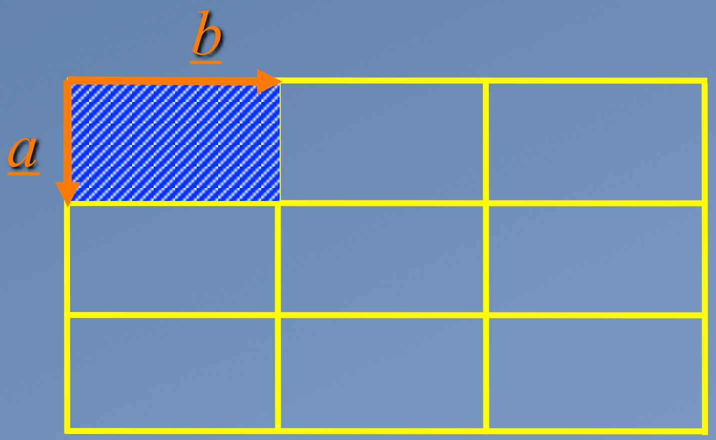

Lattice

Base vectors a, b, c set up the ***unit cell*** *of the lattice*

Crystal lattice planes

Miller indices (hkl):

smallest possible integer multiples of *reciprocal* lattice intersections

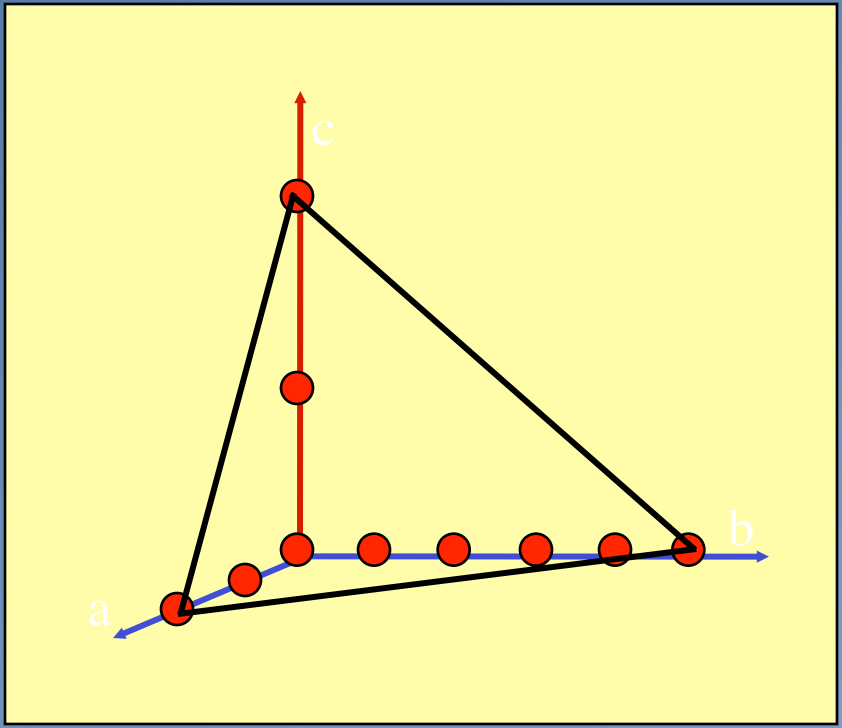

Here: (525)

Crystal lattice planes

Miller indices (hkl) not only tell the position of *one* lattice plane but of the infinite array of all parallel planes

Lattice planes of higher indices have smaller distances to each other

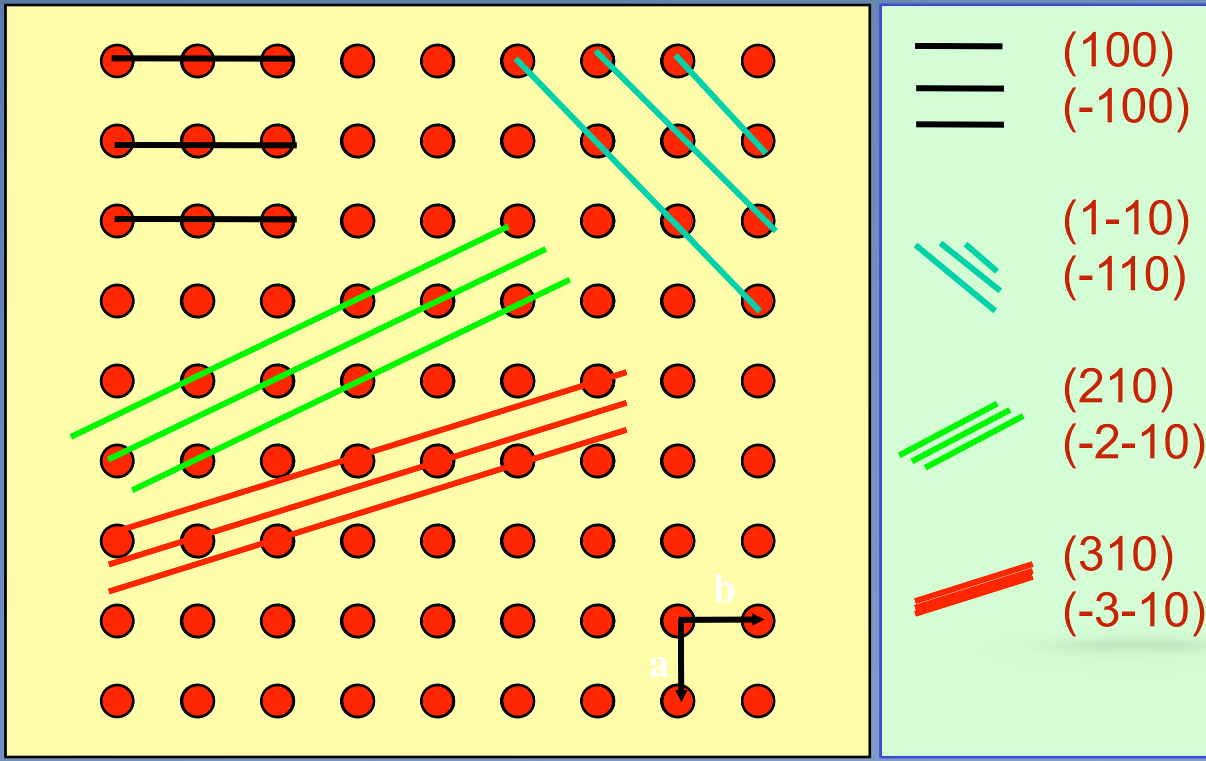

Reciprocal lattice

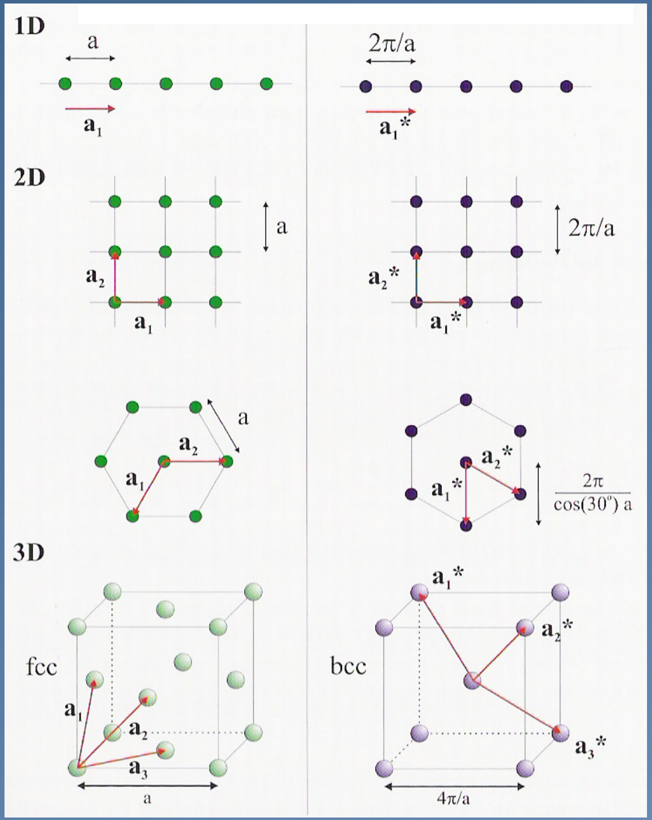

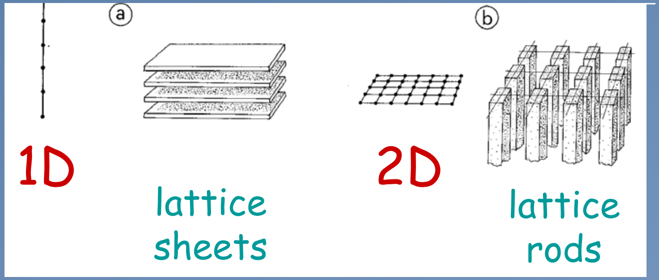

- The 3D reciprocal lattice with the basis **a***, **b*** and **c*** is the *Fourier transform* of a 3D direct lattice with the basis vectors **a**, **b**, **c**.
  - 2D example: (102) lattice planes and corresponding reciprocal lattice point 102, direct lattice grey, reciprocal lattice black. The reciprocal lattice vector **G** is $\perp$ to the planes (102). NB: **a*** is $\perp$ **c** (and **b**) and its permutations

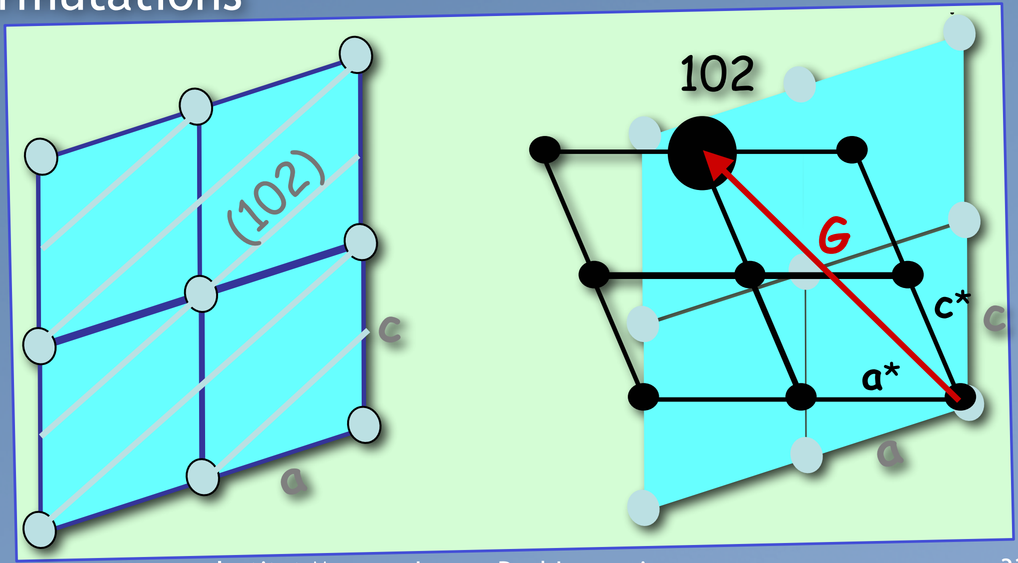

Elastic scattering geometry

- Incident radiation
  - Wave vector $\mathbf{k}_0$ $|\mathbf{k}_0|=2\pi/\lambda$
- Scattered radiation
  - Wave vector $\mathbf{k}$, $|\mathbf{k}|=2\pi/\lambda$
- Wavevector transfer
  - $\mathbf{Q} = \mathbf{k} - \mathbf{k}_0$ or $\mathbf{k} = \mathbf{k}_0 + \mathbf{Q}$
  - Scattering angle 2θ

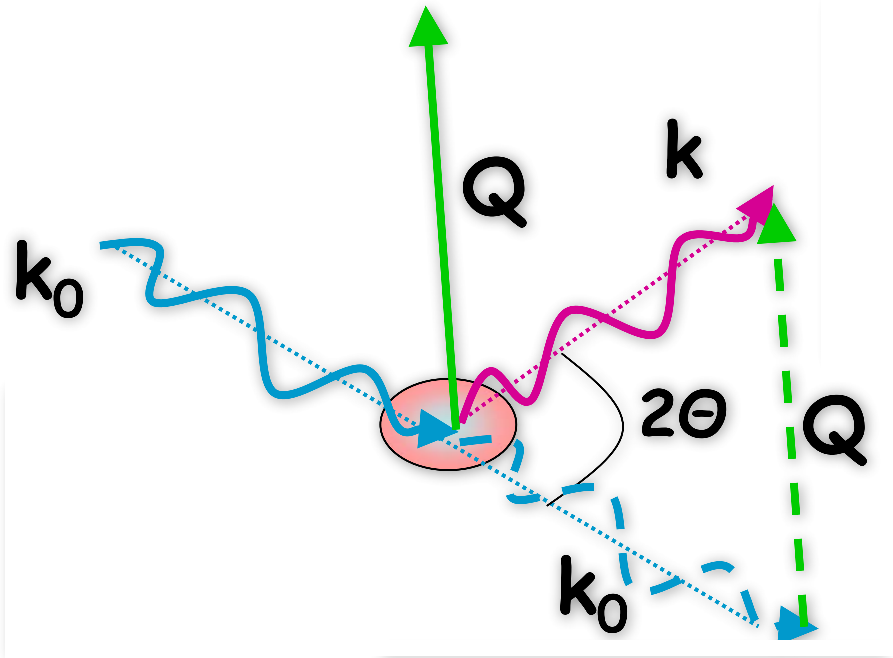

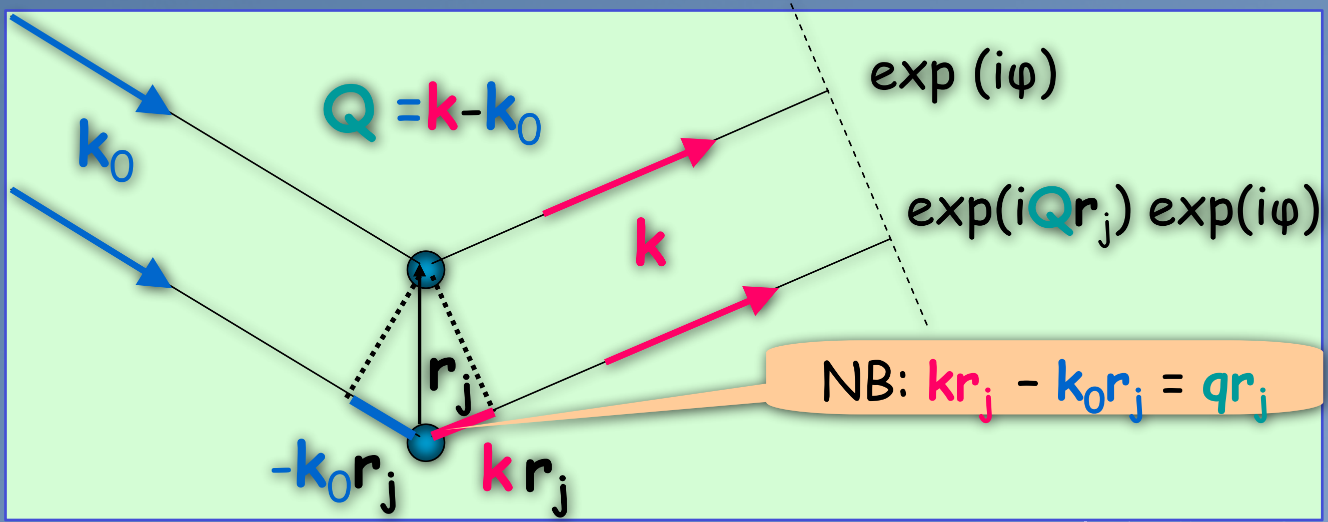

$F(\mathbf{Q}) = f \sum b_j[\exp(i\,\mathbf{Q}\,\mathbf{r}_j)]$

Sharp scattering condition

- **k a** = **k**$_0$ **a**: constructive interference
- With **Q** = 2π **h** (**h**: Miller indices hkl)
  - **Q** = **k** - **k**$_0$: F(**h**)=f ∑[exp(2π *i* **h a**)]

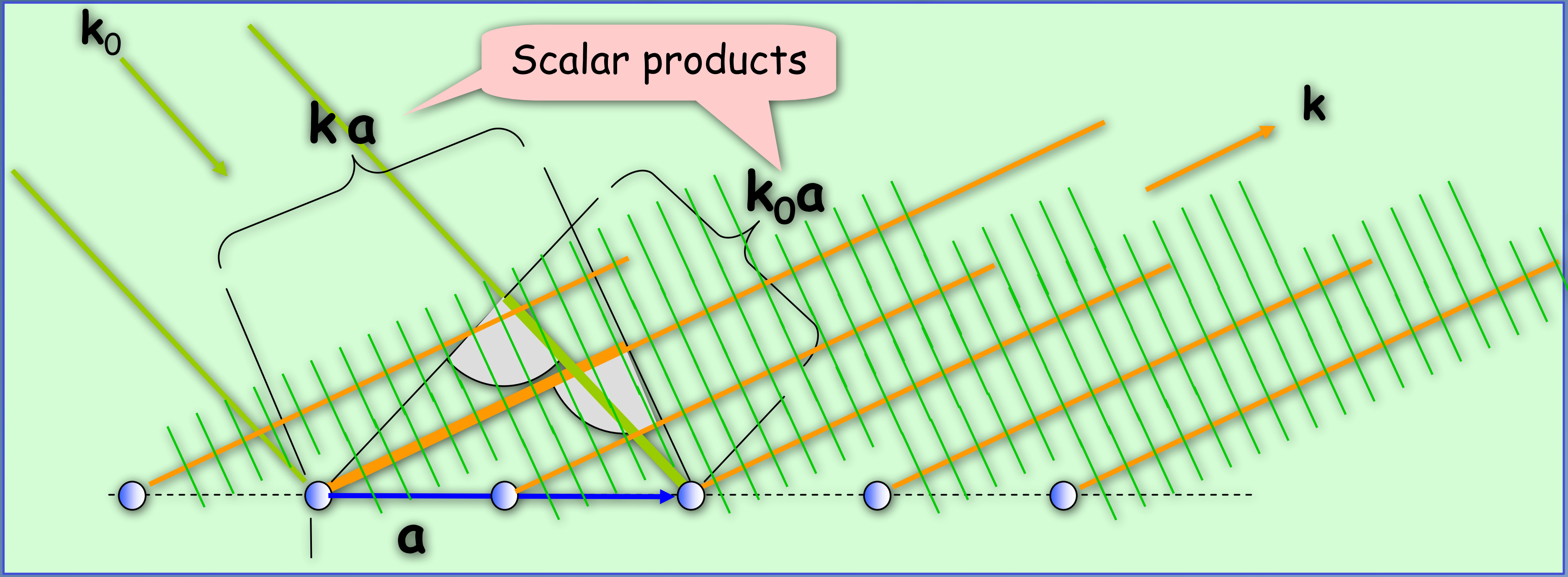

- For a given **k**$_0$ and 1D lattice vector **a**, scattering occurs only in very specific directions **k**!

Ewald construction

- Reciprocal space: Diffraction occurs when $\mathbf{k_0}$, $\mathbf{k}$ and $\mathbf{h}$ are coplanar and $\mathbf{Q}=2\pi\mathbf{h}$ ends in the Ewald sphere
  - $|\mathbf{k_0}|=|\mathbf{k}|=2\pi/\lambda$ and $|\mathbf{h}|=1/d_{hkl}$
  - The Ewald sphere is in experimental reality rather a *shell* with a finite thickness due to the fact that perfect monochromaticity does not exist

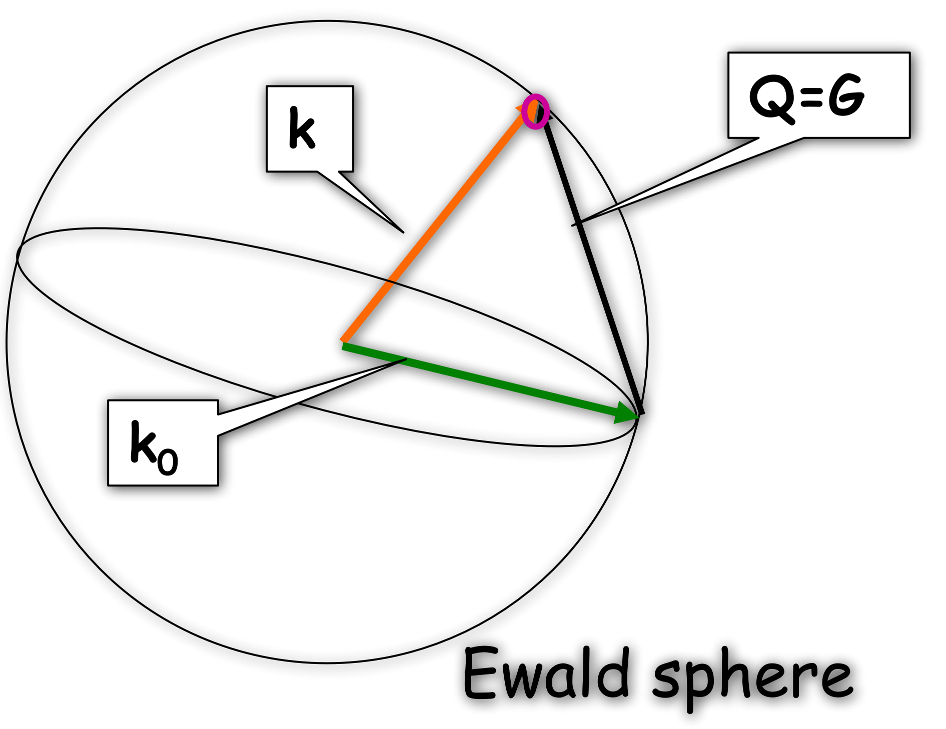

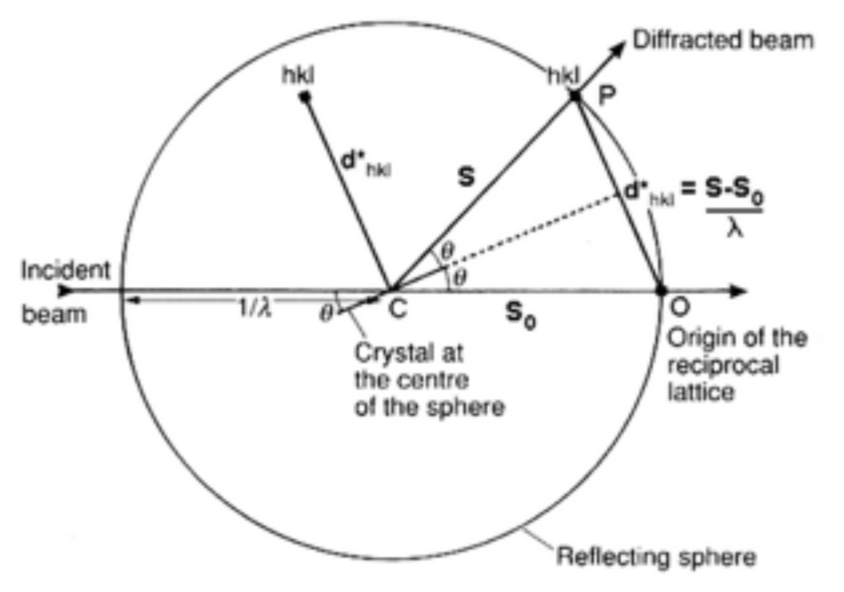

Ewald construction

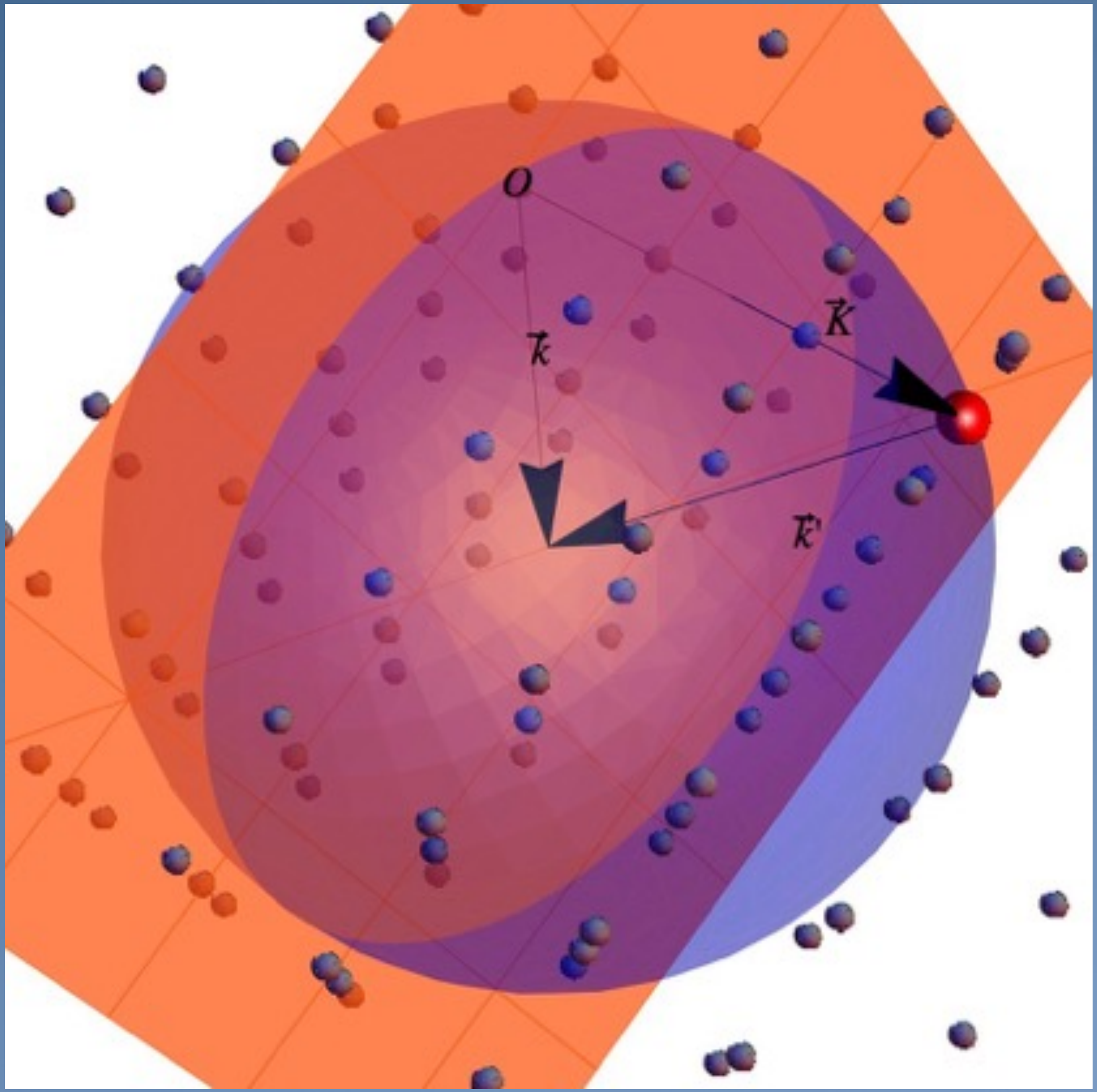

- Bragg plane
  - In reciprocal space, for a diffraction peak of a crystal to occur, the tip of a wave vector has to lie on one of the Bragg planes, which are perpendicularly bisecting the lines from the origin of the reciprocal space to the reciprocal lattice points

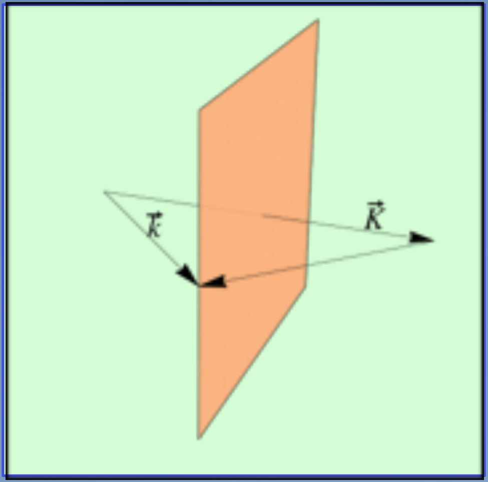

Ewald construction

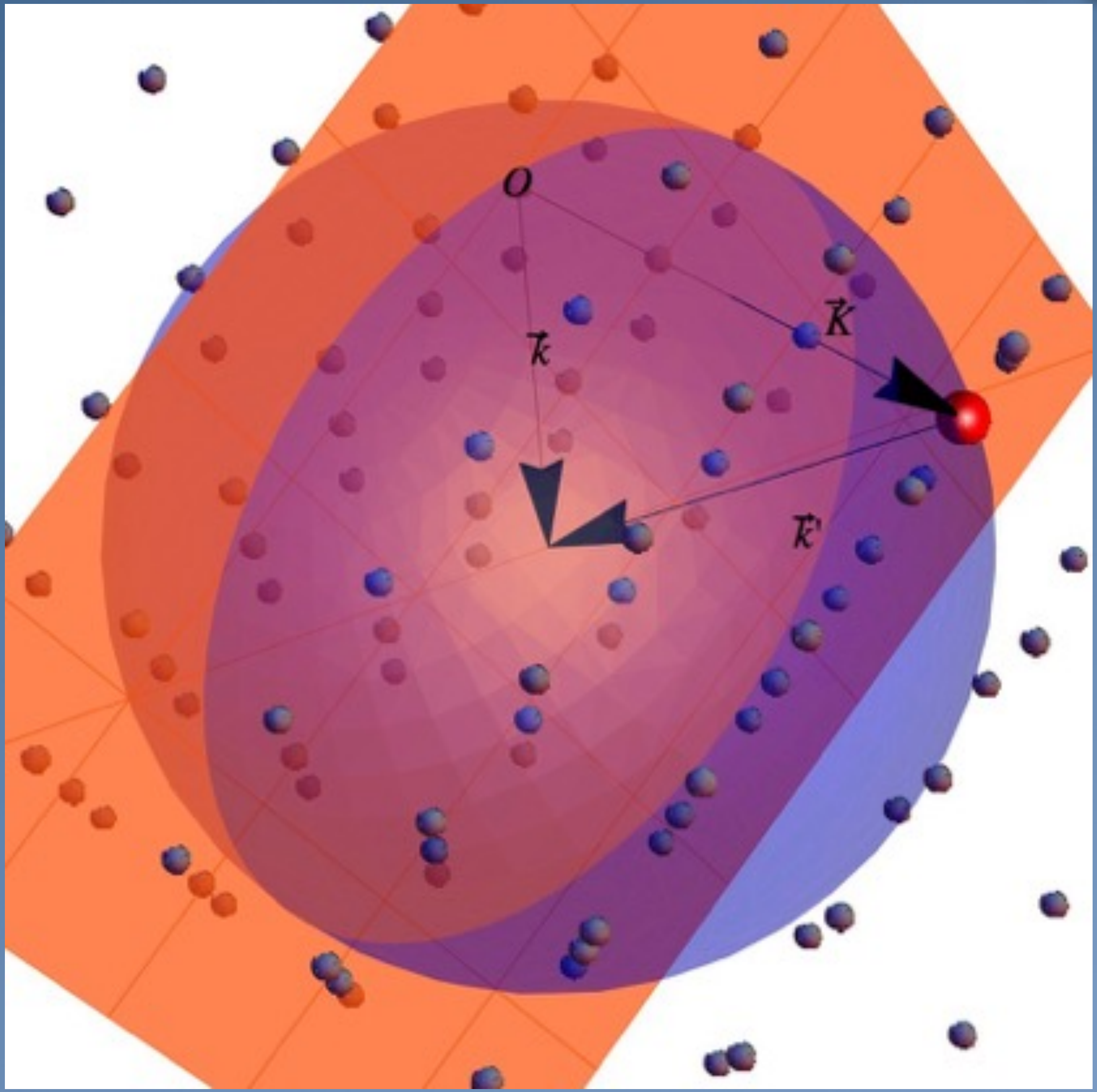

- Bragg plane
  - In reciprocal space, for a diffraction peak of a crystal to occur, the tip of a wave vector has to lie on one of the Bragg planes, which are perpendicularly bisecting the lines from the origin of the reciprocal space to the reciprocal lattice points

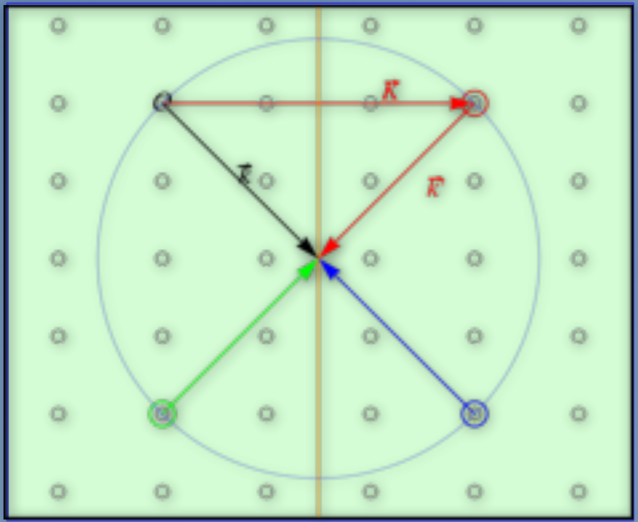

Ewald construction

- Rotating crystal
  - The rotation axis is perpendicular to the plane. The red circles are the orbits swept out by the reciprocal lattice vectors. Each intersection with the Ewald circle represents a Bragg peak

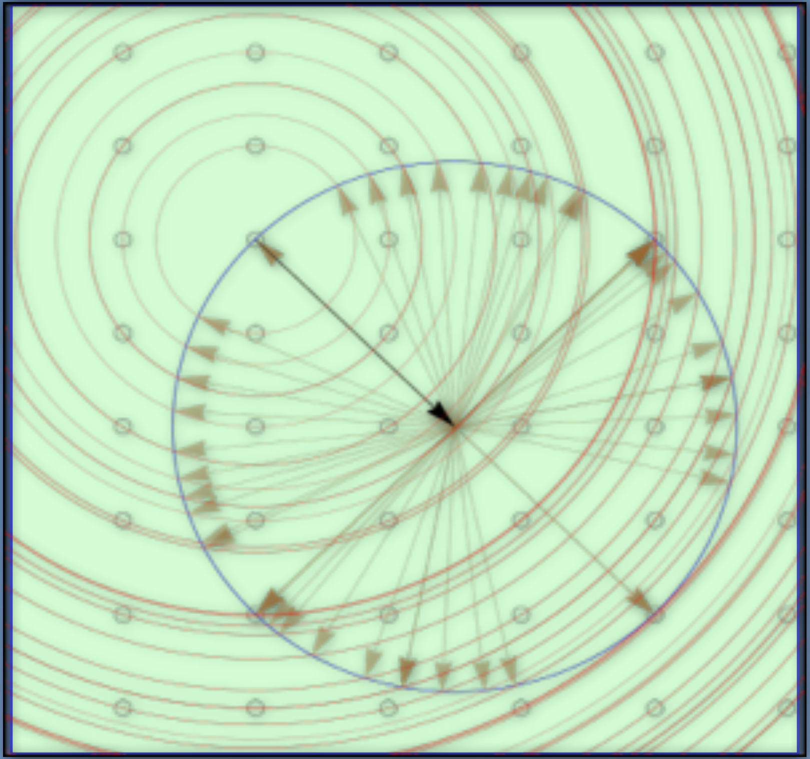

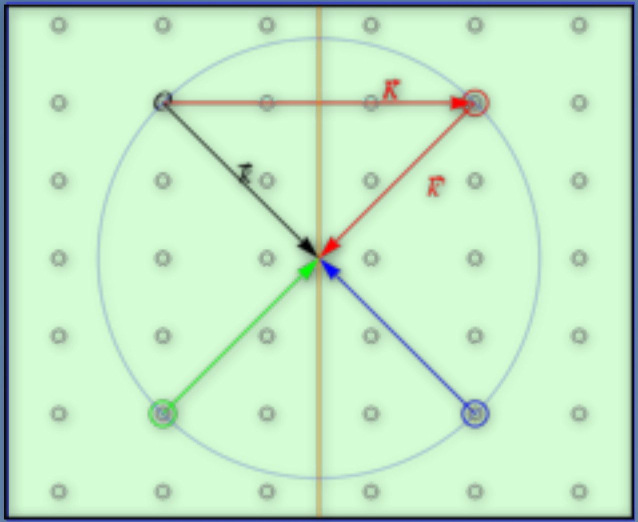

Ewald construction

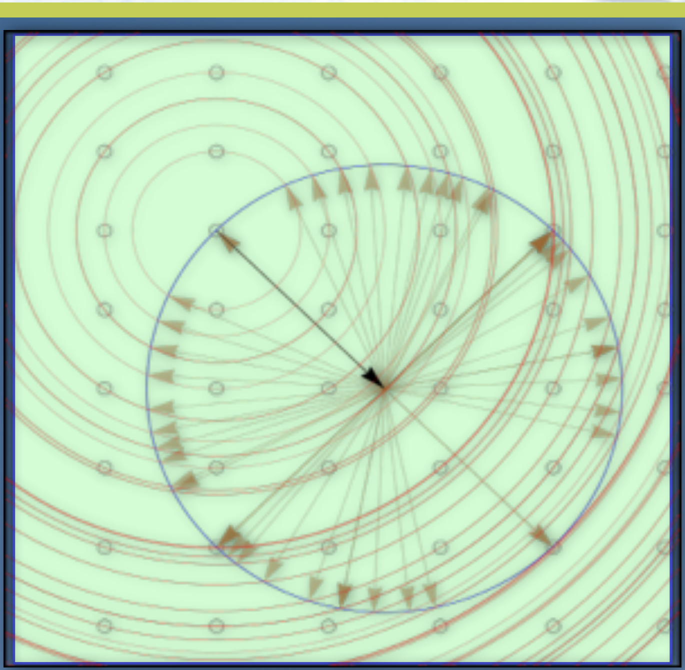

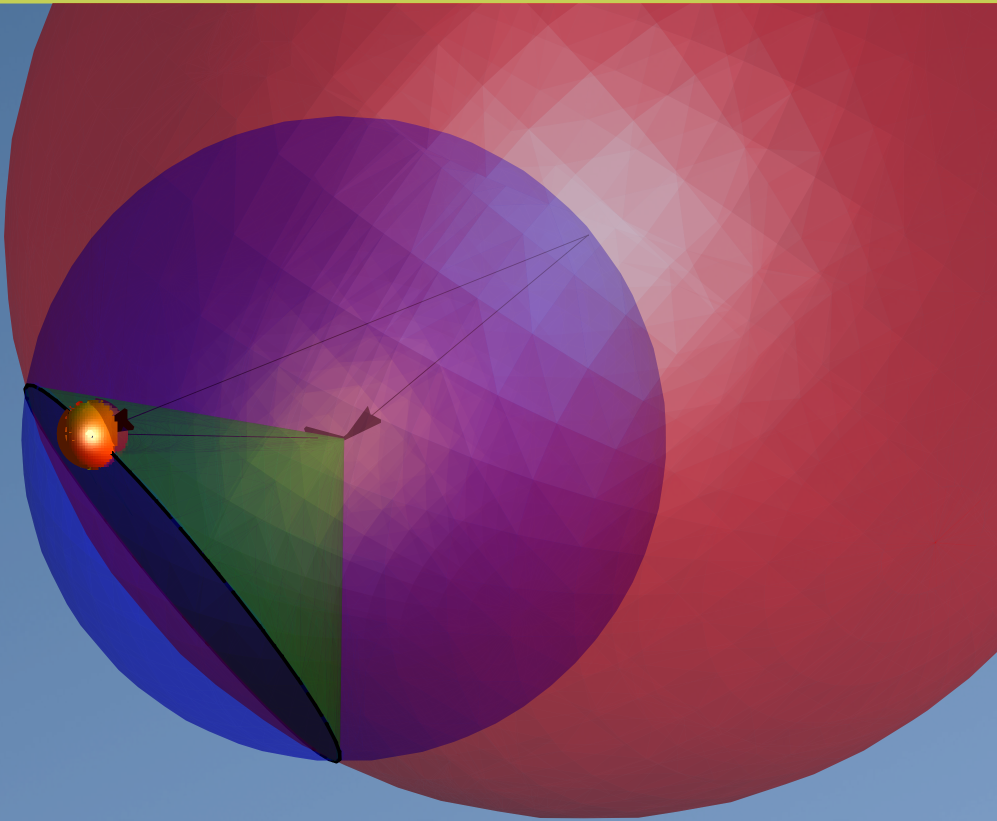

- Debye-Scherrer (powder)
  - The Ewald sphere intersects a sphere centred at the origin with a radius of K for each lattice vector with K < 2k. Bragg peaks will appear for any wave vector connecting any point on the intersection circle with the tip of the incident wave vector. For each lattice vector the scattered rays therefore lie on a so-called Debye-Scherrer cone.

Bragg's law and Laue conditions

- The Fourier transform of a 3D array of δ functions is the reciprocal lattice $G_{hkl}(\mathbf{q})$ with integer h,k,l (Miller indices).
- Laue-condition: Interference only occurs when **Q=G**
  - Geometrically equivalent to Bragg condition

Bragg: $n\lambda = 2d_{hkl} \sin\theta$ Laue: $\mathbf{Q} = \mathbf{G}_{hkl}$

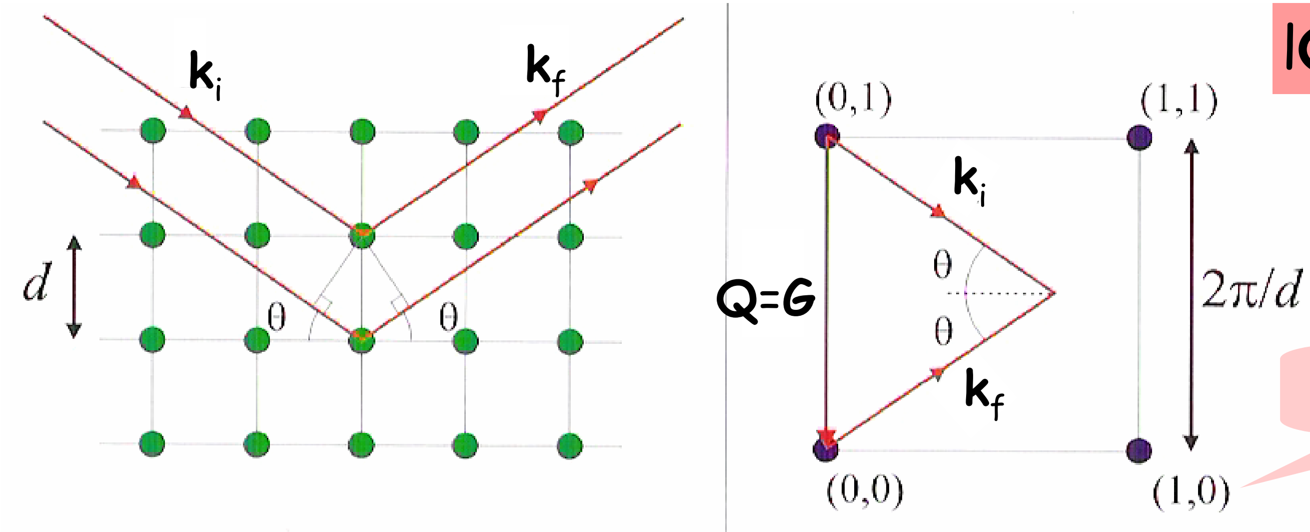

$|Q| = 4\pi \sin\Theta/\lambda$

or

$|Q| = 2\pi/d_{hkl}$

Miller indices

Structure factor

- The structure factor is the Fourier transform of the scattering density distribution of the unit cell:
  - $F(\mathbf{G})=\Sigma[b_j\cdot\exp(i\cdot\mathbf{G}\cdot\mathbf{x}_j)]$ or $F_{hkl}=\Sigma[b_j\cdot\exp[2\pi\cdot i\cdot(hx+ky+lz)]]$
  - The scalar product $\mathbf{Gx}_j$ is given as hx+hy+hz with the Miller indices hkl and the fractional atomic coordinates xyz of an atom j in the unit cell of a crystal structure; it contains the information on the phase angle
- Structure factor in complex plane
  - Each scatterer contributes with a different phase. The structure factor results from adding the individual contributions.
  - The result can be real for centroysmmetric arrangements (for each atom at ***x*** there is an equivalent one at **-*x***), phase angles φ are either 0º or 180º (structure factor positive or negative)
  - For acentric materials the result has an imaginary component

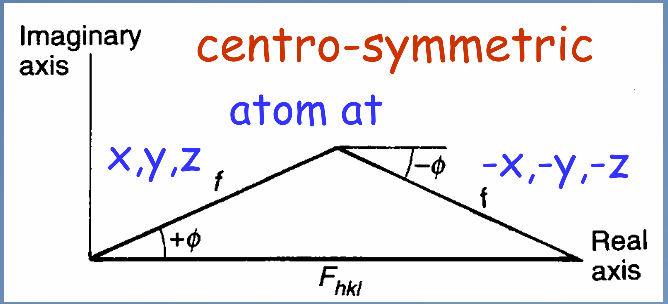

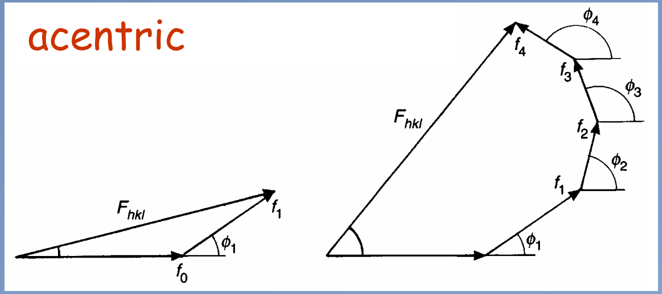

The Phase problem

- Structure factor in complex plane
    - Each scatterer contributes with a different phase. The structure factor results from adding the individual contributions.
    - The result can be real for centroysmmetric arrangements (for each atom at (xyz) there is an identical one at -(xyz), phase angles φ are either 0° or 180° (structure factor positive or negative)
    - For acentric materials the result has an imaginary component
- The Phase problem
    - The scattered intensity I is proportional to $|F_{hkl}|^2$, i.e. the product of F(**G**) with its conjugate complex F^*(**G**)
    - Fourier back-transforming I(**G**)=F(**G**)·F^*(**G**) yields the convolution ρ(**r**)·ρ(-**r**)=∫ρ(**u**)·ρ(**r**+**u**)d**u**=g(**r**)
    - g(**r**) is the pair correlation function, the so-called "Patterson function" for crystals
    - To calculate the phase, we need information on the atomic positions xyz from "Patterson techniques" of by "direct methods"

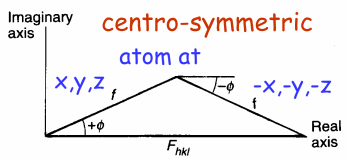

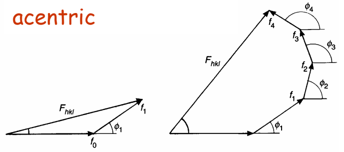

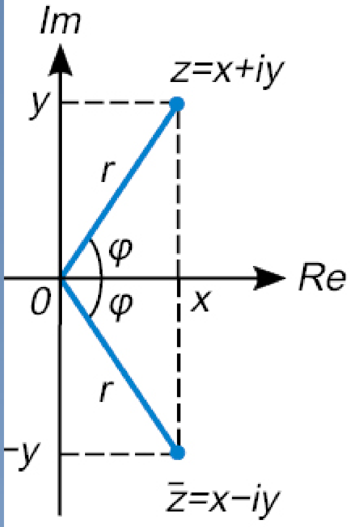

Debye-Waller factor

- Harmonic oscillator as assumption for atomic displacement
  - $F_{hkl}=\Sigma[b_j \cdot T_j \cdot \exp[2\pi \cdot i \cdot (hx+ky+lz)]]$
  - One can describe the thermal smearing of atomic positions as a convolution with the static structure.
  - The Debye-Waller factor T(**Q**) describes the averaged reduction of intensity with increasing **Q**.
  - It contains the atom-specific parameter *B* which can be seen as the surface in Å^2 of a sphere in which the atom is found most probably
    - Alternatively one finds a notation using *u* which by $8\pi^2$ smaller as it can be seen as the length in Å of the displacement vector of an atom

$$T_j = \exp(-B_j \frac{\sin^2\theta}{\lambda^2})$$

Coherent and incoherent scattering

  - Scattering length b_j depends on isotope and spin orientation!
- $I(\mathbf{Q}) = (1/V)\langle|\Sigma[b_j \cdot \exp(i\mathbf{Q}\mathbf{r}_j)]|^2\rangle$
  - Scattered intensity depends on the *relative* position of atoms:
- $I(\mathbf{Q}) = (1/V)\langle\Sigma[b_i b_j \cdot \exp(i\mathbf{q}(\mathbf{r}_i-\mathbf{r}_j))]\rangle$
  - Isotopes and spins are statistically distributed and thus uncorrelated with atomic positions
- $I(\mathbf{Q}) = (1/V) \quad \Sigma[\langle b_i b_j\rangle\langle\exp(i\mathbf{q}(\mathbf{r}_i-\mathbf{r}_j))\rangle]$

  $= (1/V)\langle b\rangle^2 \cdot \Sigma \quad \langle\exp(i\mathbf{q}(\mathbf{r}_i-\mathbf{r}_j))\rangle \quad I_{coh}$

  $+ (1/V)(\langle b^2\rangle-\langle b\rangle^2)\cdot\Sigma \quad \langle\exp(i\mathbf{q}(\mathbf{r}_j-\mathbf{r}_j))\rangle \quad I_{inc}$

  $= 1$ (no structure information)
- Dramatic for hydrogen: 1.8 vs. 79.8 barn
  - Therefore: deuteration: 5.6 vs. 2.0 barn
    - The scattering cross section σ is often given in "barn" (10^{-24}cm^2)

Kinematic vs. dynamic scattering theory

- Scattering in a perfect lattice
  - A diffracted beam can itself act as incident beam and back-diffracted into the initial direction: diffracted intensity weaker than expected
- ***Kinematical theory***
  - In far-from-perfect crystals this does not happen, intensity is proportional to sample volume
  - Shortcomings can be cured by a so-called ***extinction*** correction
- ***Dynamic theory***
  - necessary for perfect crystals

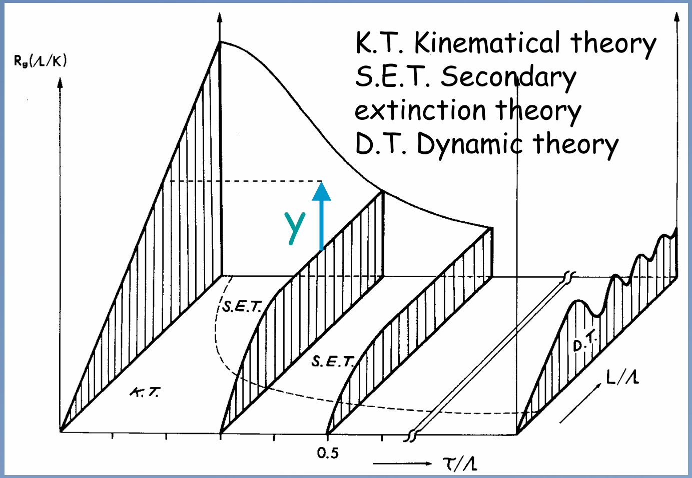

Mosaic crystal

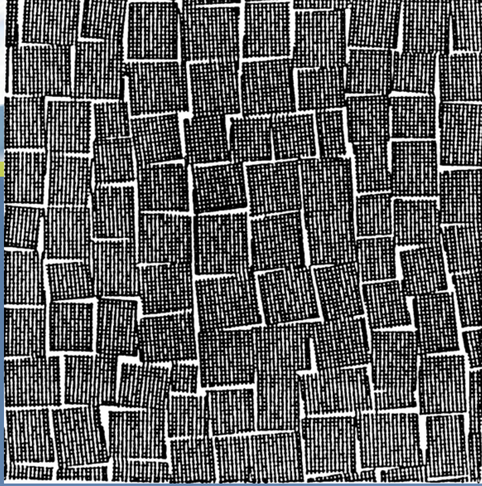

- Kinematical theory with extinction correction for imperfect crystals
    - Size of mosaic blocks
    - Misorientation
- Primary extinction
    - Blocks so large that more than one scattering event occurs within
        - Block-size counts
- Secondary extinction
    - Blocks shadowed from upstream blocks with identical orientation
        - Angular distribution of blocks counts
- Both effects may well be anisotropic

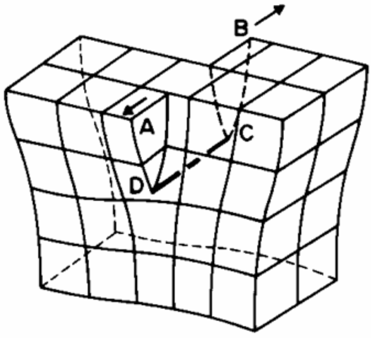

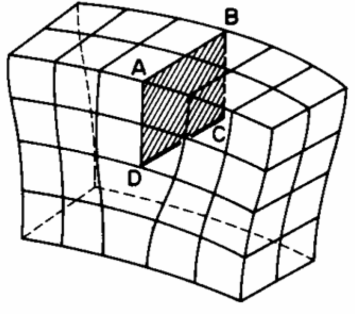

Single crystal diffraction

- The Bragg peak is a 3D volume in reciprocal space
  - One needs to integrate over a Bragg peak
  - This can be done by rotating the reciprocal lattice (thus, the crystal) through the Ewald shell
- ω-scan
  - Sensitive to angular variations of lattice planes (“rocking curve)

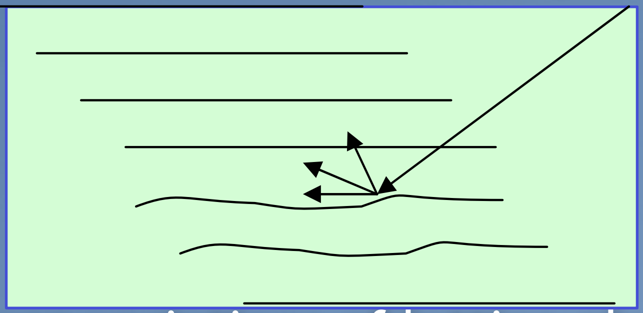

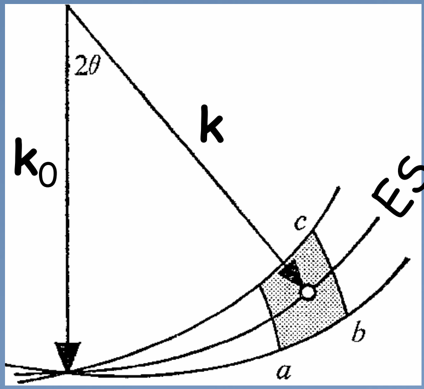

- ω-2Θ scan
  - Sensitive to distance variations of lattice planes

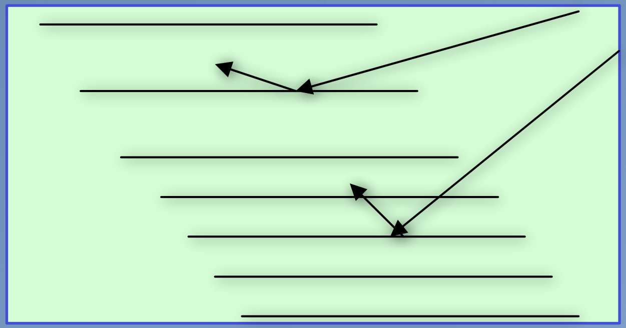

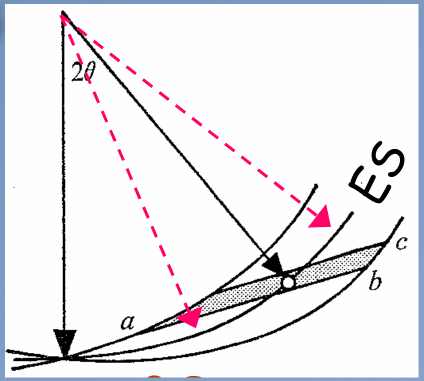

Proper integration

- How far do I need to scan?
  - Finite source size P
  - Finite detector aperture
  - Wavelength spread
- 2D detectors
  - Very large detector aperture
  - Integration in 2D by software
  - Third direction still needs to be scanned

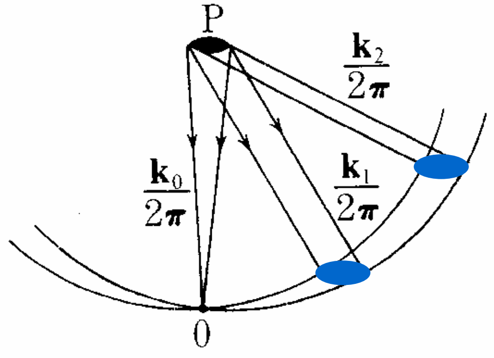

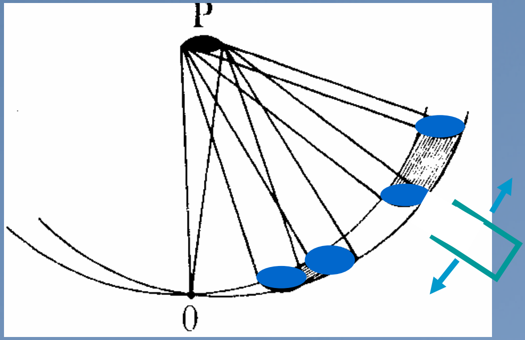

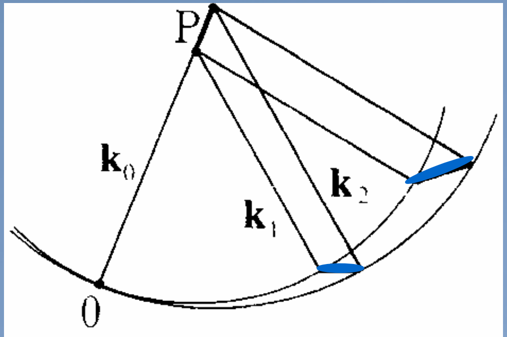

White beam: Laue method

- “White” radiation = very thick Ewald shell

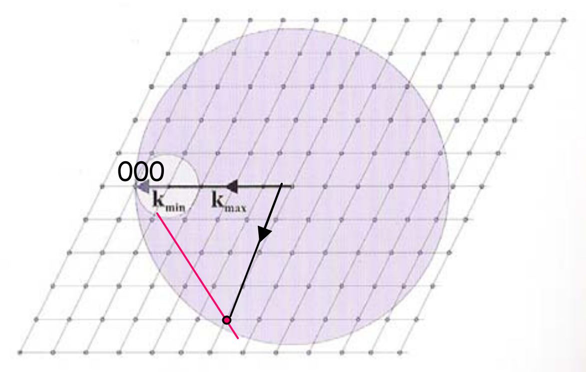

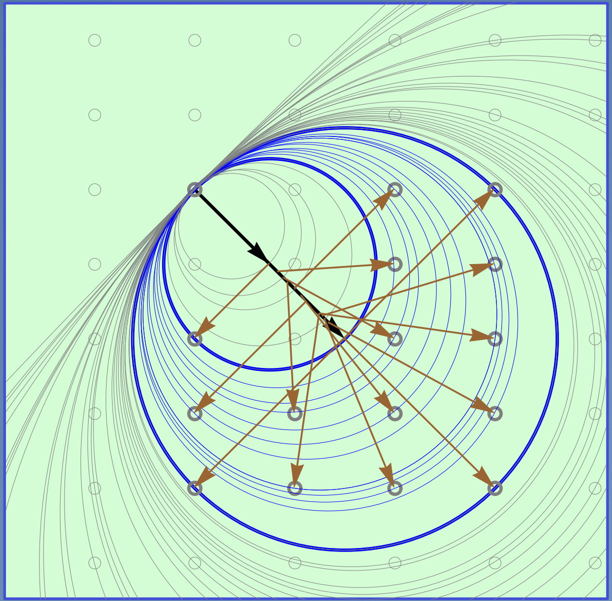

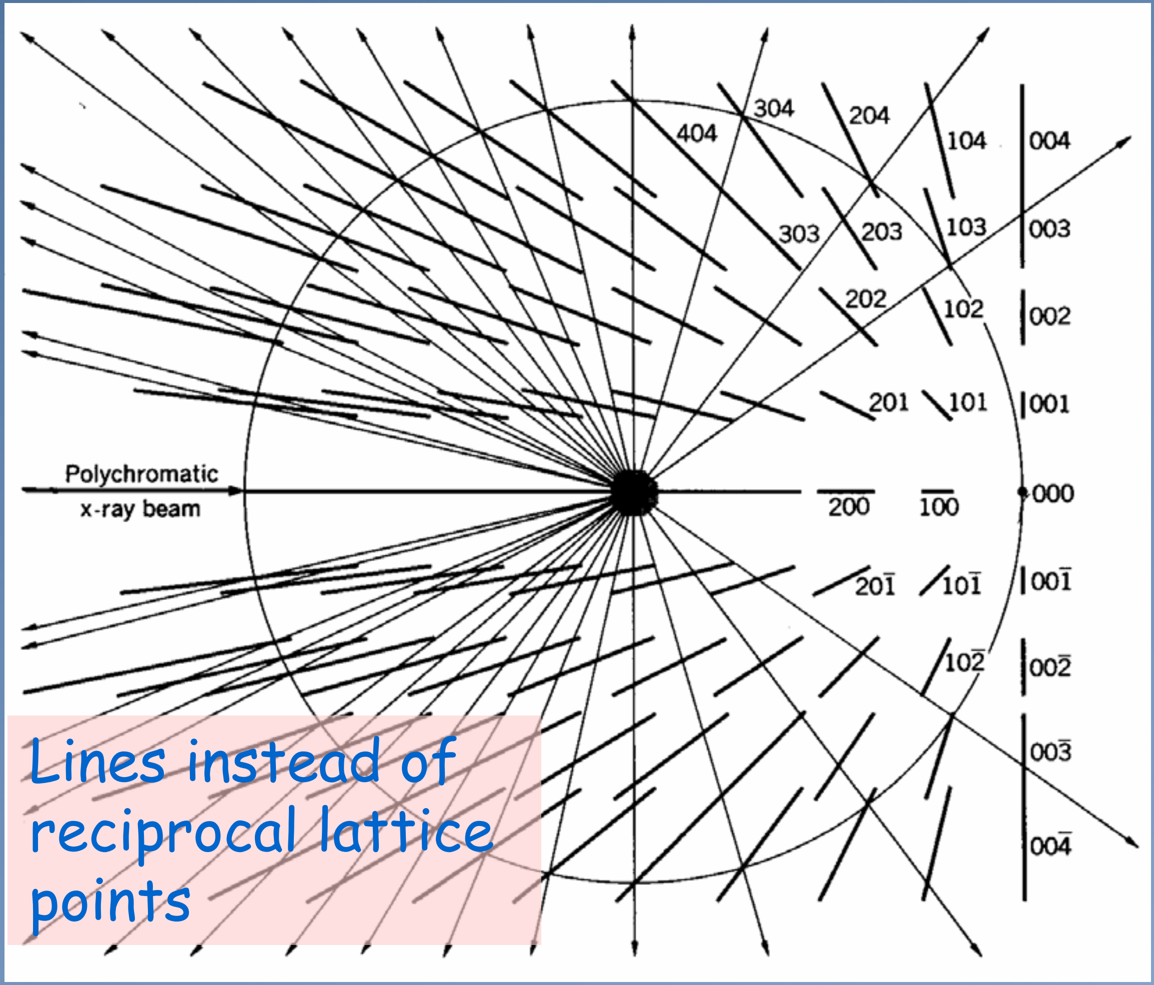

Lines instead of reciprocal lattice points

Four circle diffractometers

- Solution and refinement of crystal structures
  - Measurement of numerous reciprocal lattice point intensities
  - Accurate intensities: Scan over each reflection
- Four-cycle diffractometer
  - well collimated roughly monochromatic incident beam
  - Small sample bathed in the beam
  - Large detector (PSD) integrate neutrons scattered by the sample
  - For small mosaic spread of sample, wavelength spread of incident beam:
    - Spot in reciprocal space elongated parallel to **Q**
      - Integrated by performing a θ-2θ scan,
      - which also performs a parallel scan in reciprocal space
  - For samples with broad mosaic, the sample angle should be rocked (ω-scan).

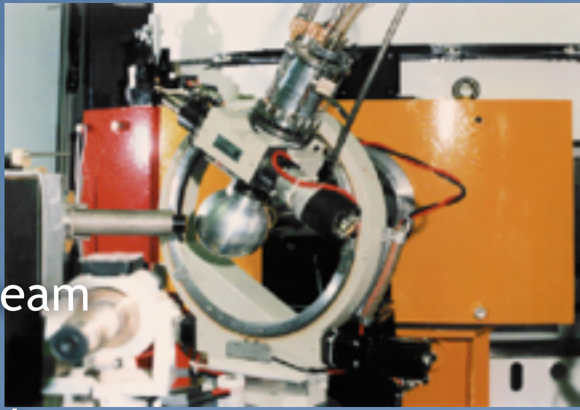

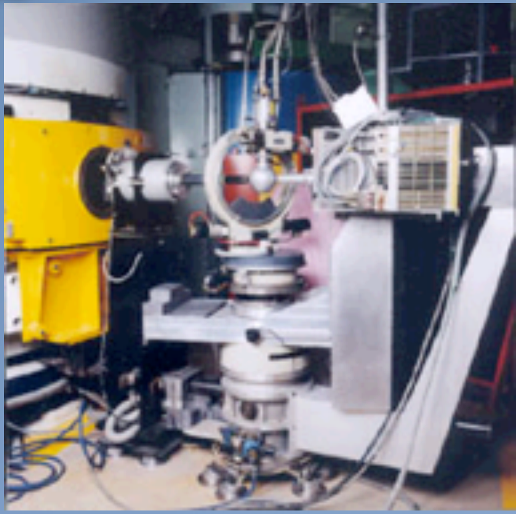

Powder Diffraction

- *Neutron (or X-ray) Powder Diffraction, why bother?*
- *Some equations and formalisms*
- *Data Analysis: The Rietveld Method*
- *Peak shape functions and microstructure*
- *Examples*

Short History of Powder Diffraction

1895	Discovery of X-rays by Röntgen
1912	von Laue demonstrates that X-rays can be diffracted by crystals
1935	Le Galley constructs the first X-ray powder diffractometer
1947	Phillips introduces the first commercial powder diffractometer
1950’s	Powder diffraction used primarily to study structural
1960’s	imperfections, phase identification, … largely by metallurgists and mineralogists
1969	**Hugo Rietveld** develops a method for whole pattern analysis of neutron powder diffraction data
1977	Cox, Young, Thomas and others first apply Rietveld method to synchrotron and conventional X-ray data

Powder Diffraction

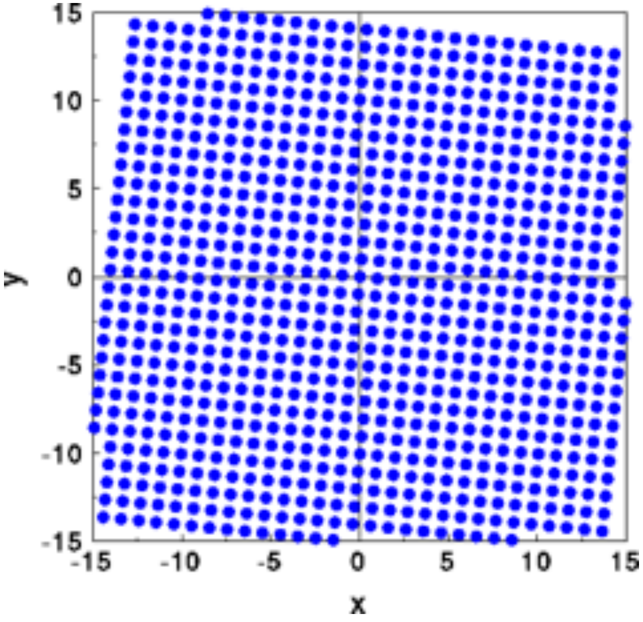

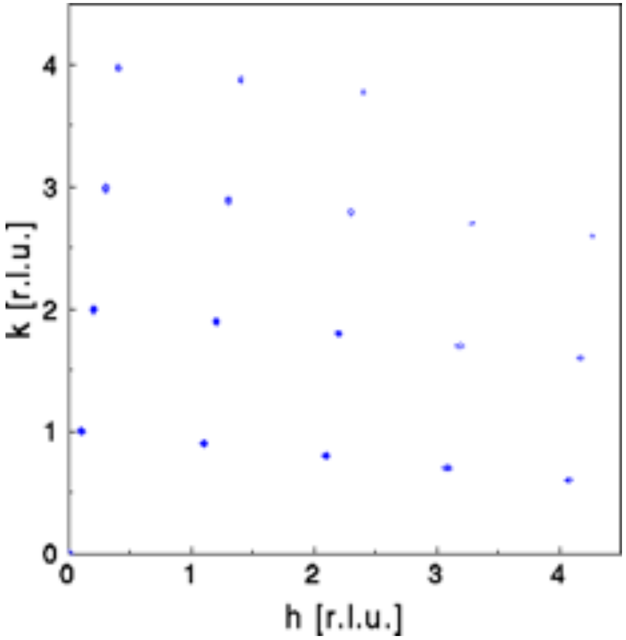

Real space

Reciprocal space

Single Crystal

Powder Diffraction

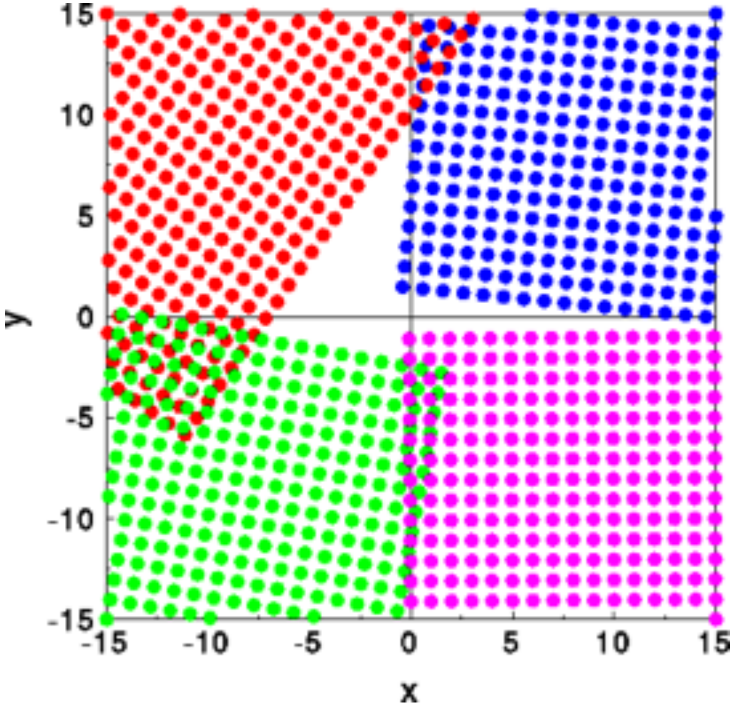

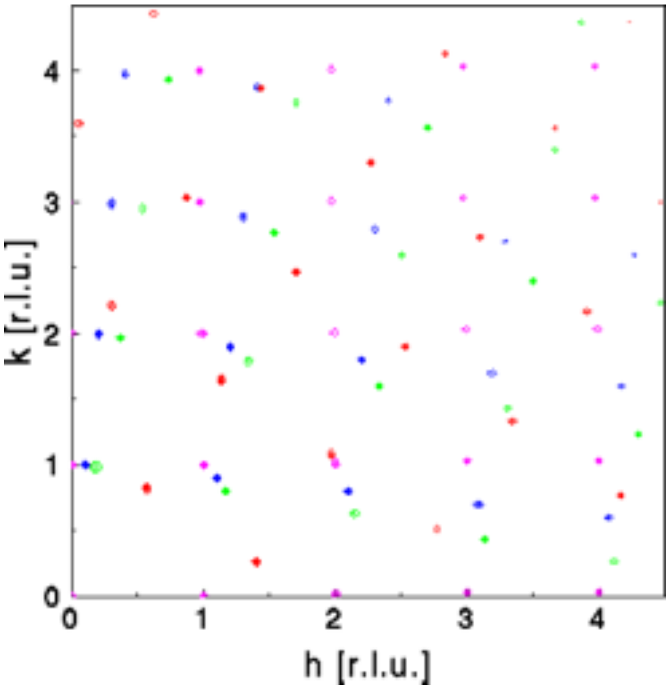

Real space

Reciprocal space

Four Single Crystals

Powder Diffraction

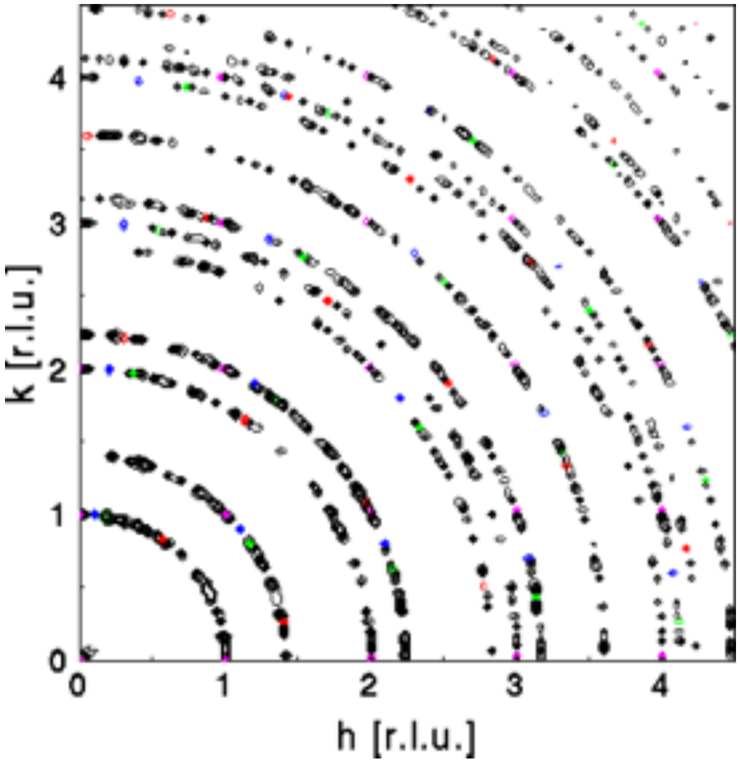

Reciprocal space

Fourty Single Crystals

Powder Diffraction

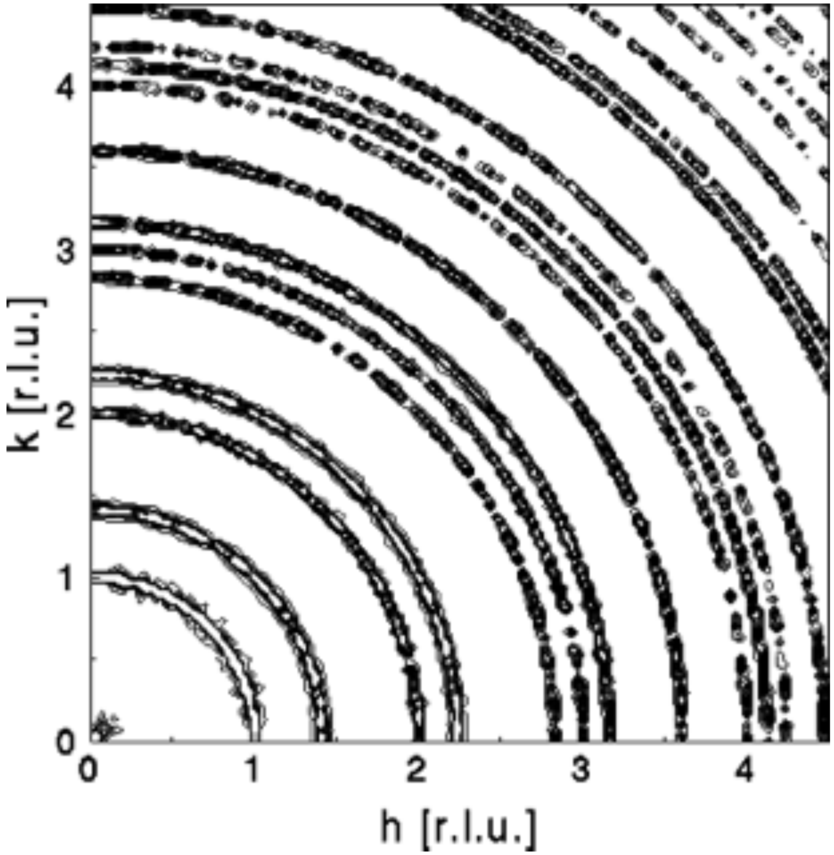

Reciprocal space

Two hundred Single Crystals

Powder Diffraction

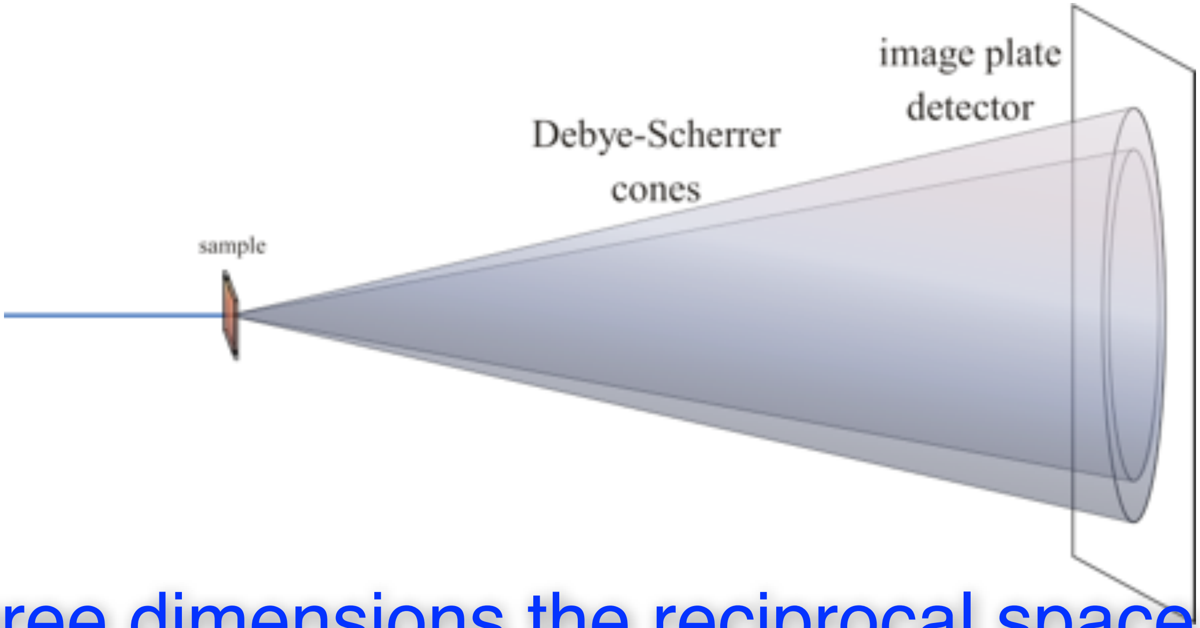

In three dimensions the reciprocal space corresponding to billions of crystals is a set of concentric spherical shells. The intersection of these shells with the Ewald Sphere gives rise to powder diffraction as a set of *Debye-Sherrer* cones

Powder Diffraction: Preferred orientation

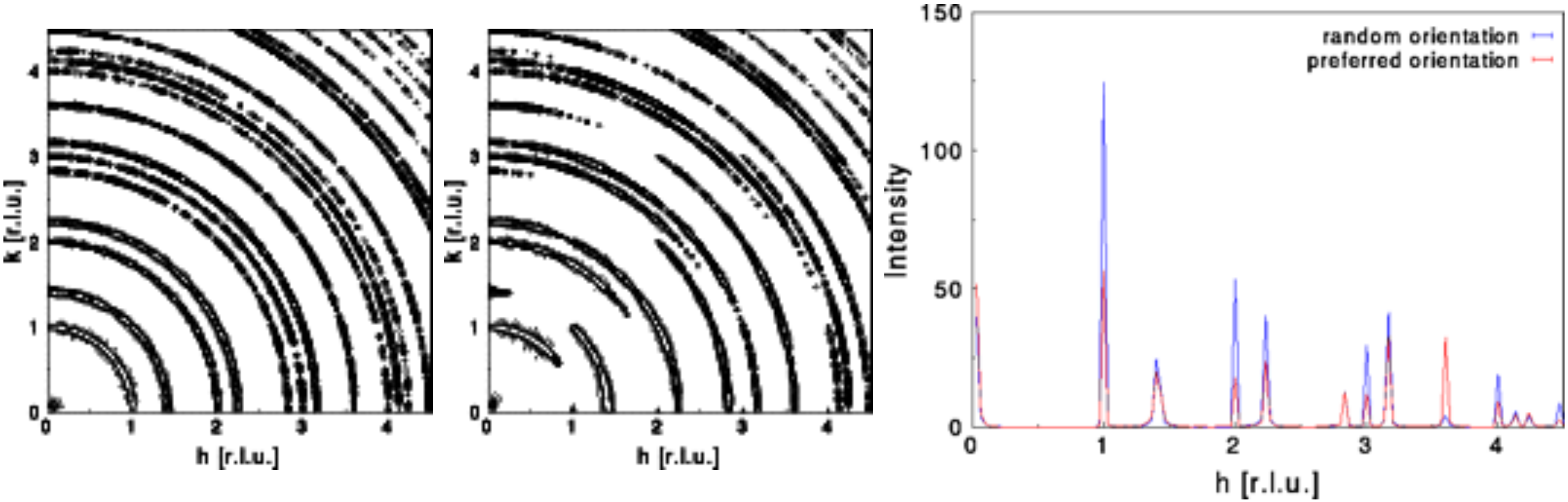

Preferred orientation is the main limitation factor for exploiting the intensities of X-ray powder diffraction. In order to use powders for structure determination and refinement one has to avoid preferred orientation

Uses of Powder Diffraction:
Applications in Physics, Chemistry, Geology, Industry, …

Qualitative Analysis
- Phase Identification

Quantitative Analysis
- Lattice Parameter (indexing & refinement)
- Phase Fraction Analysis

Structure Determination
- Reciprocal Space Methods
- Real Space Methods

Structure Refinement
- Rietveld Method

Peak Shape Analysis
- Crystallite Size Distribution
- Microstrain Analysis
- Anti-phase domains, stacking faults,…

Limitations of Powder Diffraction for solving crystal structures

- Single crystal diffraction allows solving crystal structures by using appropriate mathematical algorithms and accurate peak intensities.

- The 3D set of reflections obtained from a single crystal experiment is condensed into 1D in powder diffraction pattern. This leads to both accidental and exact peak overlap, and complicates the determination of individual peak intensities.

- Indexing may be a bottleneck for starting to solve a crystal structure. Multiphase mixtures complicates the task.

- Crystal symmetry cannot be obtained directly from powder diffraction patterns.

- Preferred orientation leads to biased peak intensities.

Scheme of a two axis diffractometer

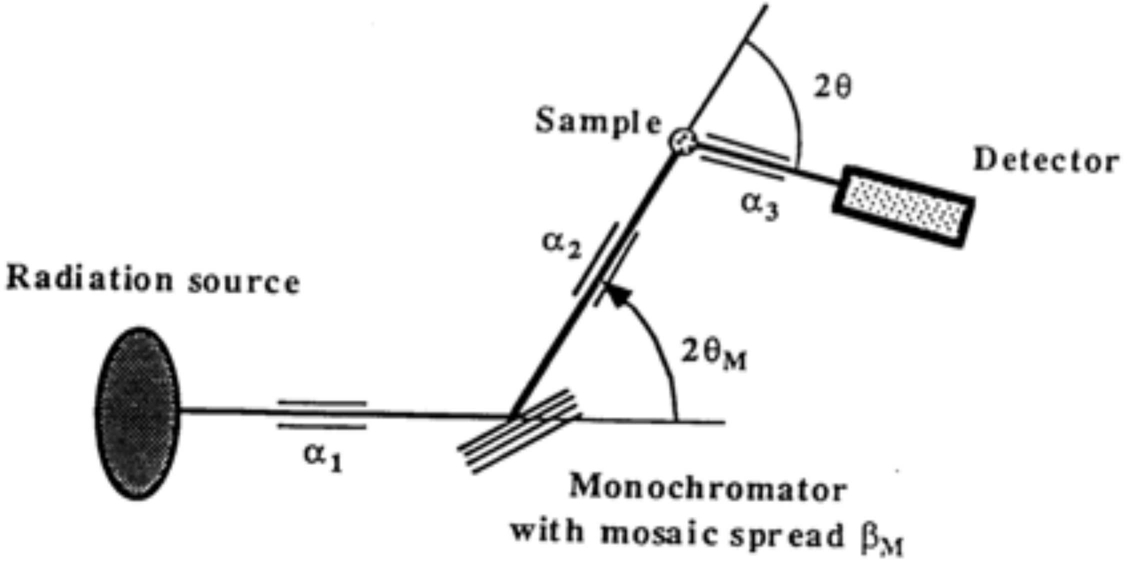

Parameters determining resolution and intensity

$$\frac{\Delta d}{d} = \frac{1}{2}\sqrt{W\cot^2\theta + V\cot\theta + U}$$

Collimators $\alpha_1, \alpha_2, \alpha_3$

Mosaicity of monochromator β_M

« take-off » angle : $2\theta_M$

$$U = \frac{\alpha_1^2 + \alpha_2^2}{\tan^2\theta_M}$$

$$V = -\frac{2\alpha_2^2}{\tan\theta_M}$$

$$W = \alpha_2^2 + \alpha_3^2$$

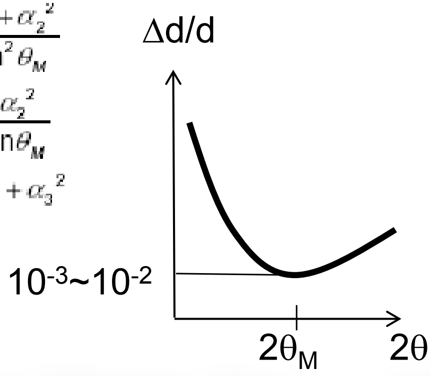

What is a powder diffraction pattern?

A powder diffraction pattern can be recorded in numerical form for a discrete set of scattering angles, times of flight or energies. We will refer to this scattering variable as : T.
The experimental powder diffraction pattern is usually given as three arrays :

$$\left\{T_i, y_i, \sigma_i\right\}_{i=1,2,\ldots n}$$

The profile can be modelled using the calculated counts: y_{ci} at the i^{th} step by summing the contribution from neighbouring Bragg reflections plus the background.

Powder diffraction profile:
scattering variable T: 2θ, TOF, Energy

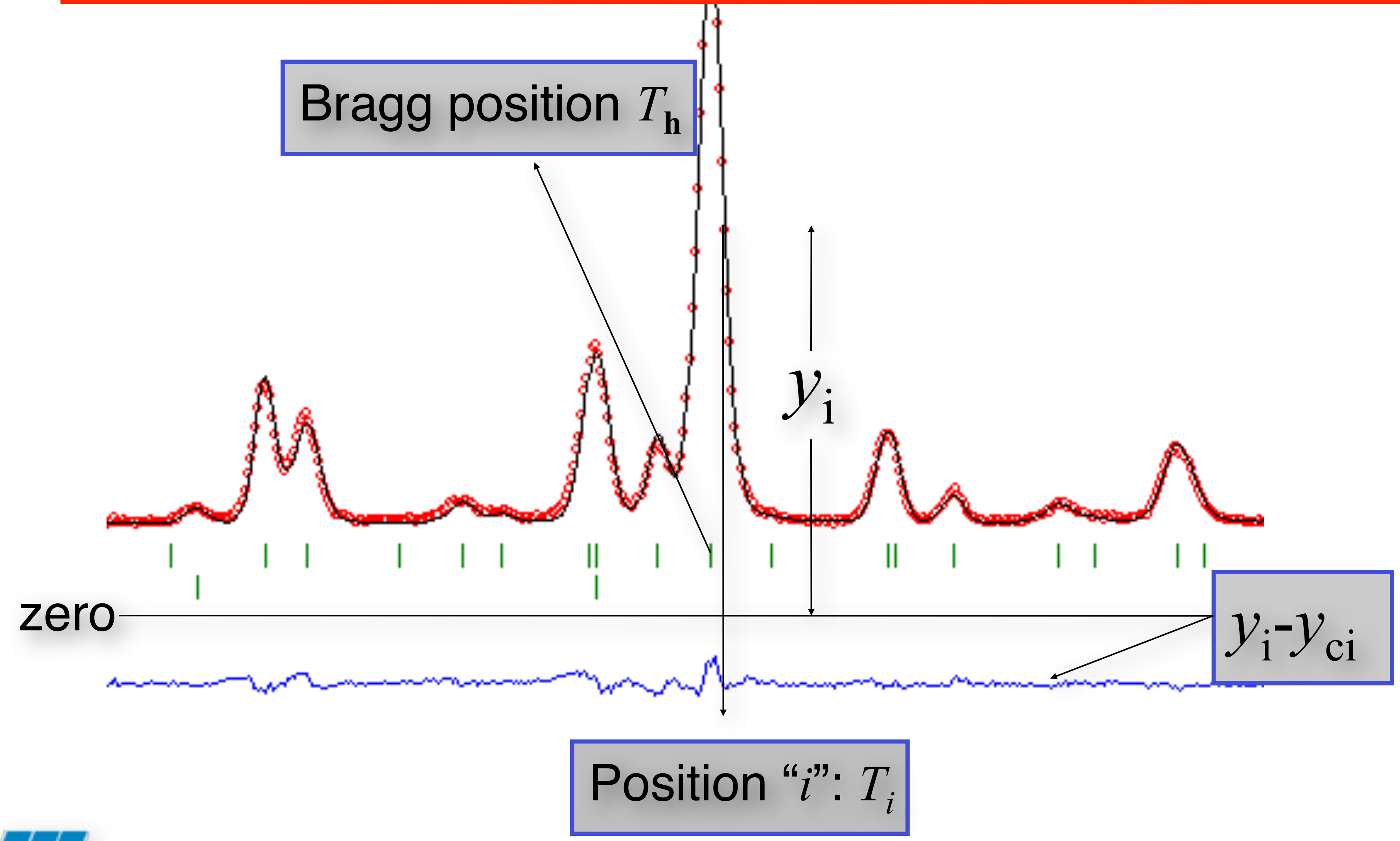

Bragg position T_{h}

y_{i}

zero

$y_{\mathrm{i}}-y_{\mathrm{ci}}$

Position "i": T_i

Constant wavelength neutron powder diffraction

$$\frac{\Delta d}{d} = \frac{1}{2}\sqrt{W\cot^2\theta + V\cot\theta + U}$$

- Resolution function determined by
  - optical diffractometer arrangements and collimators,
    - coupled to scattering angle and wavelength
- Limited Q-range
  - depends on selected wavelength
  - Hot source (low lambda):
    - gain in Q-range degraded by lower resolution
- Difficult to obtain high resolution
  - in the whole Q-range on a single instrument.
- Simple data treatment:
  - Minimal corrections of the raw data before processing.
- Simple model of peak shape:
  - faster calculations in data analysis

Time of Flight neutron powder diffraction

$$\left(\frac{\Delta d}{d}\right)_{TOF}=\sqrt{\left(\frac{\Delta t}{t}\right)^2+\left(\frac{\Delta L}{L}\right)^2+\left(\cot\theta\cdot\Delta\theta\right)^2}$$

- Resolution function determined by
  - pulse width and flight path
- Large Q-range
  - with excellent resolution for long flight path instruments
- Simple to obtain high resolution
  - in the whole Q-range on a single instrument
    - by using several detector banks
- Spectro-diffractometers:
  - study dynamics together with structural aspects
- Complex data treatment:
  - Important corrections of the raw data before processing
- Complex models of peak shape:
  - lengthy calculations in data analysis

Neutrons versus X-rays: advantages and drawbacks for Powder Diffraction

Neutrons

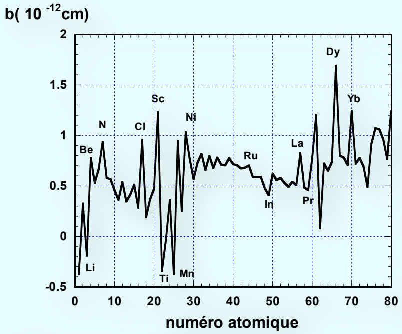

- *Constant scattering length*
- *Contrast*
- *Low absorption: easy sample environment*
- *Magnetic structures*
- *High precision in structure refinement*
- *Moderate resolution*

X-rays

- *Extremely high resolution*
- *Subtle distortions*
- *Indexing & structure determination*
- *Anomalous scattering*
- *Texture effects*
- *Form factor*

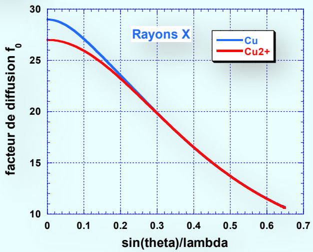

The indexing problem

- Single Crystal:
  - Unit cell and symmetry unambiguous
  - Each reflection: correct Miller indices *hkl*
  - Diffracted intensity (structure amplitude $|F|_{hkl}$) accurate
- Powder:
  - **nothing** of all this known …
  - Informations in a powder pattern:
    - Peak positions as function of unit cell dimensions
    - Peak shapes
    - Integrated intensities

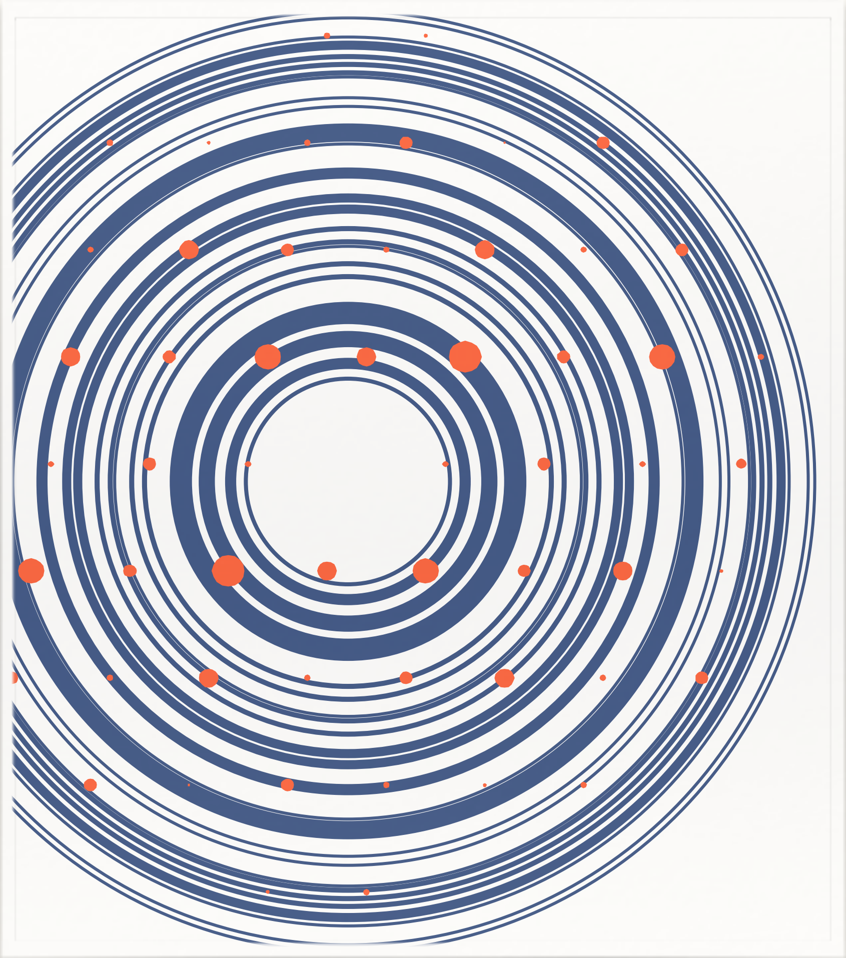

The Rietveld Method for refinement of crystal and magnetic structures

The profile of powder diffraction patterns

The model to calculate a powder diffraction pattern is:

$$y_{ci} = \sum_{\mathbf{h}} I_{\mathbf{h}} \Omega(T_i - T_{\mathbf{h}}) + b_i$$

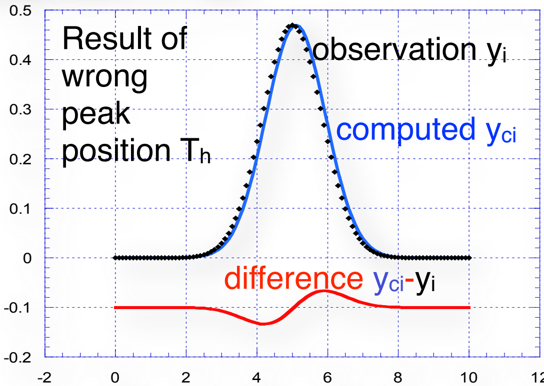

$$\int_{-\infty}^{+\infty} \Omega(x)dx = 1$$

Profile function characterized by its full width at half maximum (FWHM=H) and *shape* parameters (η, m, ...)

$$\Omega(x) = g(x) \otimes f(x) = instrumental \otimes intrinsic\ profile$$

The profile of powder diffraction patterns

$$y_{ci} = \sum_{\mathbf{h}} I_{\mathbf{h}} \Omega(T_i - T_{\mathbf{h}}) + b_i$$

$$I_{\mathbf{h}} = I_{\mathbf{h}}\left(\beta_{\mathbf{I}}\right)$$

Contains structural information:
atom positions, magnetic moments, etc.

$$\Omega = \Omega(x_{\mathbf{h}i}, \beta_{\mathbf{P}})$$

Contains micro-structural information:
instrumental resolution, defects, crystallite size, ...

$$b_i = b_i\left(\beta_{\mathbf{B}}\right)$$

Background: noise, diffuse scattering, ...

The Rietveld Method

The Rietveld Method consist of refining a crystal (and/or magnetic) structure by minimising the weighted squared difference between the observed and the calculated pattern against the parameter vector: **β**

$$\boxed{\chi^2 = \sum_{i=1}^{n} w_i \left\{ y_i - y_{ci}(\beta) \right\}^2}$$

$$\boxed{w_i = \frac{1}{\sigma_i^2}}$$

σ_i^2: variance of the "observation" y_i

Poisson statistics => $\boldsymbol{\sigma_i \approx \sqrt{y_i}\ ;\ w_i = 1/\sigma_i^2 \Rightarrow w_i = 1/y_i}$ (least squares method)

Least squares: Gauss-Newton

Minimum necessary condition: $\frac{\partial \chi^2}{\partial \beta} = 0$

A Taylor expansion of $y_{ic}(\beta)$ around β_0 allows the application of an iterative process. The shifts to be applied to the parameters at each cycle for improving χ^2 are obtained by solving a linear system of equations (normal equations)

$$\mathbf{A}\delta_{\beta_0} = \mathbf{b}$$

$$A_{kl} = \sum_i w_i \frac{\partial y_{ic}(\beta_0)}{\partial \beta_k} \frac{\partial y_{ic}(\beta_0)}{\partial \beta_l}$$

$$b_k = \sum_i w_i (y_i - y_{ic}) \frac{\partial y_{ic}(\beta_0)}{\partial \beta_k}$$

Least squares: Gauss-Newton

The shifts of the parameters obtained by solving the normal equations are added to the starting parameters giving rise to a new set

$$\beta_1 = \beta_0 + \delta_{\beta_0}$$

The new parameters are considered as the starting ones in the next cycle and the process is repeated until a convergence criterion is satisfied. The variance of the adjusted parameters are calculated by the expression:

$$\boxed{\begin{aligned} \sigma^2(\beta_k) &= (\mathbf{A}^{-1})_{kk}\chi_\nu^2 \\ \chi_\nu^2 &= \frac{\chi^2}{N - P} \end{aligned}}$$

Least squares:
a local optimisation method

- The least squares procedure provides (**if** it converges) the value of the parameters constituting the **local** minimum closest to the starting point

- A set of good starting values for all parameters is needed

- If the initial model is bad for some reasons, the LSQ procedure will not converge, but may diverge.

The structural information contained in the integrated intensities

The Integrated Intensity

$$I_{\mathbf{h}} = \left\{ L\,p\,O\,A\,C\,F^2 \right\}_{\mathbf{h}}$$

Integrated intensities are proportional to the square of the **structure factor** F.
The proportionality factors are:

- Lorentz-polarization (Lp),
- preferred orientation (O),
- absorption (A),
- other "corrections" (C) ...

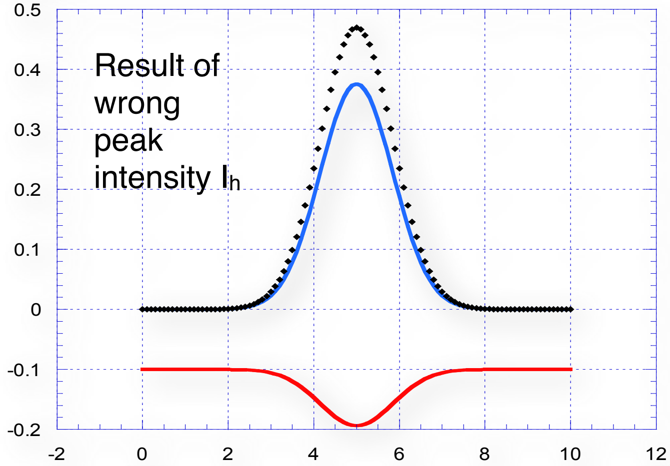

The Integrated Intensity

$$I_{\mathbf{h}} = \left\{ L p O A C F^2 \right\}_{\mathbf{h}}$$

- Lorentz-polarization (Lp) $Lp = \frac{1 - K + K \cos^2 2\theta_{Monok} \cos^2 2\theta}{2 \sin^2 \theta \cos \theta}$

  K = polarisation ratio

  Neutrons: K=0, laboratory X-rays: K=0.5 ; synchrotron K≈0.1
- preferred orientation (O) $O_h = \sum_{j=1}^{j_h} (r^2 \cos^2 \alpha_j + r^{-1} \sin^2 \alpha_j$

  Empirical March-Dollase function:

  Principal axis must be determined by inspection

  α_j: angle between (hkl) and orientation axis

  r: ratio of orientation:

    r <1 platelet type, r >1 needle type orientation
- absorption (A)
- other “corrections” (C) ...

The Integrated Intensity

$$I_{\mathbf{h}} = \left\{ L p O A C F^2 \right\}_{\mathbf{h}}$$

- Lorentz-polarization (Lp),
- preferred orientation (O),
- Absorption (A)

$$T_{\mathrm{h}} = \exp\left\{-(1.7133 - 0.0368\sin^2\theta_{\mathrm{h}})\mu R + (0.0927 + 0.375\sin^2\theta_{\mathrm{h}})(\mu R)^2\right\}$$

μ = linear absorption coefficient ; R : cylinder radius

- other “corrections” (C) ...

The Structure Factor contains the structural parameters

$$F(\mathbf{h}) = \sum_{j=1}^{n} O_j f_j(\mathbf{h})\ T_j \sum_s exp\ \left\{2\pi i \left[\mathbf{h}\{S|\mathbf{t}\}_s\, \mathbf{r}_j\right]\ \right\}$$

$$\mathbf{h}_s = (h,k,l)_s = (h,k,l)S_s^T \qquad (s = 1, 2, \ldots N_G)$$

$$\mathbf{r}_j = (x_j, y_j, z_j) \qquad (j = 1, 2, \ldots n)$$

$$T_j = \exp(-B_j \frac{\sin^2\theta}{\lambda^2})$$

Structural Parameters
(simplest case)

$\mathbf{r}_j = (x_j, y_j, z_j)$

Atom positions

up to *3n* parameters

O_j

Occupation factors
up to *n-1* parameters

B_j

Isotropic displacement (temperature) factors
up to *n* parameters

Structural Parameters (complex cases)

As in the simplest case plus additional (or alternative) parameters:

- **Anisotropic** temperature (displacement) factors
  - **Anharmonic** temperature factors
- Special form-factors (symmetry-adapted spherical harmonics), TLS for rigid molecules, etc.
- **Magnetic moments**, coefficients of Fourier components of magnetic moments, basis functions, etc.

Magnetic structures

The magnetic moments can be expressed as Fourier series

$$\mathbf{m}_{lj} = \sum_{\{\mathbf{k}\}} \mathbf{S}_{\mathbf{k}j}\, exp\left\{-2\pi i \mathbf{k}\mathbf{R}_l\right\}$$

The magnetic structure factor:

$$\mathbf{M}(\mathbf{h}) = p \sum_{j=1}^{n} O_j f_j(\mathbf{h}) T_j \sum_s M_{js} \mathbf{S}_{\mathbf{k}j}\, exp\left\{2\pi i \left[(\mathbf{H}+\mathbf{k}) \{S|\mathbf{t}\}_s \mathbf{r}_j - \psi_{\mathbf{k}js} \right] \right\}$$

Magnetic ordering of Ho and Cu ions in Ho_2BaCuO_5 (D1B)

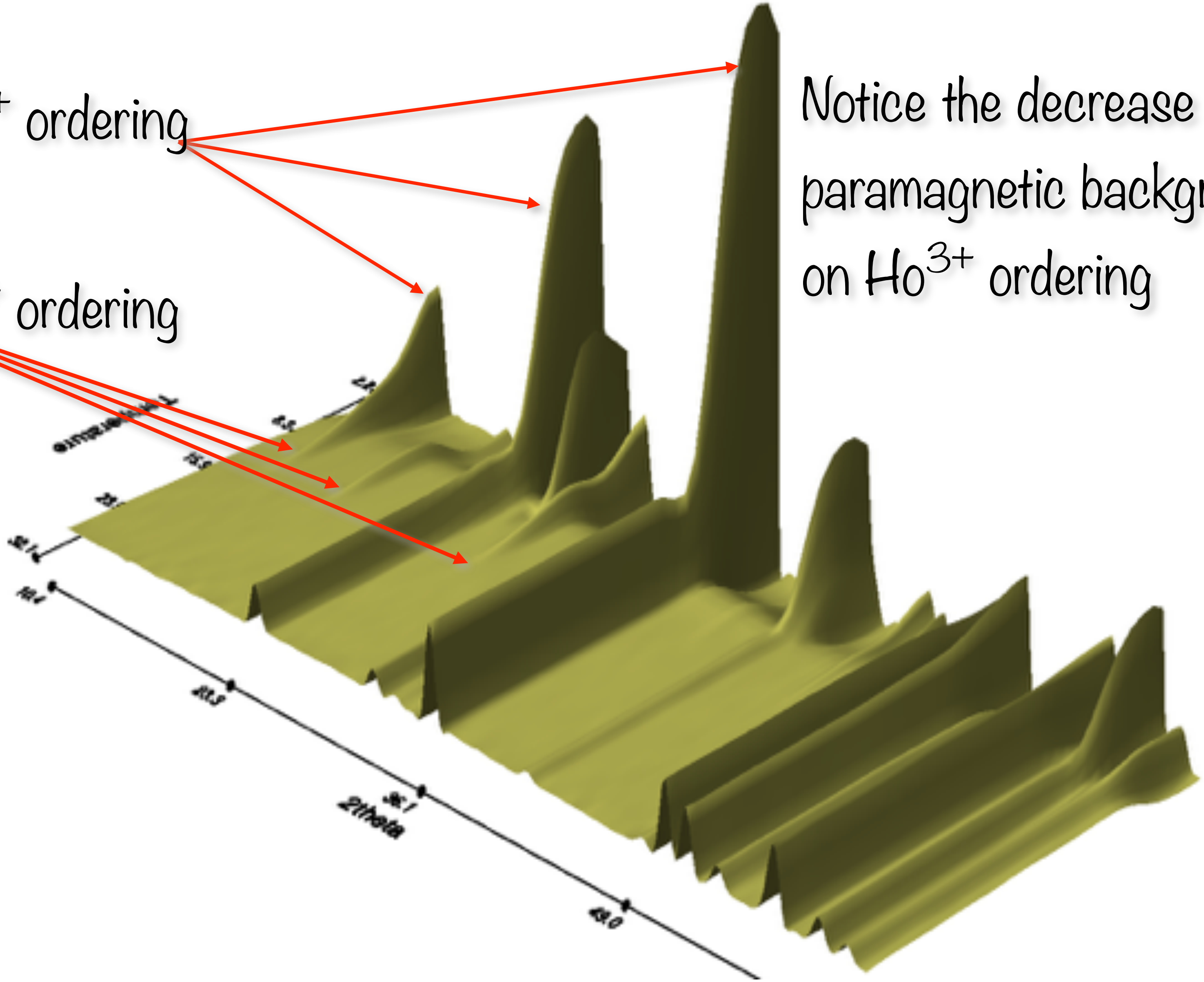

Ho^{3+} ordering

Cu^{2+} ordering

Notice the decrease of the paramagnetic background on Ho^{3+} ordering

What can we get from precise crystallographic structures?

E.g. with the Bond Valence approach:

The information contained in data bases suggest a strong correlation between average metal-oxygen distances and formal valence of metal ions

The importance of precise structural refinements

➔ *Nature of the octahedral distortions in manganite-perovskites?*

Valence state associated to a Mn site :

Directly related to the average Mn-O distance **$<d>=<d_{Mn-O}>$**

Mn^{4+} (non-JT) ions in CaMnO$_3$, T=RT

⇒ $<d_{Mn-O}>$= 1.90 Å, Δ = 0,03.10^{-4}

Mn^{3+}(JT) ions in LaMnO$_3$, T=RT< T$_{JT}$

⇒ $<d_{Mn-O}>$= 2,02 Å

l= 2.18, m=1.97, s=1.91 Å, Δ = 33,1.10^{-4}

Measure of the Jahn-Teller effect (distortion):

$$\Delta = \frac{1}{N}\sum_i \left(\frac{d_i - \langle d \rangle}{\langle d \rangle}\right)^2$$

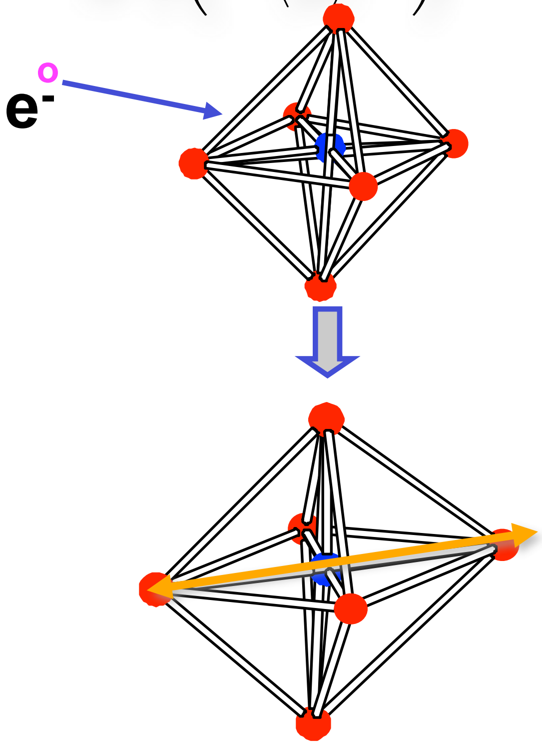

Electronic crystallisation in a Li battery material: columnar ordering of electron and holes in the spinel $LiMn_2O_4$

J. Rodríguez-Carvajal, G. Rousse, Ch. Masquelier and M. Hervieu

Physical Review Letters, **81**, 4660 (1998)

$Li_{Td}[Mn_2]_{Oct.}O_4$: $Mn^{3.5+}$

High temperature: mixed valence state

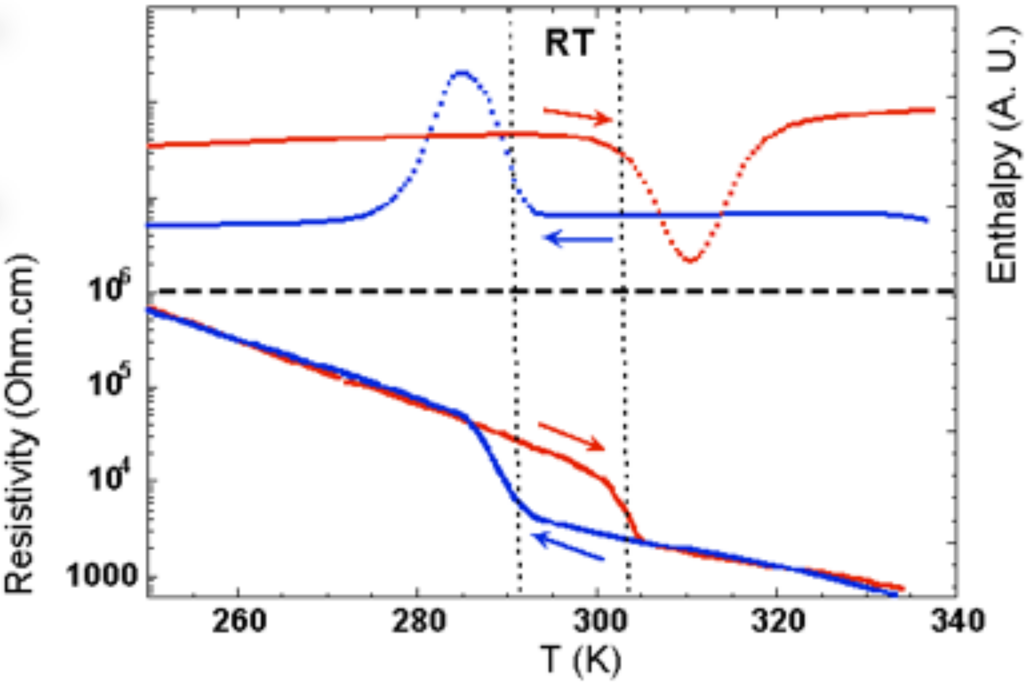

LiMn$_2$O$_4$: Electron Diffraction

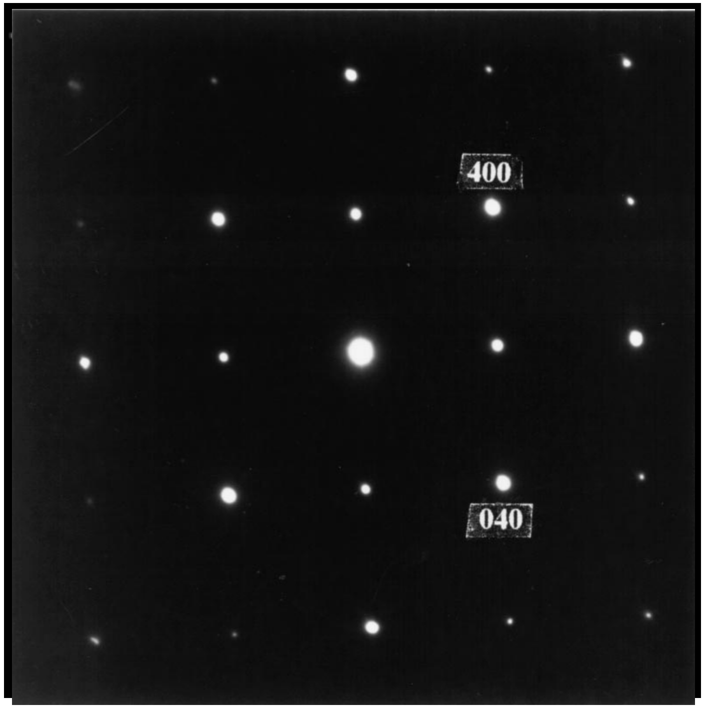

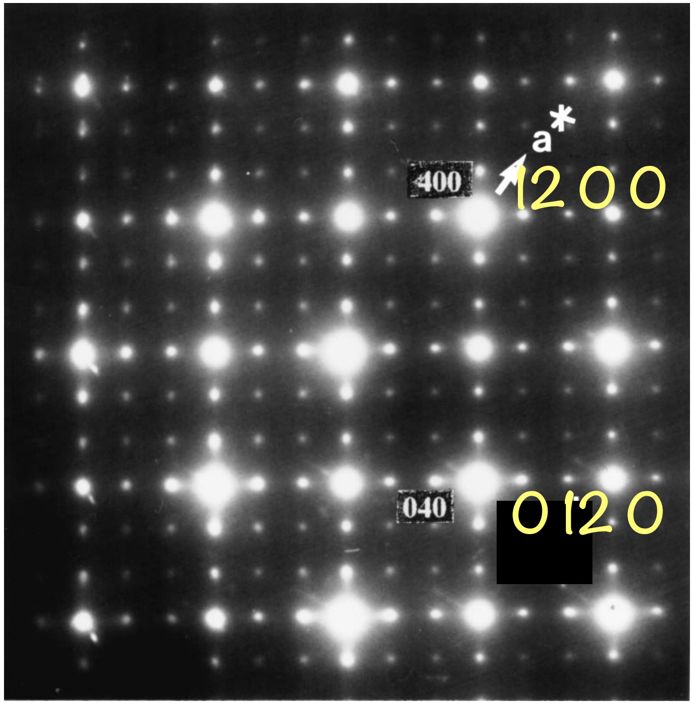

Cubic Fd$\bar{3}$m
a = 8.248(1) Å

$\xrightarrow{\times 9}$

Orthorhombic Fddd
a = 24.7435(5) Å
b = 24.8402(5) Å
c = 8.1989(1) Å

J. Rodríguez-Carvajal *et al*, *PRL*, **81**, 4660 (1998)

$LiMn_2O_4$: Neutron Diffraction, 3T2 (LLB)

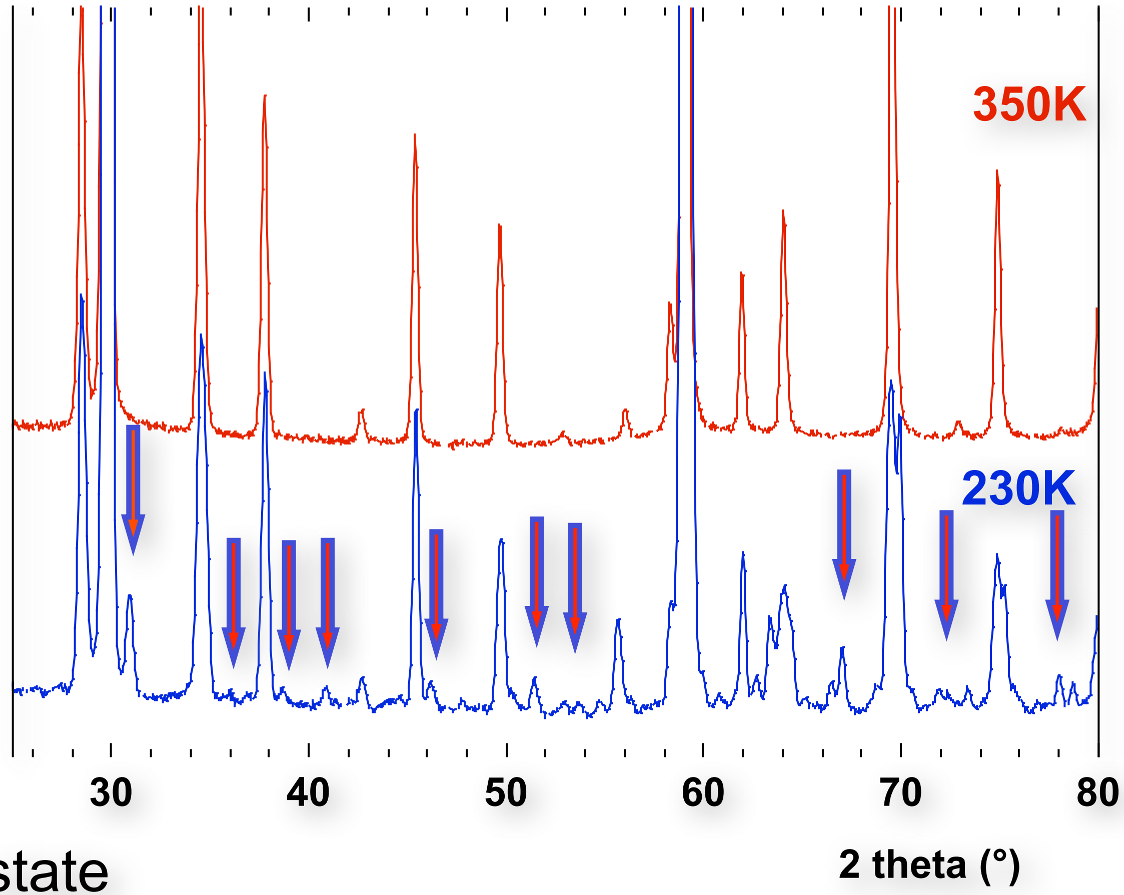

Charge ordered state

Orthorhombic Distortion

Superstructure reflections

Refinement of the high-temperature phase

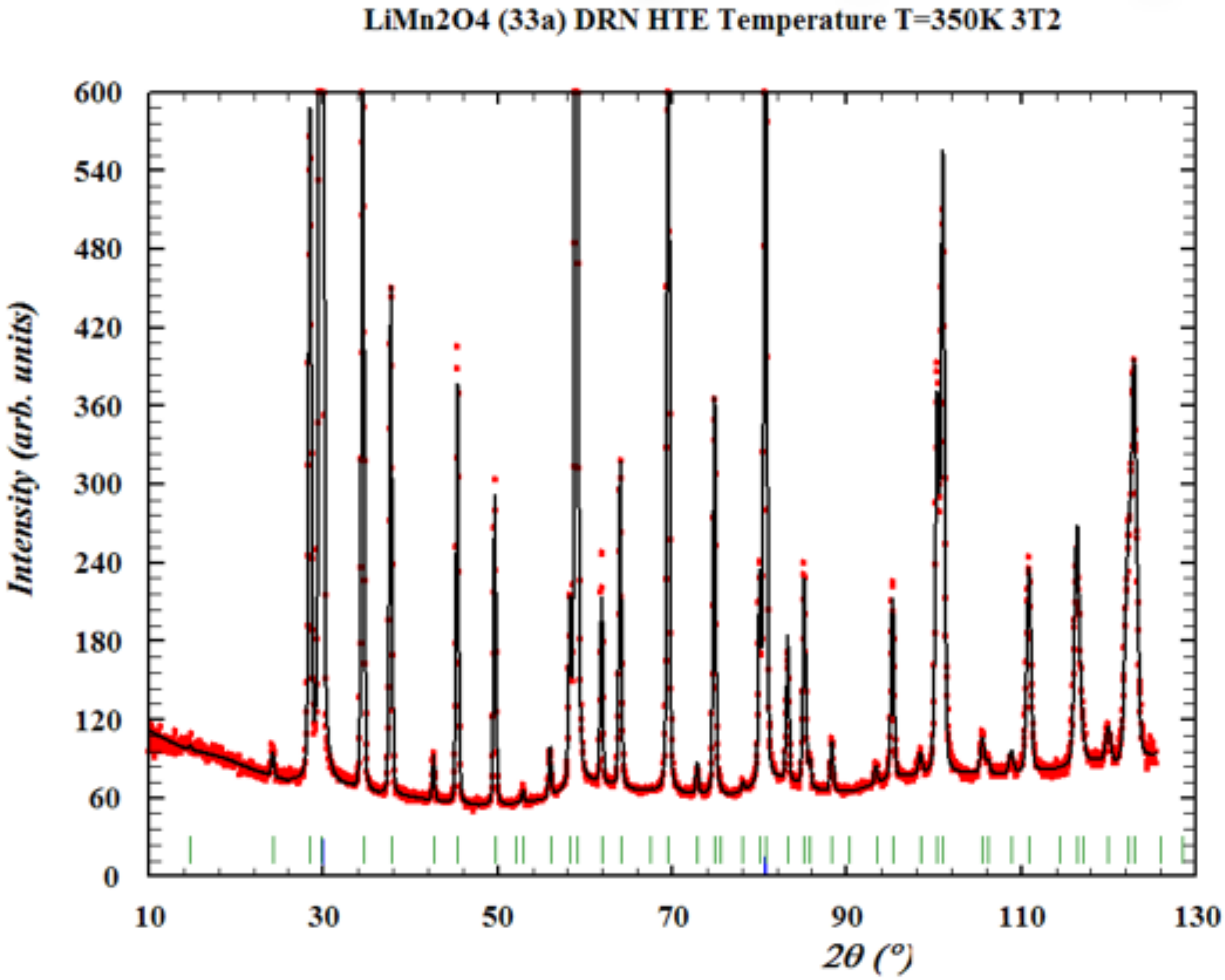

Refinement of the charge-ordered phase

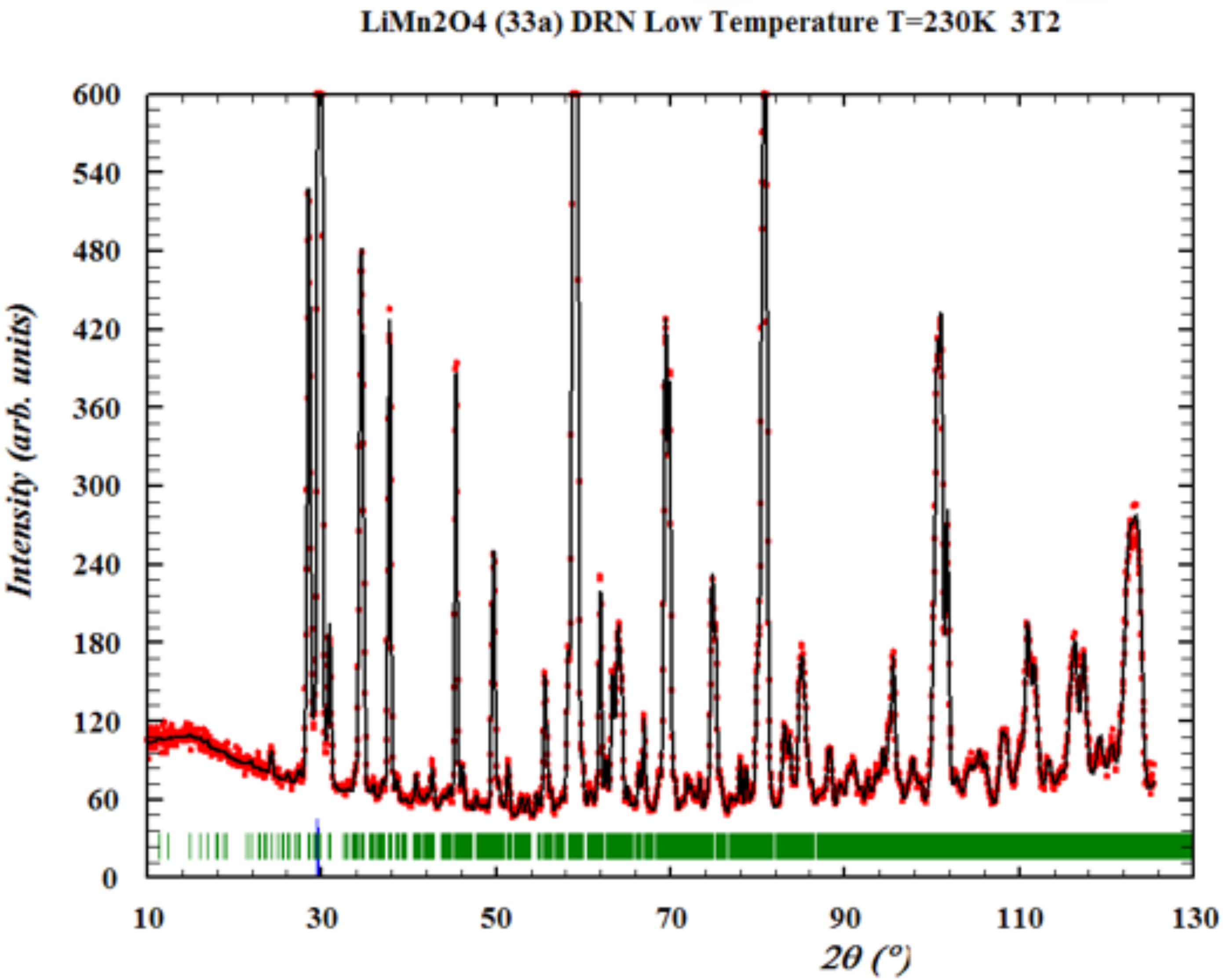

$LiMn_2O_4$: Partial Charge Ordering

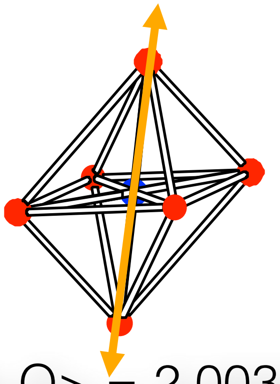

<Mn-O> = 2,003(2) Å

Mn(1) = 3.20+

Δ = 20.6

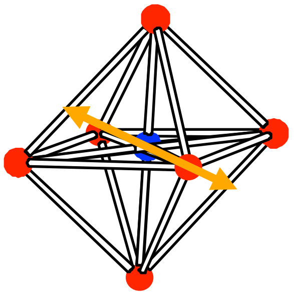

<Mn-O> = 1,996(4) Å

Mn(2) = 3.27+

Δ = 19.4

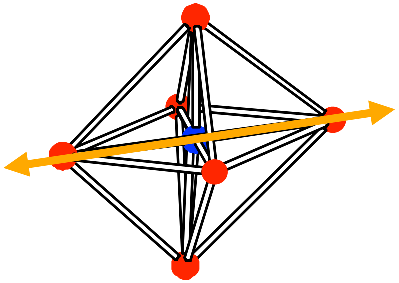

<Mn-O> = 2,020(5) Å

Mn(3) = 3.12+

Δ = 36.6

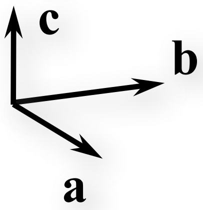

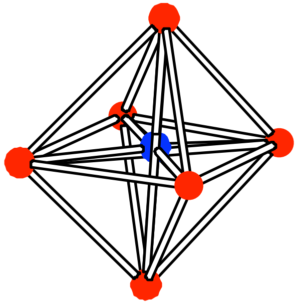

<Mn-O> = 1,903(4) Å

Mn(4) = 4.02+

Δ = 4.6

64 « Mn^{4+} »
80 « Mn^{3+} -like»
8 delocalised holes

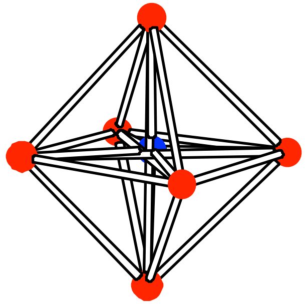

<Mn-O> = 1,915(4) Å

Mn(5) = 3.90+

Δ = 6.1

$LiMn_2O_4$: Partial Charge Ordering

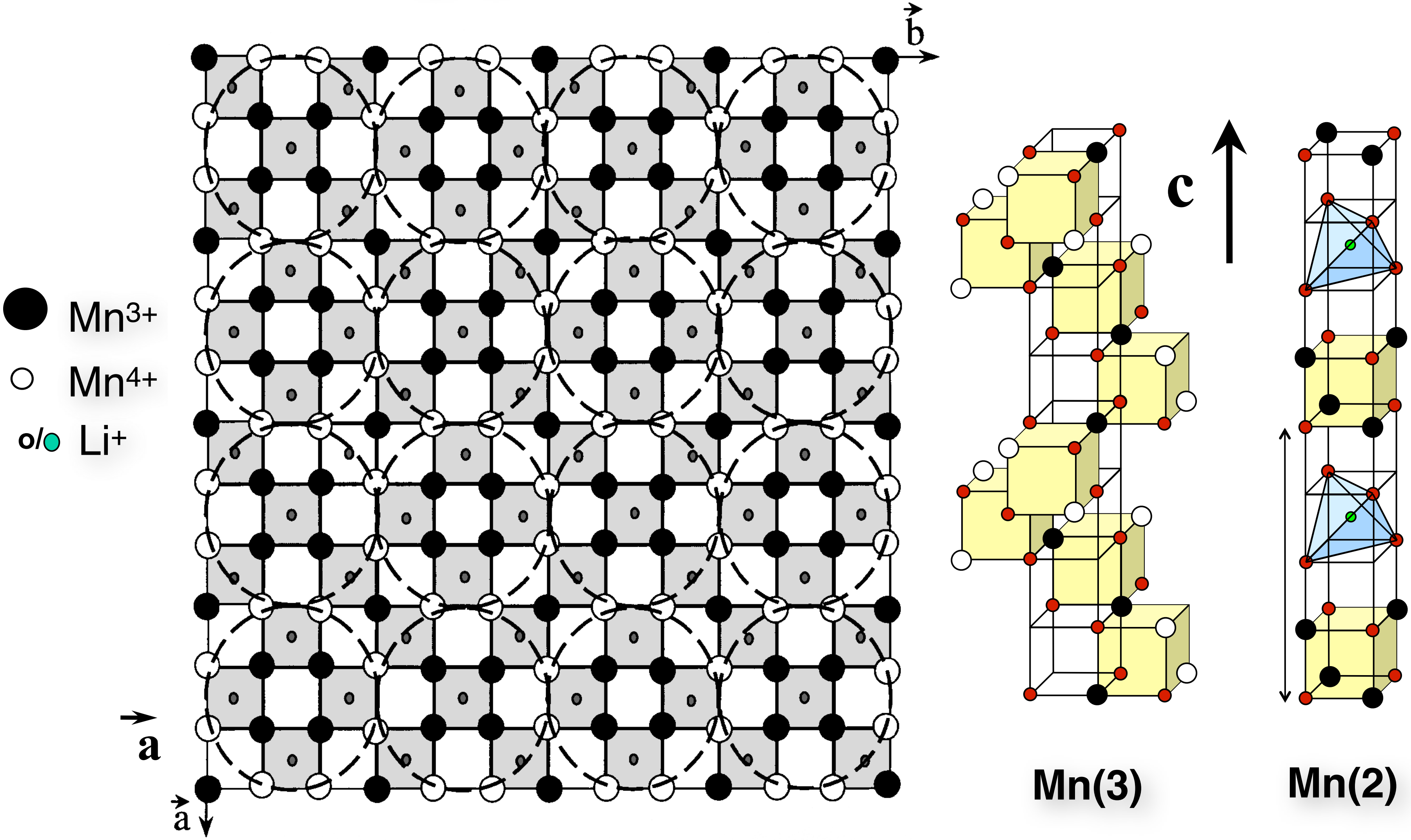

The peak shape function of powder diffraction patterns

Microstructural effects

Anisotropic peak broadening

The profile of powder diffraction patterns

The model to calculate a powder diffraction pattern is:

$$y_{ci} = \sum_{\mathbf{h}} I_{\mathbf{h}} \Omega(T_i - T_{\mathbf{h}}) + b_i$$

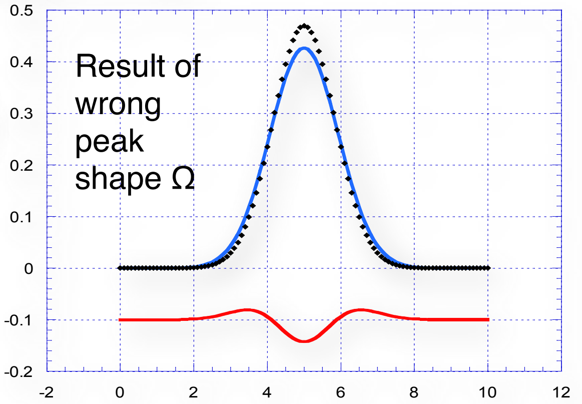

$$\int_{-\infty}^{+\infty} \Omega(x)dx = 1$$

Profile function characterized by its full width at half maximum (FWHM=H) and shape parameters (η, m, …)

$$\Omega(x) = g(x) \otimes f(x) = instrumental \otimes intrinsic\, profile$$

$$h(x) = g(x) \otimes f(x)$$ usual notation in literature

Integral breadth

The **integral breadth** of a peak is the width of a rectangle that has the same height and the same area as those of the peak

$$\beta = \frac{\int f_{hkl}(x)\,dx}{f_{hkl}(0)} \quad \left(= \frac{1}{f_{hkl}(0)} \quad \textit{if } f_{hkl} \textit{ is normalized} \right)$$

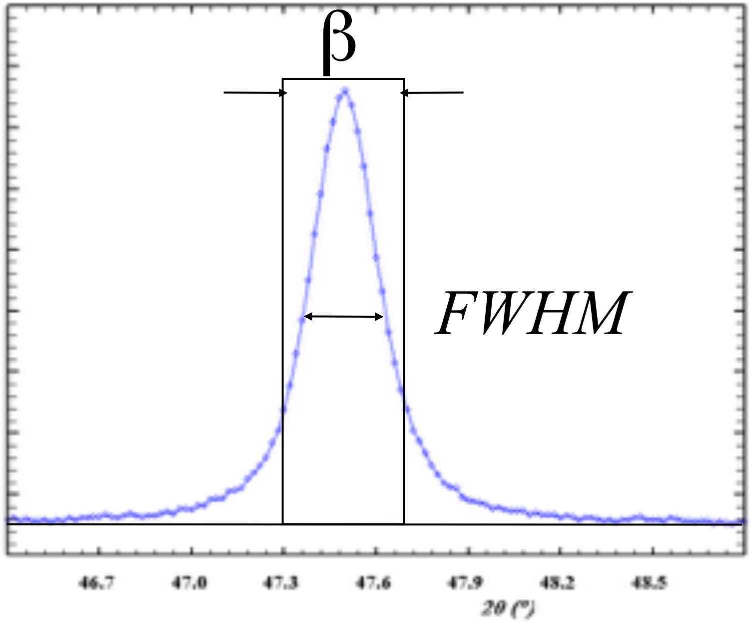

$$f_{hkl}(0) = \sum_{L} A(L)$$

$$\phi = \frac{FWHM}{\beta} < 1$$

Always less than 1

The peak shape function of powder diffraction patterns contains the *Profile Parameters* (constant wavelength case)

$$\Omega(x_{\mathbf{h}i}, \beta_{\mathbf{P}}) = \Omega(T_i - T_{\mathbf{h}}, \beta_{\mathbf{P}})$$

$$\int_{-\infty}^{+\infty} \Omega(x)dx = 1$$

The cell parameters are included, through $T_{\mathbf{h}}$, within the profile function. They determine the peak positions in the whole diffraction pattern.

The Voigt function

$$V(x) = L(x) \otimes G(x) = \int_{-\infty}^{+\infty} L(x-u)G(u)\,du$$

$$V(x) = V(x, H_L, H_G) = V(x, \beta_L, \beta_G)$$

The pseudo-Voigt function

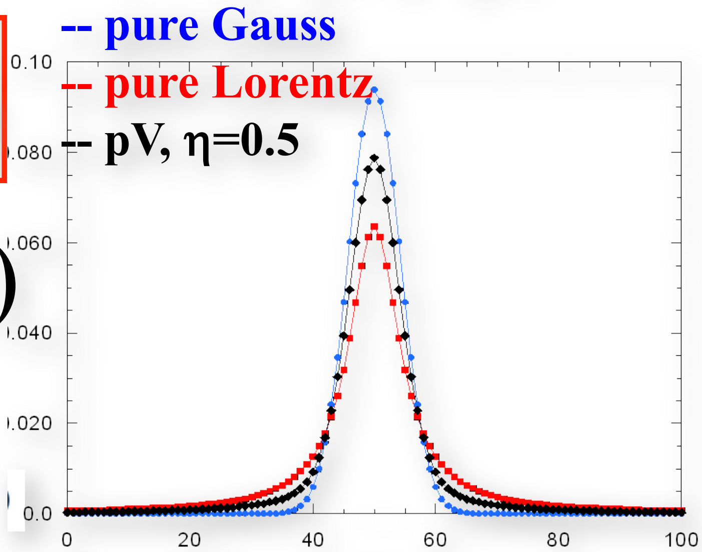

$$pV(x) = \eta L'(x) + (1-\eta)G'(x)$$

$$pV(x) = pV(x, \eta, H)$$

$$(\eta, H) = TCH(H_L, H_G) \quad \Leftrightarrow \quad (H_L, H_G) = TCH^{-1}(\eta, H)$$

“Many brilliant demonstrations starting from the well established Fourier coefficients description of diffraction profile are ending almost invariably into a pseudo-Voigt profile shape, certainly losing a bit of the original general sense by successive approximations” (A. Le Bail)

Convolution properties of Gaussian and Lorentzian functions

$$L(x,H_1)\otimes L(x,H_2)=L(x,H_1+H_2)$$

$$G(x,H_1)\otimes G(x,H_2)=G(x,\sqrt{H_1^2+H_2^2})$$

$$L(x,H_L)\otimes G(x,H_G)=V(x,H_L,H_G)$$

Properties of the Voigt function

$$V(x) = V_1(x) \otimes V_2(x)$$

"The Voigt function has proven to be a very good experimental approximation in many cases" (I. Langford)

$$\beta_L = \beta_{1L} + \beta_{2L}$$

Lorentzian breadths simply have to be summed

$$\beta_G^2 = \beta_{1G}^2 + \beta_{2G}^2$$

Gaussian breadths have to be summed quadratically

$$\beta_{fL} = \beta_{hL} - \beta_{gL}$$

$$\beta_{fG}^2 = \beta_{hG}^2 - \beta_{gG}^2$$

Correction for instrumental broadening

('Double Voigt', D. Balzar)

General 2θ dependence of the instrumental broadening (determined by a standard sample)

$$H_{hG}^{2} = (U_f + (1-\xi_f)^2 D_{fST}^{2}(\boldsymbol{\alpha}_D))\tan^2\theta + \frac{I_{fG}}{\cos^2\theta} + \boxed{H_{gG}^{2}}$$

$$H_{hL} = (X_f + \xi_f D_{fST}(\boldsymbol{\alpha}_D))\tan\theta + \frac{[Y_f + F_f(\boldsymbol{\alpha}_S)]}{\cos\theta} + \boxed{H_{gL}}$$

The Gaussian and Lorentzian components of the instrumental Voigt function are interpolated between empirically determined values. If needed, axial divergence is convoluted numerically with the resulting profile.

Some equations and formalisms

Some equations and formalisms

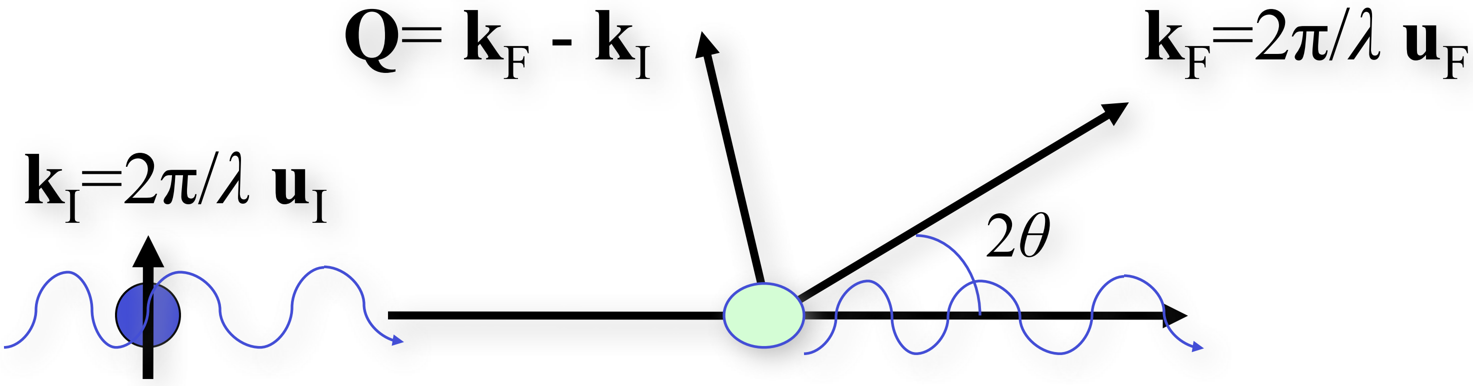

$\mathbf{Q} = \mathbf{k}_F - \mathbf{k}_I$

$\mathbf{k}_F = 2\pi/\lambda\ \mathbf{u}_F$

$\mathbf{k}_I = 2\pi/\lambda\ \mathbf{u}_I$

2θ

In scattering experiments, the incident particle (neutron, electron, photon...) experiences a change in its momentum and energy.

$$(h/2\pi)\mathbf{Q} = (h/2\pi)(\mathbf{k}_F - \mathbf{k}_I) = h\mathbf{s} \qquad h\nu = E_F - E_I$$

In the following we shall be concerned with elastic scattering ($h\nu=0$) for which $|\mathbf{k}_F| = |\mathbf{k}_I| = 2\pi/\lambda$ and $|\mathbf{Q}| = Q = (4\pi/\lambda)\sin\theta$, θ being half the scattering angle.

"crystallographic scattering vector": $\mathbf{s} = \mathbf{Q}/2\pi$

Scattering expressions for arbitrary objects

In the kinematics theory (first Born approximation), the amplitude of the wave scattered by an object is the **Fourier transform** (FT) **of its scattering density** (SD) $\rho(\mathbf{r})$ measured in cm^{-2}. Any object can be considered as constituted by atoms of SD $\rho_{aj}(\mathbf{r})$ centred at positions $\mathbf{R}_j$; the SD and the corresponding scattered amplitude and intensity can be written as:

$$\boxed{\begin{aligned} &\textit{Scattering density:} \quad \rho(\mathbf{r}) = \sum_j \rho_{aj}(\mathbf{r}-\mathbf{R}_j) \\ &\textit{Scattering amplitude:} \quad A(\mathbf{s}) = FT\left[\rho(\mathbf{r})\right] \end{aligned}}$$

$$A(\mathbf{s}) = FT\left[\rho(\mathbf{r})\right] = \int \rho(\mathbf{r}) e^{2\pi i \mathbf{s}\mathbf{r}} d^3\mathbf{r} = \int \sum_j \rho_{aj}(\mathbf{r}-\mathbf{R}_j) e^{2\pi i \mathbf{s}\mathbf{r}} d^3\mathbf{r}$$

$$A(\mathbf{s}) = \sum_j e^{2\pi i \mathbf{s}\mathbf{R}_j} \boxed{\int \rho_{aj}(\mathbf{u}) e^{2\pi i \mathbf{s}\mathbf{u}} d^3\mathbf{u}} = \sum_j \boxed{f_j(\mathbf{s})} e^{2\pi i \mathbf{s}\mathbf{R}_j}$$

$$I(\mathbf{s}) = A(\mathbf{s}) A^*(\mathbf{s}) = \sum_i \sum_j f_i(\mathbf{s}) f_j^*(\mathbf{s}) e^{2\pi i \mathbf{s}(\mathbf{R}_i - \mathbf{R}_j)}$$

Scattered Intensity of a Finite Crystal

Shape function: $g(\mathbf{r})$ is defined as $g(\mathbf{r})=1$ for $\mathbf{r}$ inside the crystal, and $g(\mathbf{r})=0$ for $\mathbf{r}$ outside the crystal ⇒ $G(\mathbf{s})=FT\{g(\mathbf{r})\}$.

$G^2(\mathbf{s})=FT\{g(\mathbf{r})\otimes g(-\mathbf{r})\}$ is the Fourier transform of the auto-correlation function:

$$\boxed{VA^S(\mathbf{r}) = \int g(\mathbf{u})g(\mathbf{r}+\mathbf{u})d^3\mathbf{u}}$$

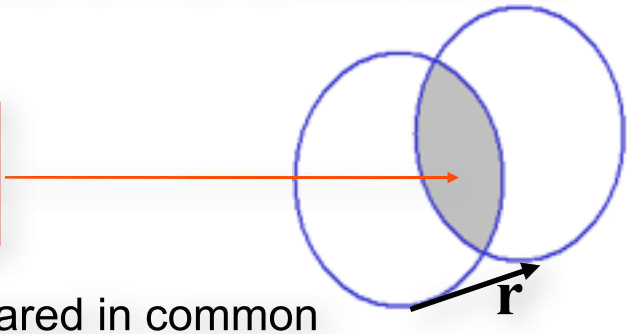

$A^S(\mathbf{r})$ is the fraction of the total volume shared in common between the object and its "ghost" displaced by the vector $\mathbf{r}$.

$A^S(0)=1$ and decreases as $\mathbf{r}$ increases. $G^2(\mathbf{s})=V\,FT\{A^S(\mathbf{r})\}$

$$\boxed{I(\mathbf{s}) \propto \frac{N}{VV_c}F(\mathbf{s})F^*(\mathbf{s})\sum_{\mathbf{H}} G^2(\mathbf{s}-\mathbf{H})}$$

Size effects in reciprocal space

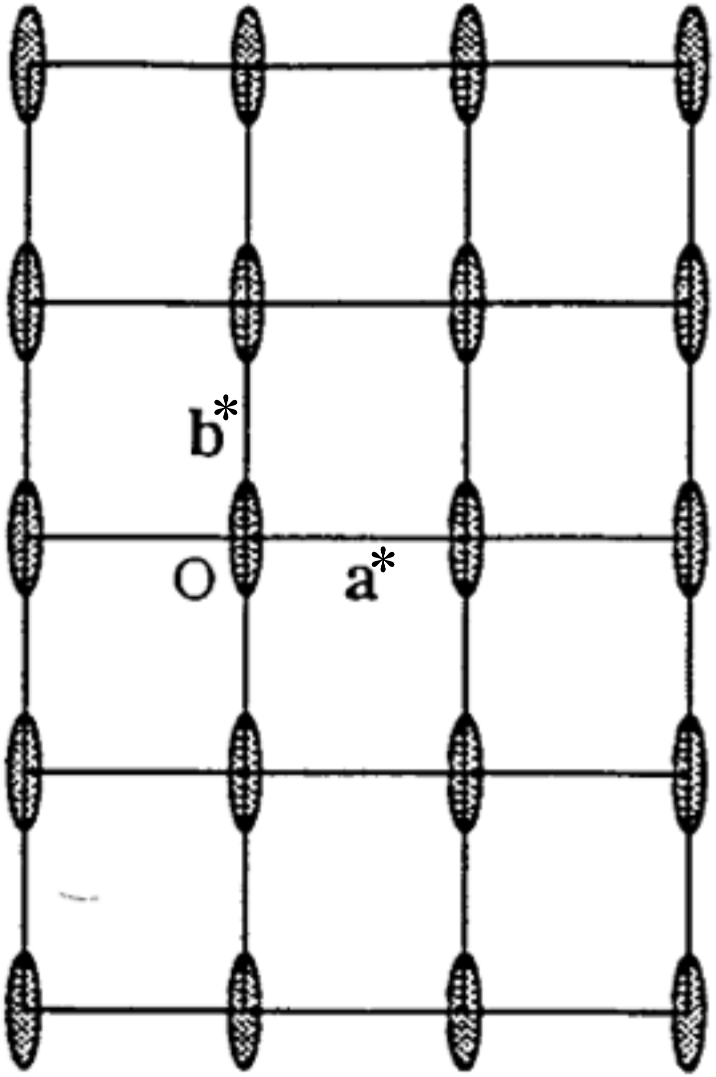

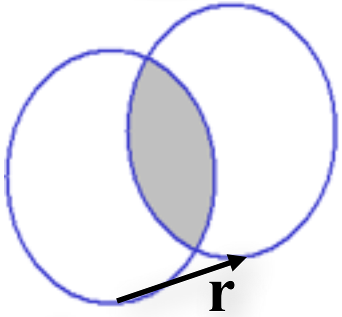

crystallographic scattering vector $\mathbf{s}=\mathbf{Q}/2\pi$
shape function $g(\mathbf{r})$
auto-correlation function $VA^S(\mathbf{r})$

$$VA^S(\mathbf{r}) = \int g(\mathbf{u})g(\mathbf{r}+\mathbf{u})d^3\mathbf{u}$$

$$G^2(\mathbf{s}) = FT\{g(\mathbf{r})\otimes g(-\mathbf{r})\} = V\,FT\{A^S(\mathbf{r})\}$$

$$\sum_{\mathbf{H}} G^2(\mathbf{s}-\mathbf{H}) \rightarrow G^2_{\mathbf{H}}(\Delta\mathbf{s}) = G^2(\Delta\mathbf{s})$$

***G* determines the shape of the peak profile and it is the same for all reciprocal nodes**

Peak width increases in 2θ space with $(\cos\theta)^{-1}$
Apart from spheres, the width depends on the direction in reciprocal space

Scattered Intensity of a Real Crystal

crystallographic scattering vector $\mathbf{s}=\mathbf{Q}/2\pi$
auto-correlation function $VA^S(\mathbf{r})$

Defects: **average lattice + structure factor depending on unit cell**

$$I(\mathbf{s}) \approx \sum_n \Big(\sum_m F_m F^*_{m+n} \Big) \exp\{2\pi i\, \mathbf{s}\, \mathbf{R}_n\}$$

$F_m = F_m(\mathbf{s})$ is the **structure factor** of the cell m.

$p_n(\mathbf{R}_n,\mathbf{s})=\langle F_m F^*_{m+n}\rangle$ is independent of m, but depends on $\mathbf{s}$.

The number of terms in the inner sum is given by $VA^S(\mathbf{R}_n)/V_\mathrm{c}$ and the equation can be transformed to:

$$\begin{aligned} I(\mathbf{s}) &= \frac{V}{V_c} \sum_n A^S(\mathbf{R}_n) \left\langle F_m F^*_{m+n} \right\rangle \exp\{2\pi i\, \mathbf{s}\, \mathbf{R}_n\} \\ &= N \sum_n A^S(\mathbf{R}_n)\, p_n(\mathbf{R}_n, \mathbf{s}) \exp\{2\pi i\, \mathbf{s}\, \mathbf{R}_n\} \end{aligned}$$

Strained Crystals

A crystal is said to be "strained" if the structure factor of the cell m can be written in the form:

$$F_m = F\exp\{2\pi i\,\mathbf{s}\,\mathbf{u}_m\}, \quad \left(with\ F = \frac{1}{N}\sum_n F_n \right)$$

Defining the quantity: $A^D(\mathbf{R}_n, \mathbf{s}) = \left\langle \exp\{2\pi i\,\mathbf{s}(\mathbf{u}_m - \mathbf{u}_{m+n})\} \right\rangle$

$$\boxed{I(\mathbf{s}) = NF^2 \sum_n A^S(\mathbf{R}_n)\, A^D(\mathbf{R}_n, \mathbf{s}) \exp\{2\pi i\,\mathbf{s}\,\mathbf{R}_n\}}$$

If $\mathbf{s}=\mathbf{H}+\Delta\mathbf{s}$, the scattered intensity around a Bragg peak is given by:

$$\boxed{I_{\mathbf{H}}(\Delta\mathbf{s}) = NF_{\mathbf{H}}^2 \sum_n \underset{\text{size}}{A^S(\mathbf{R}_n)}\, \underset{\text{strain}}{A_{\mathbf{H}}^D(\mathbf{R}_n)} \exp\{2\pi i\,\Delta\mathbf{s}\,\mathbf{R}_n\} \approx F_{\mathbf{H}}^2 f_{\mathbf{H}}(\Delta\mathbf{s})}$$

Strain effects in reciprocal space

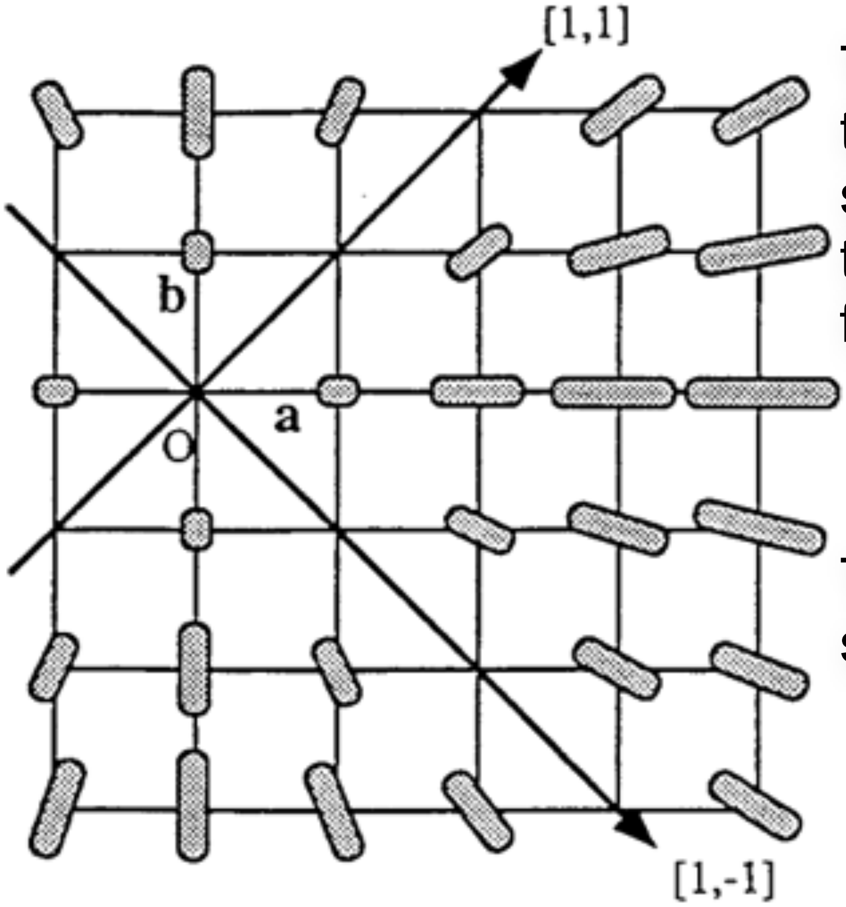

The interpretation of the peak shape in the case of strains is not so straightforward as that of size because there are many possible physical origins for strain broadening:

dislocations, interstitials, vacancies, compositional fluctuations, etc.

The important point is that the peak shape and width depend on **both**

particular reflection **and**

direction in reciprocal space.

Peak width increases in 2θ space with $\tan\theta$

Simplified methods for treating the intrinsic profile

The method of *Warren-Averbach*, based in the Fourier series representing the intrinsic profile of a powder diffraction peak, has drawbacks when overlap is strong. Moreover, not enough statistics make this **de-convolution** method extremely unstable.

$$\boxed{\begin{aligned}\beta\,(size) &= \frac{\lambda}{D\cos\theta}\\ \beta\,(strain) &= 4e\tan\theta\end{aligned}}$$

Integral breadth methods, combined with an analytical approximation for f, g and Ω, are, by far, much more simple and robust: ***strain*** and size parameters are volume averaged quantities

They separate **peak broadening effects due to size and strain**, by adding peak width terms with distinct Q-dependencies.

The peak shape function of powder diffraction patterns contains the *Profile Parameters* (constant wavelength case)

$$\Omega(x_{\mathbf{h}i}, \beta_{\mathbf{P}}) = \Omega(T_i - T_{\mathbf{h}}, \beta_{\mathbf{P}})$$

$$\int_{-\infty}^{+\infty} \Omega(x)\,dx = 1$$

The cell parameters are included, through $T_{\mathbf{h}}$, within the profile function. They determine the peak positions in the whole diffraction pattern.

The Voigt function

$$V(x)=L(x)\otimes G(x)=\int_{-\infty}^{+\infty}L(x-u)G(u)du$$

$$V(x)=V(x,H_L,H_G)=V(x,\beta_L,\beta_G)$$

The pseudo-Voigt function

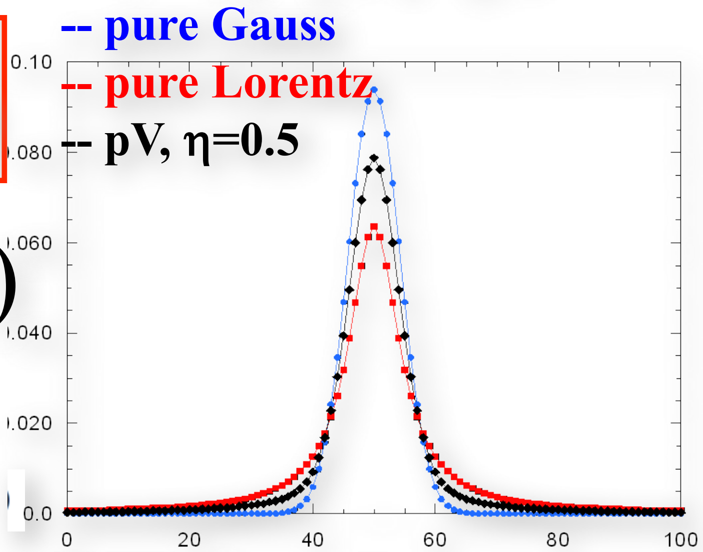

$$pV(x)=\eta L'(x)+(1-\eta)G'(x)$$

$$pV(x)=pV(x,\eta,H)$$

$$(\eta,H)=TCH(H_L,H_G)\quad\Leftrightarrow\quad(H_L,H_G)=TCH^{-1}(\eta,H)$$

“Many brilliant demonstrations starting from the well established Fourier coefficients description of diffraction profile are ending almost invariably into a pseudo-Voigt profile shape, certainly losing a bit of the original general sense by successive approximations” (A. Le Bail)

Convolution properties of Gaussian and Lorentzian functions

$$L(x, H_1) \otimes L(x, H_2) = L(x, H_1 + H_2)$$

$$G(x, H_1) \otimes G(x, H_2) = G(x, \sqrt{H_1^2 + H_2^2})$$

$$L(x, H_L) \otimes G(x, H_G) = V(x, H_L, H_G)$$

Properties of the Voigt function

$$V(x) = V_1(x) \otimes V_2(x)$$

"The Voigt function has proven to be a very good experimental approximation in many cases" (I. Langford)

$$\beta_L = \beta_{1L} + \beta_{2L}$$

Lorentzian breadths simply have to be summed

$$\beta_G^2 = \beta_{1G}^2 + \beta_{2G}^2$$

Gaussian breadths have to be summed quadratically

$$\beta_{fL} = \beta_{hL} - \beta_{gL}$$

$$\beta_{fG}^2 = \beta_{hG}^2 - \beta_{gG}^2$$

Correction for instrumental broadening
('Double Voigt', D. Balzar)

Profile parametrization

- $h(x) = g(x) \otimes f(x)$
- ***Instrument resolution function*** *modeled by the parameters* $(U, V, W, X, Y)_g$ *:*
    - *total profile:Voigt function with* (H_G, H_L)

$$H_{hG}^2 = (U_g + U_f + (1-\xi_f)^2 D_{fST}^2(\boldsymbol{\alpha}_D))\tan^2\theta + V_g \tan\theta + W_g + \frac{I_{fG}}{\cos^2\theta}$$

$$H_{hL} = (X_g + X_f + \xi_f D_{fST}(\boldsymbol{\alpha}_D))\tan\theta + \frac{[Y_g + Y_f + F_f(\boldsymbol{\alpha}_S)]}{\cos\theta}$$

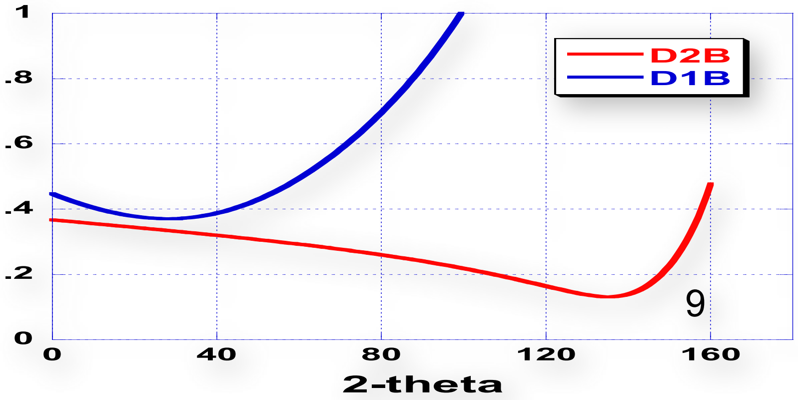

Spherical harmonics to simulate the average shape of crystallites

Arbitrary shapes of crystallites can be simulated using spherical harmonics.

$$\frac{1}{D_{\mathbf{h}}} = \sum_{lmp} a_{lmp} P_{lm}\left(\cos\Theta_{\mathbf{h}}\right)\begin{Bmatrix}\cos m\Phi_{\mathbf{h}} \\ \sin m\Phi_{\mathbf{h}}\end{Bmatrix}; \qquad p = +/-$$

$\left(\Theta_{\mathbf{h}}, \Phi_{\mathbf{h}}\right)$: Polar angles of reciprocal vector $\mathbf{h}$ w.r.t. crystal frame

$$\beta_S = \frac{\lambda}{\cos\theta}\sum_{lmp} a_{lmp} P_{lm}\left(\cos\Theta_{\mathbf{h}}\right)\begin{Bmatrix}\cos m\Phi_{\mathbf{h}} \\ \sin m\Phi_{\mathbf{h}}\end{Bmatrix}$$

Profile parameterisation

- $h(x) = g(x) \otimes f(x)$
- ***Instrument resolution function** modelled by the parameters* $(U, V, W, X, Y)_g$ *:*
    - *total profile:Voigt function with* (H_G, H_L)

$$H_{hG}^2 = (U_g + U_f + (1-\xi_f)^2 D_{fST}^2(\boldsymbol{\alpha}_D))\tan^2\theta + V_g \tan\theta + W_g + \frac{I_{fG}}{\cos^2\theta}$$

$$H_{hL} = (X_g + X_f + \xi_f D_{fST}(\boldsymbol{\alpha}_D))\tan\theta + \frac{[Y_g + Y_f + F_f(\boldsymbol{\alpha}_S)]}{\cos\theta}$$

$$H_{hG}^2 = (U_g + U_f)\tan^2\theta + V_g \tan\theta + W_g + \frac{I_{fG}}{\cos^2\theta}$$

$$H_{hL} = (X_g + X_f)\tan\theta + \frac{Y_g + Y_f}{\cos\theta}$$

General 2θ dependence of the instrumental broadening (determined by a standard sample)

$$H_{hG}^{2} = \boxed{U_f \tan^{2}\theta + \frac{I_{fG}}{\cos^{2}\theta}} + \boxed{H_{gG}^{2}}$$

$$H_{hL} = \boxed{\overset{\text{strain}}{X_f} \tan\theta + \frac{\overset{\text{size}}{Y_f}}{\cos\theta}} + \boxed{H_{gL}}$$

The Gaussian and Lorentzian components of the instrumental Voigt function are interpolated between empirically determined values.
If needed, axial divergence is convoluted numerically with the resulting profile.

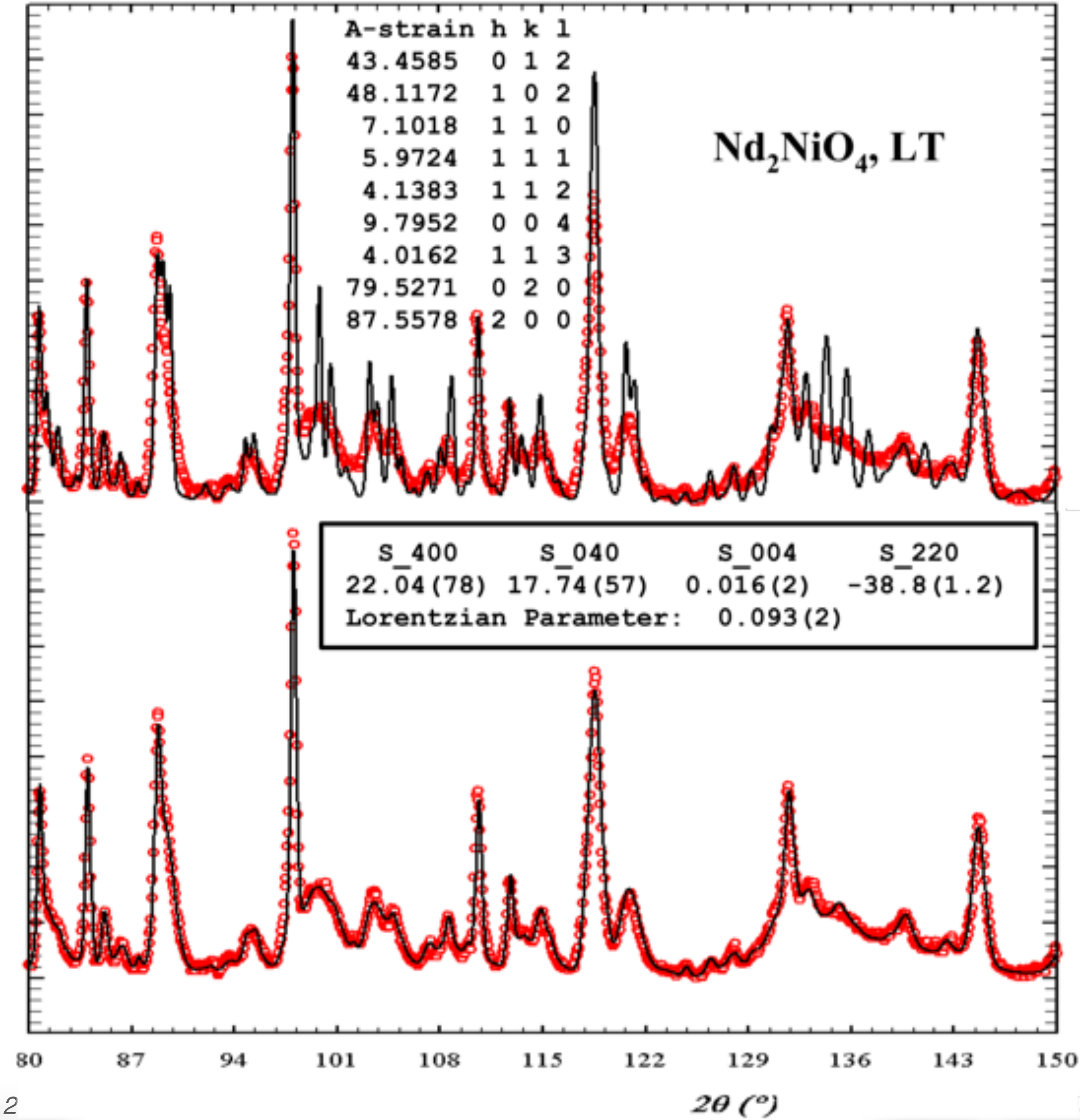

A-strain	h	k	l
43.4585	0	1	2
48.1172	1	0	2
7.1018	1	1	0
5.9724	1	1	1
4.1383	1	1	2
9.7952	0	0	4
4.0162	1	1	3
79.5271	0	2	0
87.5578	2	0	0

S_400	S_040	S_004	S_220
22.04(78)	17.74(57)	0.016(2)	-38.8(1.2)

Lorentzian Parameter: 0.093(2)

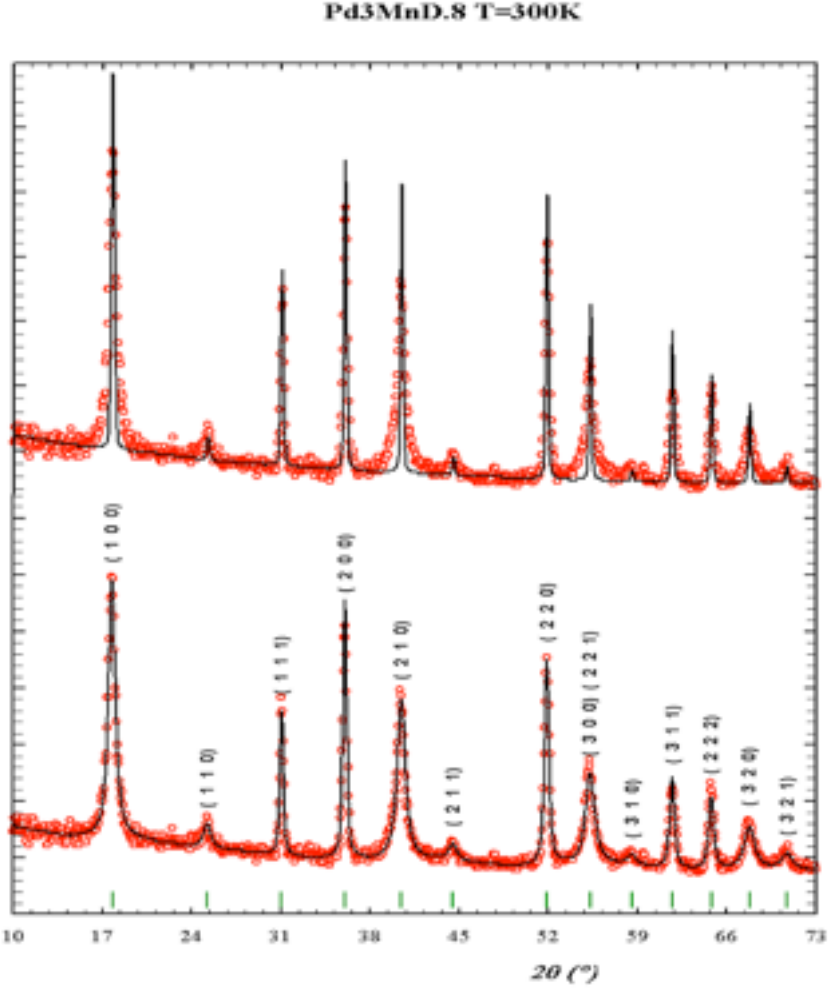

Portion of the neutron diffraction pattern of $Pd_3MnD_{0.8}$ at room temperature obtained on 3T2 (LLB, λ = 1.22 Å). On top, the comparison with the calculated profile using the resolution function of the instrument. Below the fit using `IsizeModel` = -14. Notice that only the reflections with indices of different parity are strongly broadened. An isotropic strain, due to the disorder of deuterium atoms, is also included for all kind of reflections.

Example: Simulated data of anisotropic size effects using Spherical Harmonics (based in unpublished real data)

The sample was a component of a catalyst, mostly constituted by a tetragonal alumina polymorph

Comparison of the experimental pattern with the resolution function of the diffractometer

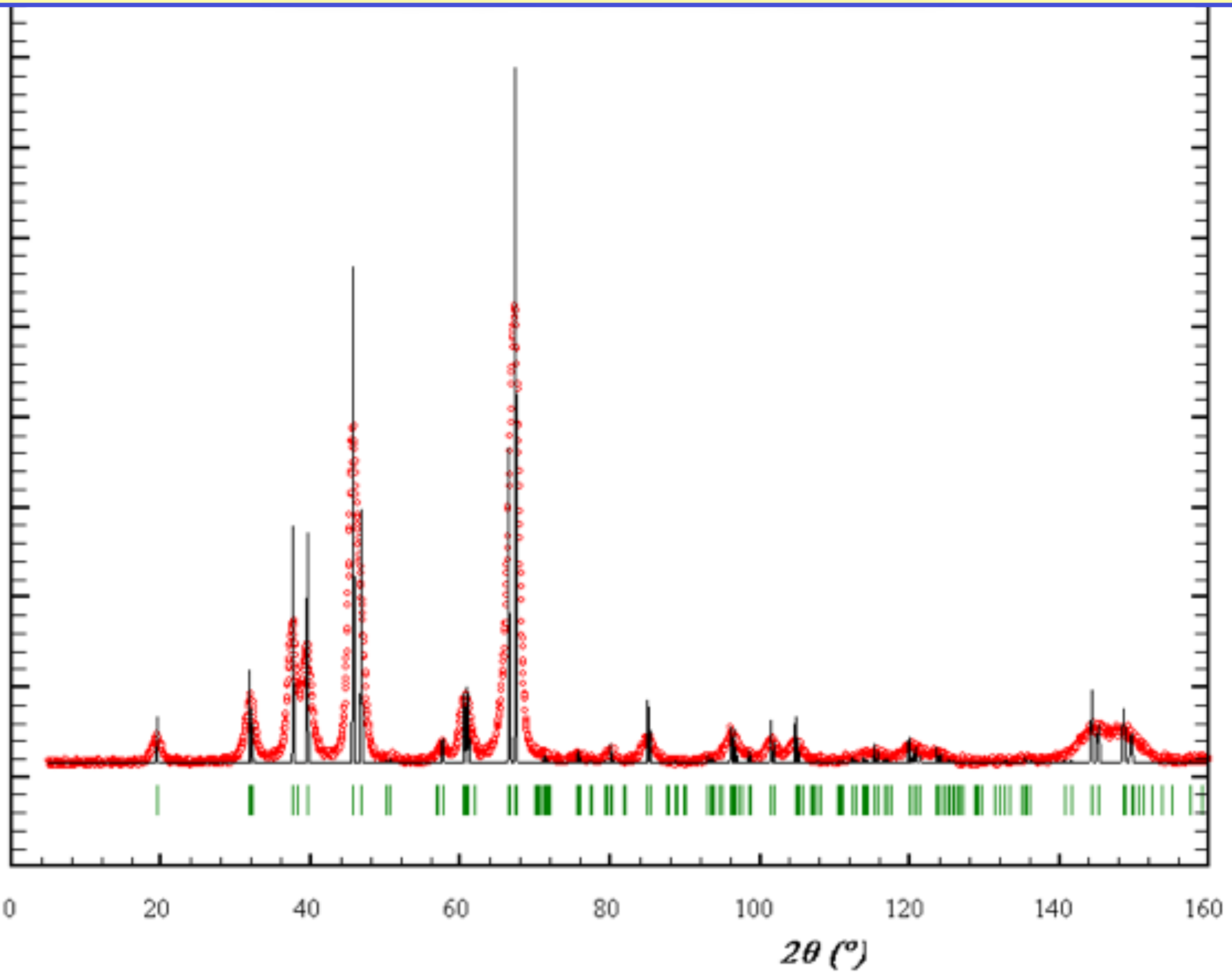

Refinement using isotropic Lorentzian and Gaussian parameters: Average crystallite size 58.3 Å

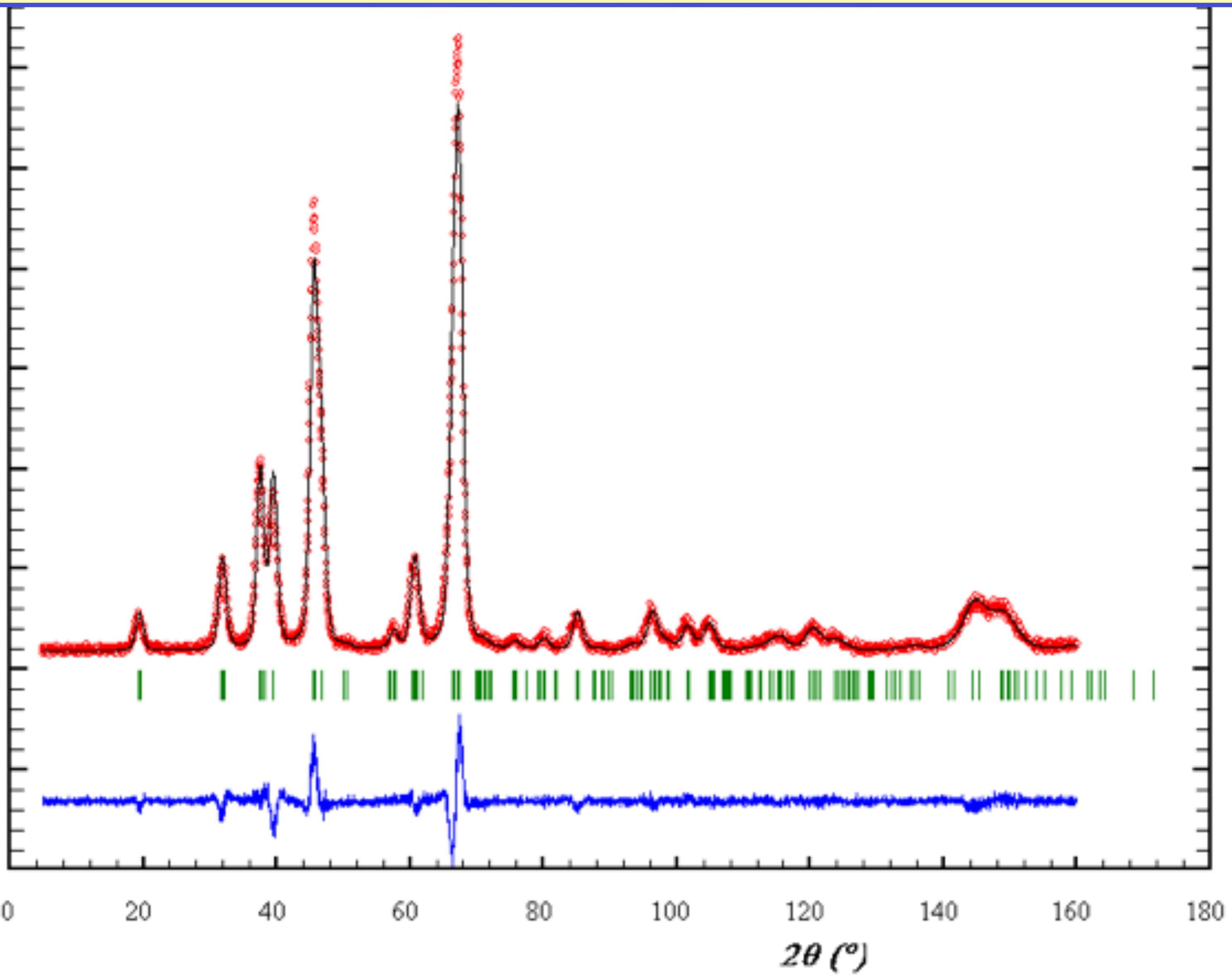

Refinement using anisotropic Lorentzian and isotropic Gaussian size parameters: Average crystallite size (anisotropy): 56.31 (7.74)

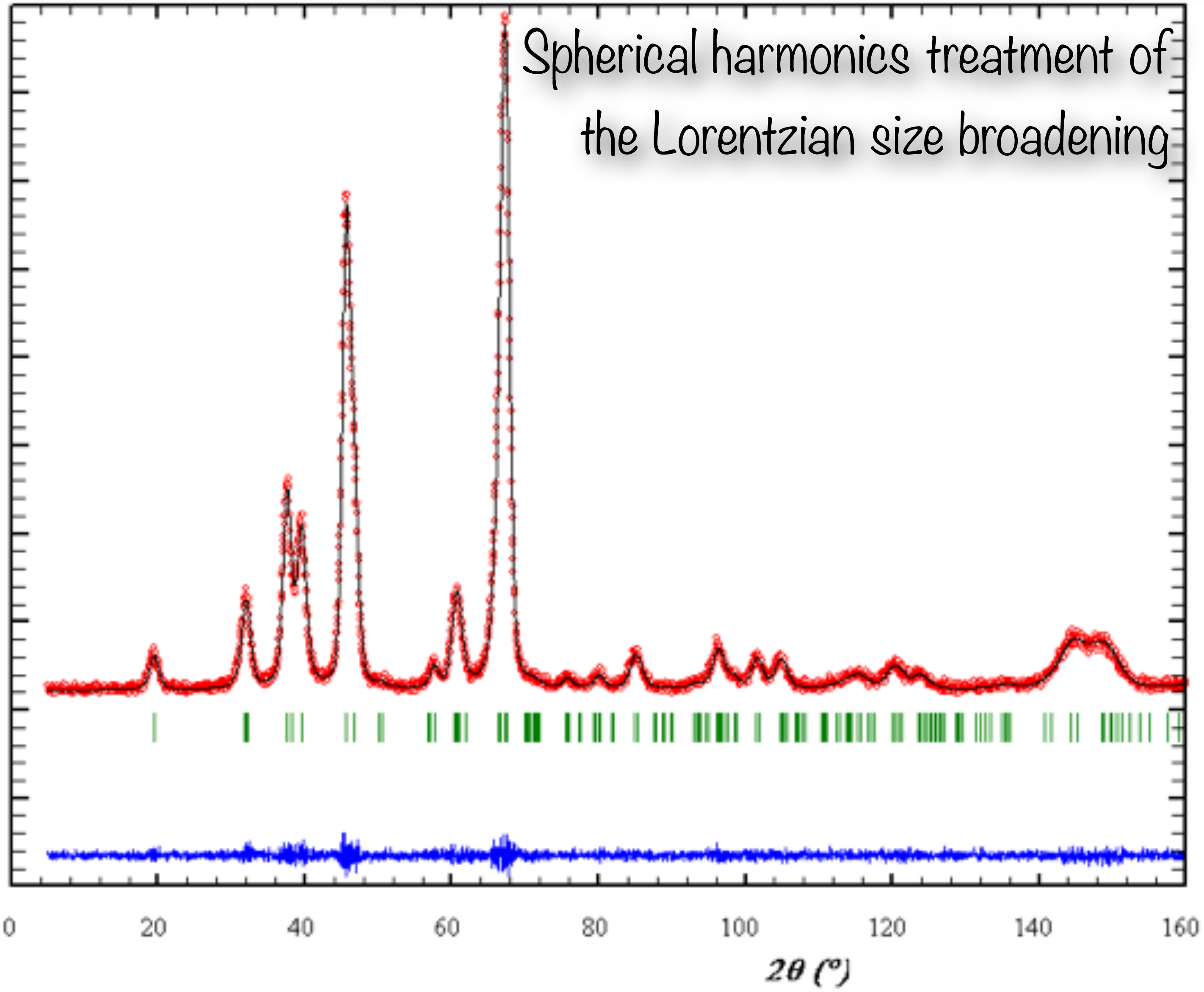

Spherical harmonics treatment of the Lorentzian size broadening

Anisotropic crystallite size

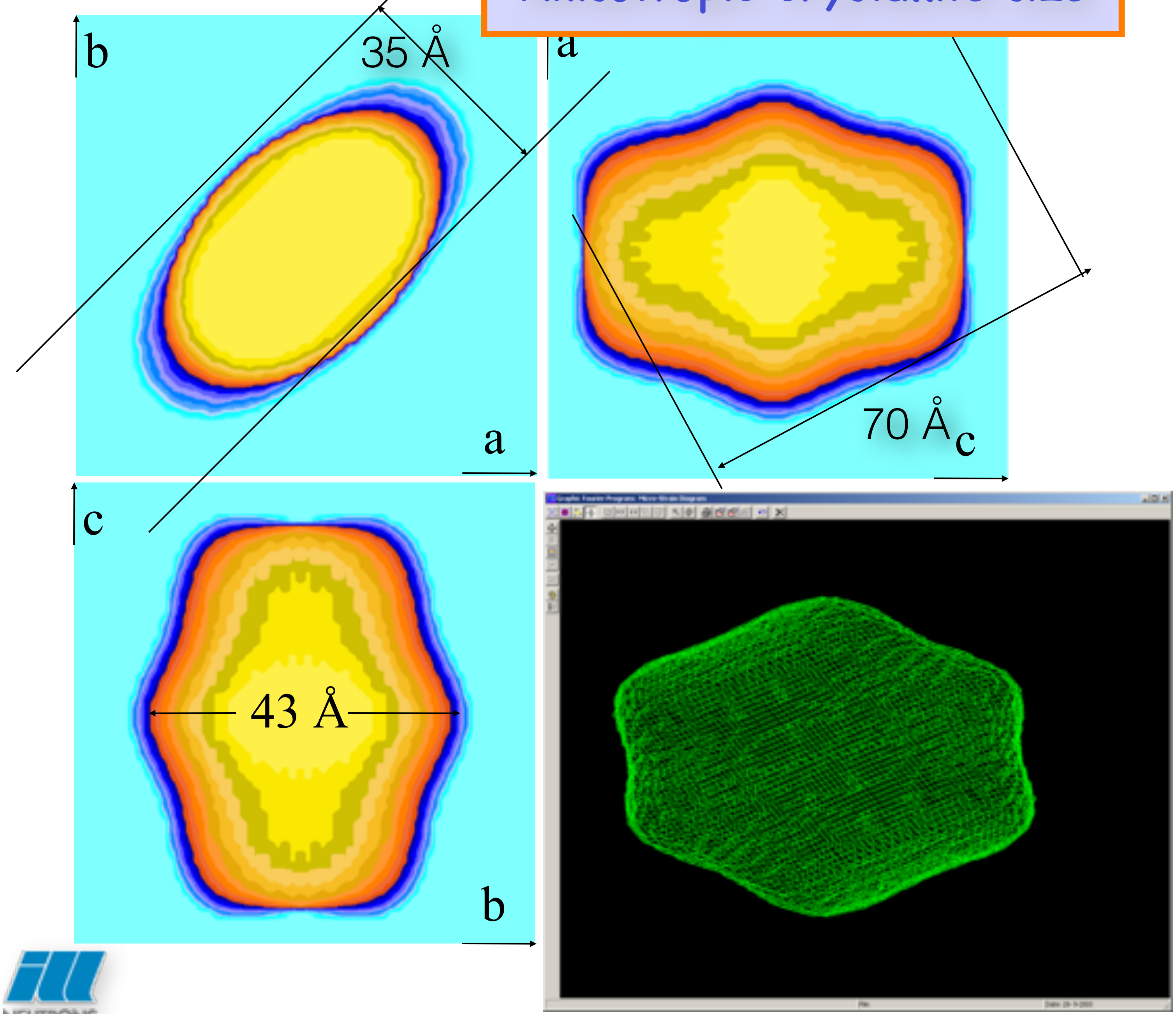

Size broadening in $Ni(OH)_2$